

1997

# Argonne National Laboratory

## THE EBR-I MELTDOWN - PHYSICAL AND METALLURGICAL CHANGES IN THE CORE

by

J. H. Kittel, M. Novick and R. F. Buchanan

LOS ALAMOS NATIONAL LABORATORY



3 9338 00347 6164

## LEGAL NOTICE

This report was prepared as an account of Government sponsored work. Neither the United States, nor the Commission, nor any person acting on behalf of the Commission:

- A. Makes any warranty or representation, express or implied, with respect to the accuracy, completeness, or usefulness of the information contained in this report, or that the use of any information, apparatus, method, or process disclosed in this report may not infringe privately owned rights; or
- B. Assumes any liabilities with respect to the use of, or for damages resulting from the use of any information, apparatus, method, or process disclosed in this report.

As used in the above, "person acting on behalf of the Commission" includes any employee or contractor of the Commission to the extent that such employee or contractor prepares, handles or distributes, or provides access to, any information pursuant to his employment or contract with the Commission.

ARGONNE NATIONAL LABORATORY  
P O. Box 299  
Lemont, Illinois

THE EBR-I MELTDOWN -  
PHYSICAL AND METALLURGICAL CHANGES IN THE CORE

by  
J. H. Kittel, M. Novick<sup>1</sup> and R. F. Buchanan<sup>2</sup>

Final Report - Metallurgy Program 7.2.18

Portions of the material in this report have appeared  
in ANL-5717, the Metallurgy Division Quarterly Report  
for January, February, and March 1957

Metallurgy Division

November 1957

<sup>1</sup>Novick - Idaho Division  
<sup>2</sup>Buchanan - ANL Chemistry Division

Operated by The University of Chicago  
under  
Contract W-31-109-eng-38

## TABLE OF CONTENTS

	<u>Page</u>
ABSTRACT . . . . .	11
INTRODUCTION . . . . .	11
REMOVAL OF THE CORE FROM THE REACTOR . . . . .	13
INITIAL CORE DISASSEMBLY . . . . .	14
FINAL CORE DISASSEMBLY . . . . .	17
METALLOGRAPHIC STUDIES . . . . .	21
CHEMICAL AND MASS SPECTROGRAPHIC ANALYSES . . . . .	22
SIMULATED MELTDOWN EXPERIMENTS . . . . .	24
CONCLUSIONS. . . . .	25
ACKNOWLEDGMENTS . . . . .	25
REFERENCES . . . . .	27

## LIST OF TABLES

<u>No.</u>	<u>Title</u>	<u>Page</u>
I.	Location of areas in which metallographic and chemical samples were taken. See also Figures 42 and 43 . . . . .	29
II.	Microhardness values obtained on samples from EBR-I Core. Five determinations were made on each specimen, using a 1-kg load and a Vickers diamond indenter . . . . .	29
III.	Chemical and Mass Spectrographic Analyses of Samples from Damaged Core Assembly. See Table I and Figures 42 and 43 for locations from which samples were taken . . . . .	30

## LIST OF FIGURES

<u>No.</u>	<u>Title</u>	<u>Page</u>
1.	Horizontal cross section of EBR-I at the reactor midplane . . . . .	31
2.	Simplified drawing of a typical fuel element from the EBR-I second loading. The diameter of the assembled fuel element is 0.45 in. . . . .	32
3.	Intermetallic compound layers formed as a result of interdiffusion between uranium and Type 347 stainless steel after six days at 700°C. Total thickness of the layers is 0.0018 in. . . . .	33
4.	Construction of temporary cave above EBR-I before closure of front face. The top of the reactor is shown at the center of the cave floor. After lifting the core assembly from the reactor tank, it was suspended from the bracket shown at the upper left. . . . .	34
5.	Completed temporary cave built over EBR-I for removal of core assembly . . . . .	35
6.	Core assembly after removal of blanket rods. The fuel section is enclosed in the hexagonal separator . . . . .	36
7.	Core assembly after removal of bottom plate. The tips of the fuel rods in the hexagonal separator are visible . . . . .	37
8.	Holes drilled in hexagonal separator to facilitate removal from core assembly . . . . .	38
9.	Interior surfaces of hexagonal separator, showing superficial alloying of molten phase with separator, particularly on sides 2, 4, and 6 . . . . .	39
10.	Damaged EBR-I core after removal of hexagonal separator . . . . .	40
11.	Typical fuel element from the first (outer) row of the damaged EBR-I core . . . . .	41

## LIST OF FIGURES

<u>No.</u>	<u>Title</u>	<u>Page</u>
12.	Typical fuel element from the second row of the damaged EBR-I core . . . . .	41
13.	Fuel element from outer row of damaged EBR-I core assembly, showing that although the outer jacket has been severely damaged by melting, the stainless steel spacer between adjacent fuel slugs is undamaged. . . . .	42
14.	The stainless steel jacket shown above in Figure 13 has been peeled back, and it can be noted that the surface of the fuel slug and the interior surface of the jacket were unaffected by the meltdown. . . . .	42
15.	Damaged EBR-I core after removal of outer fuel elements . . . . .	43
16.	Thimble used to contain damaged core. Argon gas is being led into the thimble by the tube on the left . . . . .	44
17.	Appearance of core assembly after all remaining fuel rods has been sawed through . . . . .	45
18.	Gas-tight container and cage assembly used for shipment of the damaged EBR-I core assembly . . . . .	46
19.	Lead cask used to ship the damaged EBR-I core assembly. The cask is 43 inches high, 40 inches in diameter, and weighs 10,800 lbs . . . . .	47
20.	View of some of the instrumentation outside the cave used for final disassembly of the EBR-I core. The equipment at the left recorded air-borne particulate activity in the cave atmosphere. The equipment at the center recorded oxygen level in the cave atmosphere. Other instruments, not visible, measured nitrogen flow rate, temperature, humidity, and gamma and neutron levels in the cave . . . . .	48

## LIST OF FIGURES

<u>No.</u>	<u>Title</u>	<u>Page</u>
21.	Area in left part of cave used for disassembly of EBR-I core. The top of the cage assembly used for shipment, shown in Figure 18, is at the lower left. The device in the center background is a pipe cutter, and the object in the right background is a hydraulic chisel. An electric impact chisel is suspended at the extreme right. All powered equipment was remotely operated . . . . .	49
22.	Area in right part of cave used for weighing and sealing cans of separated enriched material. The numbered bottles in the foreground were used for chemical samples. A partition at the left divided this area of the cave from the disassembly operations in the left area . . . . .	50
23.	Typical piece of fuel being loaded into a storage can. After each filled can was weighed it was moved to the can sealer shown in Figure 24 . . . . .	51
24.	Remotely operated equipment shown sealing a can of enriched fuel . . . . .	52
25.	Procedure used for loading unenriched blanket material . . . . .	53
26.	Appearance of the top of the damaged EBR-I core before final disassembly operations were started . . . . .	54
27.	Remotely operated pipe cutter being used to cut outer jacket on a fuel element near the junction of fuel and blanket. The blanket section at the right end of the element has already been removed with the pipe cutter, and the tip of a fuel slug is visible . . . . .	55
28.	Clump of upper blanket rods from near the center of the core assembly. The blanket section begins about one-half in. above the lower end, and it can be noted that the molten fuel alloy has moved upward between the rods for approximately 5 in. . . . .	56

## LIST OF FIGURES

<u>No.</u>	<u>Title</u>	<u>Page</u>
29.	Stainless steel outer jacket from the upper blanket. The left end originally was attached to the fuel section. Most of the adhering fuel alloy has been removed, and it can be noted that the jacket does not appear to have been damaged by melting . . . . .	57
30.	Use of thermocouple wires embedded in the fuel section to lift the fuel and lower blanket assembly from the thimble used for shipping . . . . .	58
31.	Appearance of the damaged EBR-I core after removal of the upper blanket section . . . . .	59
32.	Cross section of damaged EBR-I core at the midplane of the fuel section. Two distinct sponge-like zones are present. Thermocouple wires in the fused mass are undamaged . . . . .	60
33.	Side view of core assembly after partial removal of lower blanket section . . . . .	61
34.	Bottom of fuel section, after partial removal of lower blanket rods . . . . .	62
35.	Stainless steel outer jacket from the lower blanket. The upper end was originally attached to the fuel section. Most of the adhering fuel alloy has been removed, and it can be noted that the jacket does not appear to have been damaged by melting . . . . .	63
36.	Vertical cross section of the lower half of the core. The junction between fuel and lower blanket is at the 6-1/4-in. level . . . . .	64
37.	Partially dissolved fuel slugs embedded in dense material from near bottom of fuel section . . . . .	65
38.	Partially dissolved fuel slugs separated from adjoining material . . . . .	66
39.	Illustration of voids which were found in the dense zone in the lower fuel section . . . . .	67

## LIST OF FIGURES

<u>No.</u>	<u>Title</u>	<u>Page</u>
40.	Artist's reconstruction of a vertical cross section through the damaged EBR-I core. The most reliable values for the densities of the various areas shown at the left . . . . .	68
41.	Appearance of samples removed for metallographic examination. Reading left to right, sample numbers are: top, 31 and 32; bottom: 33, 29, and 30. Locations from which the samples were taken are given in Table I . . .	69
42.	Approximate location of samples taken from a horizontal cross section of the core for chemical analyses and metallographic studies. . . . .	70
43.	Approximate location of samples taken from a vertical cross section of the core for chemical analyses and metallographic studies . . . . .	71
44.	Typical porosity in sample No. 29, from coarse sponge zone. . . . .	72
45.	Typical porosity in sample No. 30, from fine sponge zone. . . . .	72
46.	Typical porosity in sample No. 31, from material between blanket rods. . . . .	73
47.	Porosity in material adhering to partially dissolved fuel slug, in sample No. 32. . . . .	73
48.	Typical porosity in sample No. 33, from high-density zone . . . . .	74
49.	Exudation of NaK oxide and resulting deliquescence in porous samples removed from damaged core. From left to right, the samples are from the coarse sponge zone, the fine sponge zone, and material solidified between lower blanket rods . . . . .	75
50.	Microstructure in sample No. 29, from coarse sponge zone. The light phase is believed to be analogous to $UFe_2$ and the dark phase analogous to $U_6Fe$ . . . . .	76

## LIST OF FIGURES

<u>No.</u>	<u>Title</u>	<u>Page</u>
51.	Microstructure in sample No. 30, from fine sponge zone. The light phase is believed to be analogous to $UFe_2$ and the dark phase analogous to $U_6Fe$ . . . . .	76
52.	Microstructure in sample No. 31, from material between blanket rods. The light phase is believed to be analogous to $UFe_2$ and the dark phase analogous to $U_6Fe$ . . . . .	77
53.	Microstructure of sample No. 32, showing junction between embedded fuel slug and adjoining material. The undissolved fuel slug is shown in the upper half of the photograph. The light phase is believed to be analogous to $UFe_2$ and the dark phase analogous to $U_6Fe$ . . . . .	77
54.	Microstructure in sample No. 33, from high-density zone. The light phase is believed to be analogous to $UFe_2$ and the dark phase analogous to $U_6Fe$ . . . . .	78
55.	Cross section of first casting made by pouring uranium-stainless steel alloy into NaK. A small amount of NaK was trapped in the casting, as evidenced by the traces of NaK oxide . . . . .	78
56.	Porosity in casting shown in Figure 55 . . . . .	79
57.	Microstructure of casting shown in Figure 55. The light phase is believed to be analogous to $UFe_2$ and the dark phase analogous to $U_6Fe$ . . . . .	79
58.	Cross section of second casting made by pouring uranium-iron alloy into NaK. . . . .	80
59.	Metallographic section of above casting . . . . .	80
60.	Microstructure of casting shown in Figure 58. The light phase was identified as $UFe_2$ and the dark phase is believed to be $U_6Fe$ . . . . .	81

# THE EBR-I MELTDOWN - PHYSICAL AND METALLURGICAL CHANGES IN THE CORE

by

J. H. Kittel, M. Novick and R. F. Buchanan

## ABSTRACT

As a result of the partial meltdown which occurred in EBR-I on November 29, 1955, it was necessary to remove the core assembly from the reactor and to separate the enriched fuel section from upper and lower unenriched blanket sections. A temporary cave was constructed on top of the reactor in order to remove the core assembly, and at this time about one-fourth of the fuel elements were removed. In order to perform further disassembly operations under less hazardous conditions, the core assembly was shipped from the Idaho Division of Argonne National Laboratory, at the National Reactor Testing Station, to the Lemont, Illinois, site of the Laboratory, where disassembly was completed in a protective atmosphere. It was found that approximately 40 to 50% of the core had melted and reached temperatures ranging between approximately 850°C and 1400°C, and that the molten portion had separated into three clearly defined zones characterized by different porosities. Densities of the zones ranged from 2.5 to 15.4 gm/cm<sup>3</sup>, depending upon the degree of porosity. It was also found that molten fuel alloy had traveled upward 5 inches and downward 3 inches between the blanket rods. Chemical and mass spectrographic analyses indicated that relatively little mixing occurred in the core during the period in which it was molten, that the fuel alloy which penetrated the blanket sections originated primarily from the outer part of the molten zone, and that the blanket did not enter the molten phase. Observations during disassembly of the core and subsequent simulated meltdown experiments indicated that the porous structure which formed in the molten core could have resulted from the vaporization of entrained NaK.

## INTRODUCTION

EBR-I (Experimental Breeder Reactor No. 1) is a NaK-cooled, solid-fuel fast reactor built to determine and investigate factors which are important to the development of a fast breeder system. The reactor, which is shown in cross section in Figure 1 and which has been described in detail

previously,<sup>(1)</sup> was designed and built by Argonne National Laboratory and put into operation by the Laboratory at the National Reactor Testing Station in Idaho in 1951 with a core of enriched unalloyed uranium. The fuel slugs had been prepared by rolling at 300°C, followed by quenching from the beta phase, a procedure which had been shown to greatly reduce the dimensional instability which uranium displays when subjected to irradiation.<sup>(2)</sup> This first core produced over  $3 \times 10^6$  kilowatt-hours of heat.

During the period of time when the reactor was operating with its first loading, experiments at Argonne National Laboratory showed that castings of uranium - 2 w/o zirconium alloy were capable of much better performance under irradiation than beta-quenched unalloyed uranium.<sup>(3)</sup> Fuel specimens made of the uranium-zirconium alloy were not only more resistant to irradiation growth, but also were free of the irradiation-induced surface roughening which characterizes beta-quenched uranium.<sup>(4)</sup> Accordingly, in the early part of 1954, a second core was installed which had been fabricated by centrifugally casting uranium - 2 w/o zirconium alloy for both fuel and blanket slugs.<sup>(5)</sup> At this time certain other changes were also made in the design of the stainless steel jackets which contained the fuel slugs.

Figure 2 shows a drawing of a typical fuel element used in the second loading. The fuel section was made up of two  $4\frac{1}{4}$  in. long bare slugs, 93.21% enriched, which were separated by a 0.005-in. thick stainless steel spacer. The lower blanket slug, also  $4\frac{1}{4}$  in. long, was made of unenriched uranium and was encased in a drawn-on stainless steel jacket. The upper blanket section, also of unenriched uranium, consisted of two  $3\frac{3}{4}$ -in. long slugs encased in a single drawn-on stainless steel jacket. The fuel slugs were separated from the jacketed blanket slugs by 0.005-in. thick stainless steel spacers. The diameter of the jacketed blanket slugs and the bare fuel slugs was 0.384 in. Surrounding these slugs was a 0.012-in. thick NaK annulus and a stainless steel outer jacket with a 0.021-in. wall. As mentioned previously, both the fuel and blanket slugs were made of centrifugally cast uranium - 2 w/o zirconium alloy. As can be seen from Figure 2, numerous possible contacts are present for uranium and stainless steel to interdiffuse. When the EBR-I was in its initial design stages, in 1947 and 1948, a study was made of the diffusion problems in this reactor.<sup>(6)</sup> It was found that uranium and stainless steel were among the two elements which diffused into each other most rapidly, and Figure 3 shows a typical diffusion zone between uranium and stainless steel which developed after six days at 700°C. Diffusion zones also formed at temperatures as low as 500°C, although at a slower rate.

An additional consideration presented by the close proximity of the stainless steel is the fact that the uranium forms low-melting eutectics with the three main constituents in stainless steel, namely, iron, nickel and chromium. These eutectics melt at temperatures from 270° to 400°C lower

than the melting point of unalloyed uranium. It was anticipated, therefore, that should any serious overheating occur in the reactor a eutectic would very likely form between the uranium fuel slugs and the jackets in which they were contained. However, the economic advantage of using stainless steel was such that the reactor was constructed of this alloy, and a special heat of Type 347 alloy was made for this purpose.<sup>(7)</sup>

Although the second core performed quite satisfactorily with regard to dimensional stability of the fuel and blanket slugs under irradiation, an increased positive reactivity temperature coefficient was noted. The possible origins of the increased coefficient were subsequently investigated by operating the reactor with various core temperatures, amounts of excess reactivity, etc. On November 29, 1955, experiments at high core temperature and with a short reactor period culminated in a partial meltdown of the fuel. The circumstances surrounding the experiment, which resulted in damage to the core assembly, and an analysis of the incident itself have been described elsewhere<sup>(8,9)</sup> and will not be repeated here.

This report describes the procedure by which the damaged core assembly was removed from the reactor early in 1956 and how, a few months later, the fuel section was disassembled from its upper and lower blanket. The description is given in some detail to aid as much as possible others who might be confronted with a similar operation. The primary purpose of the report, however, is to describe the physical and metallurgical changes which were noted in the core as disassembly proceeded.

## REMOVAL OF THE CORE FROM THE REACTOR

Following the incident and after a reasonable decay time, an attempt was made to remove the blanket and core elements from the reactor. All of the outer blanket rods were removed in the conventional manner by withdrawing them into the transfer coffin above the reactor tank. There was no difficulty and no indication of any damage was noticed.

The next step involved removing the rods from the core. Corner elements which contained blanket material again came free with no evidence of overheating. However, when it was attempted to remove the rods containing fuel from the outer rows of the lattice, considerable force was required, and damage to the jackets was observed. It was then decided to lift the core out as a complete unit and disassemble it outside the reactor tank. Fortunately, it has been anticipated in the original design of the reactor that situations could arise where fuel elements might become too distorted for normal removal, so the reactor was designed in such a way that the entire core assembly could be lifted out of the tank and thus be accessible from all sides.

Since the expended core was very radioactive, it was realized that it would be necessary to work through a shield wall with the assembly in a cell with controlled ventilation. Therefore, it was decided to build this temporary cave above the reactor tank on the permanent shield top.

Measurements of the core activity indicated that 30-in. thick walls would be sufficient for limited access time. Since portable shield blocks from the Borax-III reactor would become available during the unloading of fuel elements from that reactor for reprocessing, it was decided to wait for them in the construction of this cell. The blocks measured 60 in. x 30 in. x 15 in. and were readily handled by means of the building overhead crane.

The front face was constructed of standard concrete building blocks and included two 18-in. square by 36-in. thick shield windows. Access holes were provided in the front face to line up with disassembly points on the core. Two Model 8 master-slave manipulators were installed to allow remote operations. The windows were borrowed from an existing facility at EBR-I, and the manipulators were borrowed from a cave at the Lemont, Illinois, site of Argonne National Laboratory. Inside dimensions of the cell measured 14 ft long by 5 ft wide by 12 ft high with 30-in. thick walls and a 36-in. thick face.

A bracket consisting of a frame work of 6-in. I beams was constructed to support the assembly during the cutting operation in the cave, and the top of the cell was closed with 1-in. thick steel plate.

Figure 4 shows the construction prior to the building of the front face. Steel pans were placed on the floor of the cave and at a position immediately under the location the core would occupy when it was supported by the steel structure. Sodium lights were borrowed from one of the hot cells in EBR and installed. The completed cave appears in Figure 5.

The ventilation system consisted of two type 25 Fg media pre-filters, two 24 in. x 24 in. CWS absolute filters in parallel and a 3700-cfm centrifugal fan. This fan was one which normally served in the emergency reactor cooling system. Its discharge was piped to the exhaust stack on the EBR building.

#### INITIAL CORE DISASSEMBLY

When the cave was completed and the necessary tools had been constructed, the initial disassembly operation was begun. The first step involved the removal of as much as possible of the NaK coolant which was trapped in the reactor tank. This was accomplished by drawing it up into a portable tank to which a vacuum had been applied. The second step was the lifting of the assembly out of the tank by means of the building crane and placing it on the support stand provided in the cave.

Figure 6 shows the appearance of the core assembly after the remaining NaK had been allowed to oxidize. Before the core rods were accessible, the bottom plate and the hexagonal separator, shown in this figure, had to be removed. Bottom nuts were unscrewed by means of special wrenches through which torque could be applied from the outside of the cave. The bottom plate was removed with little difficulty, as shown in Figure 7.

At this point the hexagonal separator which enclosed the fuel section should have slipped off easily. However, it proved to be held tightly to the core and had to be cut off. This was accomplished by drilling a vertical row of holes down one corner, as shown in Figure 8, and splitting it open. When this was done the separator came off easily.

Subsequently, at the Lemont site of the Laboratory, the hexagonal separator was split down each corner to provide specimen material for determination of the effects of irradiation on the mechanical properties of the stainless steel. Figure 9 shows a photograph of the six interior faces of the separator, and it can be noted that the material formed during the temperature excursion had alloyed superficially with the separator in certain areas, particularly on sides 2, 4, and 6.

The appearance of the damaged core after removal of the hexagonal separator is shown in Figure 10. The molten core alloy was found to have extruded into the coolant channels and to have finally solidified into a mass surrounding the fuel section and molded into shape by the separator can. The solidified material was heavily covered with oxides of NaK.

The process of removing individual rods was then undertaken. This was done by cutting them off at the by-pass section immediately below the lowest plate of the assembly, using saber saws. These were operated through access holes in the front face of the shield. As each rod was cut off it was placed in a prepared thimble in a coffin which had been located in the cave. This was then lifted out, and the thimble and rod were transferred to the regular rod storage area. Using this method, the entire outer row and part of the second row were removed. Several of these fuel elements were sent to the Lemont site of the Laboratory where they were disassembled and examined.

Typical fuel rods from this group are shown in Figures 11 and 12. Although the outer jackets were damaged on most of the fuel elements in the outer row, as shown in Figure 11, it was evident that any jacket melting resulted from external causes, rather than from the fuel slugs which they contained. This is clearly shown in Figure 13, in which can be seen an undamaged stainless steel spacer between fuel slugs contained in an outer jacket which had been subjected to melting damage. Had these particular slugs overheated, the spacer, being at the center of the fuel section, would have formed a eutectic before any jacket damage occurred.

Additional evidence that the fuel in the outer row of elements did not participate in the molten phase is shown in Figure 14. Here, the damaged jacket shown in Figure 13 has been peeled back to expose one of the fuel slugs, and it can be noted that the surface of the slug and the interior surface of the stainless steel jacket have not been affected by the meltdown. For the outer row of fuel elements, therefore, it appears that the fuel temperature did not exceed about 850° to 950°C, which have been reported<sup>(10)</sup> to be the lowest temperatures at which uranium and stainless steel form a liquid phase for short heating periods.

The appearance of the core assembly after removal of the outer fuel elements is shown in Figure 15. It is evident that severe melting damage had occurred in the fuel section, which had slumped somewhat so that the lower half was tightly packed with solidified material. The upper half, on the other hand, contained numerous cavities. Evidently many of the jackets, after forming a molten phase with the fuel slugs they contained, sloughed off and left the partially dissolved fuel still more or less in place. It was subsequently learned during final disassembly that the partially dissolved fuel still in position was confined generally to the second row of fuel elements, i.e., the row next to the outermost row. Moving inwardly from the second row, damage was more extensive.

After the core assembly had been reduced to the 153 fuel elements shown in Figure 15, it was apparent that the facilities at the reactor site were not adequate for further operations to be conducted in a safe manner. The pyrophoric nature of the damaged core presented a serious fire hazard, a condition which was further aggravated by the presence of large amounts of entrained NaK. After several small NaK fires were observed in debris resulting from removal of the outer fuel elements, it was decided to stop further disassembly operations at the Idaho site and to ship the core assembly to the Lemont site of the Laboratory, where more complete hot laboratory facilities existed and where disassembly could be completed in an inert atmosphere. Accordingly, as shown in Figure 16, a stainless steel thimble was pulled up and supported around the assembly, leaving the upper part of the rods visible. Argon gas was allowed to fill the thimble to prevent fire. Saber saws were again used to cut through the entire assembly below the bottom plate, and all remaining fuel elements were sawed through, permitting the assembly to drop into the thimble as shown in Figure 17.

Although one-fourth of the 52 kilograms of  $U^{235}$  originally present in the reactor had been removed, the remaining 39 kilograms, fused into an assembly of small volume and well-reflected from top and bottom, presented a shipping problem because of the hazard of accidental criticality, a condition which now had to be considered in addition to the pyrophoric hazard mentioned above. In order to ship the core assembly under safe conditions the assembly shown in Figure 18 was constructed. It consisted of a container just large enough to hold the thimble and core assembly

shown in Figure 17. The flange closure was completed with a flexitallic gasket so that an inert atmosphere, once placed in the container to prevent fires, could be maintained indefinitely after the flange was bolted down. The container was surrounded by a cage which physically prevented any reflecting surface, including the shipping cask, from approaching the container within less than 10 inches. The shipping cask, which is shown in Figure 19, was made with 4-in. thick lead walls and with interior dimensions just large enough to accommodate the cage assembly. The outer edge of the shipping cask lid was gasketed with neoprene and tightly bolted to prevent entry of liquids. The shipping cask, which weighed 10,800 lb, had an external diameter of 40 in. and stood 43 in. high. As an additional safety measure, using a neutron source, multiplication measurements were made during the loading of the core assembly into the shipping cask.

### FINAL CORE DISASSEMBLY

A cave capable of containing 10,000 curies of 1-Mev gamma activity was made available for final disassembly of core at ANL. This cave has been described elsewhere.<sup>(11)</sup> Although the cave was not designed for gas-tight operation, it was apparent that the final disassembly operations had to be conducted in an atmosphere of low oxygen content. Accordingly, the Model 6 manipulators with which the cave was equipped were removed and Model 8 manipulators, booted for minimum air in-leakage,<sup>(12)</sup> were installed. All ports and other openings into the cave were taped shut or gasketed as required. A trial run, with a negative pressure in the cave of 0.05 in. water, showed approximately 1-cfm in-leakage of air.

It was hoped that operations could be conducted in an atmosphere containing as much as 2% oxygen. This amounted to a ten-fold dilution of air leaking into the cave, so that approximately 10 cfm of inert gas would be required while operations were in progress. Possible inert gases narrowed to a choice between argon, helium, and dry nitrogen. The above rate of gas flow, coupled with the amount required to purge the cave at the start of each day's operations, ruled out the use of relatively expensive argon. Helium appeared attractive because its high thermal conductivity would help quench incipient fires. However, supply problems arose because of the remoteness of a rail siding, and delivery by truck of adequate amounts of helium could not be established. This left only nitrogen, which fortunately is available with a dew-point of  $-70^{\circ}\text{F}$  in large quantities and at low cost in the Chicago area. Although uranium is not inert in nitrogen,<sup>(13)</sup> the reaction rate is substantially less than in air. A piping system was then installed to run nitrogen through a flowmeter and into the cave from loaded trailers delivered by the commercial supplier. Equipment was installed in the cave to measure and record oxygen content and to measure humidity. Subsequently, after disassembly operations had begun, it was found that metal fires were still occurring with the cave atmosphere at 2% oxygen.

The nitrogen flow rate was therefore increased to 20 cfm to maintain the oxygen level between 1 and 1.5%. With the increased flow rate the relative humidity of the cave atmosphere ranged from 1.6 to 2.1%.

Instruments were also installed to continuously measure in the cave with portable probes gamma-ray and neutron-radiation intensities, temperature, and air-borne particulate activity. Figure 20 shows some of the instrumentation outside the cave. A number of special tools were placed in the left area of the cave for disassembly operations, as shown in Figure 21. The tools included an electric impact chisel, hydraulically operated equipment including a chisel, pipe cutter, and vise, and grappling tools to handle the core assembly which weighed approximately 250 lb. In order to protect the cave window from flying fragments of metal, a safety-glass window was installed at the front of the area.

It was decided to seal the fuel pieces, after they were separated from the unenriched blanket, into cans containing approximately 1 kilogram of material. For this purpose a Mettler type K-5 balance reading directly to 2000 grams was installed in the right area of the cave, along with a remotely operated can sealer and about 100 cans, approximately 3 in. in diameter and 2 in. high. Figure 22 shows an over-all view of this area of the cave. Views of the method by which the fuel cans were loaded and the can sealer are shown in Figures 23 and 24. As shown in Figure 22, this area of the cave was separated from the disassembly area by a partition approximately two feet high. It was subsequently found that each fuel can, when loaded and sealed, showed a gamma activity at one-inch distance of about 100 r/hr. Larger cans, 3 in. in diameter and 10 in. high, were used for containment of blanket material. Loading of typical blanket material is shown in Figure 25.

The criticality hazard was handled by arranging bench tops so that the core could not be reflected by more than one adjacent surface (in addition to the attached upper and lower blanket sections). The cage in which the core was shipped was installed in the cave as shown in Figure 21, both to help with the avoidance of criticality and to provide a fire-safe vault for overnight storage. Finally, hydrogenous material was also excluded from the cave because of criticality considerations. The only exceptions were hydraulic oil lines which were installed so that in the event of leakage they could not empty into the cave by gravity.

After the cage assembly was placed in the cave and the protective atmosphere established, the container in which the core assembly had been shipped was opened. The appearance of the top of the core assembly is shown in Figure 26. It was found that most of the fuel elements could be broken off near the junction between the upper blanket and the fuel section. Accordingly, the upper parts of most of the fuel elements were removed individually, without removing the fuel section and lower blanket from the thimble and cage assembly in which they were placed at the Idaho site.

Since one of the main purposes of disassembly was to separate and recover the enriched fuel, each upper rod section, after being removed from the cage assembly, was parted so as to separate any remaining fuel from the blanket. A few rods were removed from the outer row which were relatively undamaged, and the fuel and blanket sections in these rods were separated by cutting with the remotely operated pipe cutter through the outer jacket near the junction of fuel and blanket, as shown in Figure 27. The remaining rods were too badly damaged for this operation, however, so they were cut with the hydraulic chisel. All cuts with the chisel were made about one-half inch above the junction of fuel and blanket to ensure that all enriched material was removed from the blanket scrap. Separation of fuel and blanket material was verified by means of radiation measurements.

During removal of the upper blanket section, it was observed that considerable amounts of molten fuel had penetrated into the coolant passages between the outer jackets of the upper blanket. A clump of upper blanket rods near the center is shown in Figure 28, and it can be noted that the maximum upward travel was approximately five inches. This material was easily detached from the stainless steel jackets and, as shown in Figure 29, no evidence of melting damage was observed, as was the case in the jackets of the outer fuel section shown in Figure 13. Furthermore, as nearly as could be determined by observation, no evidence could be seen of the unenriched blanket alloy slugs being damaged by melting.

The only upper fuel element sections which could not be detached from the remainder of the core assembly were three special rods, each of which contained chromel-alumel thermocouples. These wires, which were firmly embedded in the fuel section, were to prove invaluable in furnishing a convenient means of attaching the lifting crane in the cave to the balance of the core assembly, which was now estimated to weight approximately 150 lb.

By means of the thermocouple wires, the fuel section and lower blanket were then lifted from the cage assembly, as shown in Figure 30. The appearance of the core assembly at this stage is shown in Figure 31. A cut was then made with the impact chisel through the horizontal midplane of the fuel section (the  $1\frac{1}{2}$ -in. level in Figure 31). A photograph of the cross section thus obtained is shown in Figure 32. It was observed that two distinct sponge-like zones of porosity had formed, with a well-defined boundary between them containing white oxides of NaK. The inner zone was characterized by pores ranging up to about  $1/4$  in. in diameter, along with several larger cavities. The pores in the outer zone were much smaller, with a maximum size not exceeding about  $1/16$  in. Many of the freshly opened pores in each of the two zones were observed to contain NaK. The structure of the material in both zones showed no traces of the original fuel element components, so that alloying appeared to be complete. The material in both zones, particularly the center zone, was friable and easily

broken, and exhibited no traces of ductility. It was observed that the thermocouple wires mentioned above were intact and unalloyed with the solidified fuel alloy in which they were embedded. Although their braided glass insulation was gone, it apparently prevented contact and subsequent alloying between the molten phase and the wires. The fact that the wires were intact indicated that the center of the fuel section had not exceeded 1400°C, the approximate melting point of chromel and alumel.

Measurements of the radioactivity of the exposed cross section gave a reading of 700 r/hr at 1 in. A thermocouple probe was used to measure the temperature in voids near the center of the mass. A reading of 2°C above ambient was obtained.

The next part of the core assembly that was removed was about half of the lower blanket rods. As was the case with the upper blanket section, it was found that the lower blanket rods broke away from the fuel section, as shown in Figures 33 and 34. Also, as was the case in the upper blanket, the coolant passages in the lower blanket were filled with solidified material from the fuel section. It was noted that this material when freshly broken was black, but on standing for an hour or two became covered with white oxide. The material had moved downward between the outer jackets for varying distances depending upon the distance from the center of the reactor. The maximum downward travel was approximately three inches and occurred at the center of the reactor. The solidified material could easily be removed from the outer jackets of the lower blanket section, and, as shown in Figure 35, no melting damage was observed.

The half of the fuel section from which the lower blanket had been removed, shown projecting upward in Figures 33 and 34, was then split off to make a vertical cross section of the lower half of the core assembly, shown in Figure 36. The junction between fuel and lower blanket is at the  $6\frac{1}{4}$ -in. level of the adjoining scale. This section showed that the lower side of the coarse and fine sponge-like zones terminated abruptly and that the lower part of the fuel section consisted of a dense, relatively non-porous mass. This material could be fractured only with difficulty because it was tough and somewhat ductile. It was observed that this material evidently also contained entrapped finely dispersed NaK. When freshly broken it showed a bright silvery appearance, which turned dark within about a minute. Several hours later, if sufficient oxygen were present, the black product, which was perhaps nitrides or sub-oxides of NaK, was replaced with normal white oxide.

This dense zone was found to contain at least 12 or 15 partially dissolved fuel slugs which were jumbled together near the center line of the reactor. Although three fuel slugs can be seen in the photograph in Figure 36, the piece of material shown in Figure 37 shows more clearly the random manner in which the fuel slugs were embedded in the dense

material. Several fuel slugs which were separated from adjoining material are shown in Figure 38. All had a characteristic point on one end. It is probable that these fuel slugs originated from the upper fuel section and were held in place until much of the fuel alloy had entered the molten phase and dripped from the lower end, thus accounting for the point on one end. Several large voids were also found in the dense zone, as shown in Figure 39.

The remainder of the core disassembly was accomplished with no additional unusual features of interest being found.

Based on observations and measurements made on the core itself during disassembly and on photographs, an artist's reconstruction of a vertical section through the damaged core was made as shown in Figure 40. Also shown in the figure are what are considered to be the most reliable values of densities of the various areas. The greater density of the partially dissolved fuel slugs evidently permitted them to fall completely through the molten volume, and they finally came to rest at the bottom of the fuel section. It appeared that between 40 and 50% of the volume of the fuel section had entered a molten phase during the meltdown, and that the shape of the molten volume approximated that of a prolate spheroid.

#### METALLOGRAPHIC STUDIES

During disassembly operations at Argonne National Laboratory, the five representative samples shown in Figure 41 were removed for metallographic studies. The locations from which these samples were taken, as well as 27 chemical samples which will be discussed in the next section, are listed in Table I. Figures 42 and 43 show approximate locations in the core from which all samples were removed.

Prior to metallographic examination or chemical analysis, the density of each sample was measured by determination of weight loss in  $\text{CCl}_4$ . As expected, a wide range of densities was observed, depending upon the region of the core assembly from which samples were taken. It was realized, however, that density determinations by immersion would show fictitiously high values for the more porous materials because of the penetration of immersant into open pores. A material balance<sup>(14)</sup> made for the meltdown also showed that the porous zones could not be as dense as indicated by the immersion tests. By measuring the amount of matrix relative to voids in metallographic sections of the porous samples, shown in Figures 44 through 48, and assuming the density of the matrix to be  $15.4 \text{ gm/cm}^3$  (the average density shown by samples from the nonporous mass), bulk densities of the porous areas were obtained. The most reliable density values obtained for each of the zones in the damaged core have been summarized in Figure 40. If the larger cavities in the fuel section were taken into account, even lower densities than those indicated in that part of the core in Figure 40 would be obtained.

A few minutes after removal of porous samples from the protective cave atmosphere into air of normal composition and humidity, the samples were observed to begin exuding oxides of NaK, as shown in Figure 49. Since these oxides are highly deliquescent, considerable moisture collection also occurred, which then reacted intermittently with the entrapped NaK. Metallographic sections also became covered with NaK oxides soon after polishing was stopped.

Figures 50 through 54 show the microstructures present in the five metallographic samples. The samples were all characterized by a two-phase structure, which in some samples appeared to be near a eutectic composition. The two phases which formed the eutectic are believed to be analogous to  $UFe_2$  and  $U_6Fe$ , which form a eutectic in the U-Fe system.<sup>(15)</sup> The relative amounts of each phase present in the samples depended upon their original location in the core. Thus, samples 29 and 30 from the porous zones, shown in Figures 50 and 51, contained an excess of the " $UFe_2$ " phase, sample 31 from the material between the lower blanket rods, shown in Figure 52, appeared to be near the actual eutectic composition, and the dense samples 32 and 33, shown in Figures 53 and 54, contained large amounts of the " $U_6Fe$ " phase.

Results of microhardness tests using a Vickers diamond indenter and a 1-kg load are given in Table II. The solidified material formed during the meltdown was found to be significantly harder than the undissolved fuel specimen. The solidified material adhering to the undissolved fuel showed intermediate hardness readings.

## CHEMICAL AND MASS SPECTROGRAPHIC ANALYSES

As mentioned earlier, a total of 27 samples were removed from the damaged core for chemical analyses. Original locations of the samples are listed in Table I and shown in Figures 42 and 43. All samples were analyzed for iron and potassium, with results as shown in Table III. It was assumed that the nickel and chromium would be in the same proportion to the iron in the samples as they were in the original stainless steel, and that the sodium would be present in proportion to the potassium as it was in the original eutectic NaK. On this basis, the iron contents shown in Table III should be multiplied by 0.26 to obtain chromium content and by 0.19 to obtain nickel; similarly the potassium values should be multiplied by 0.28 to obtain sodium. It was generally noted that when all known and calculated metallic constituents were totaled, less than 100% composition was obtained. The discrepancy is believed to be due to oxide contamination which was observed on most of the samples.

The wide variations of iron content in the samples indicated that the core was far from being chemically homogeneous, even within areas of like structure and density. Evidently, even though alloying was apparently

complete, the amount of mixing was not sufficient to homogenize the alloy. Considering only the volumes of stainless steel and fuel alloy present in the core before meltdown, the theoretical composition of an alloy formed from the fuel section in the core would be 7.23% iron. Actually, the average analyzed composition in the melted-down section was 7.87% iron. The extra iron probably came from the jackets of outer fuel elements, such as that shown in Figure 13.

The potassium analyses confirm the observations made during disassembly and on metallographic specimens in that they show that the samples taken contained up to 35 volume percent NaK. Actually, this figure would be higher had a sampling technique been available which would have retained the NaK in surface pores in the samples.

As shown in Table III, some of the samples were selected for more complete analyses, including uranium, mass spectrographic analyses of the uranium and plutonium, and radiochemical analyses of  $Ce^{144}$  and  $Pu^{238}$ . The primary purpose of the more complete analyses was to provide information on the relative movement of the fuel alloy during the time it was molten.

For example, the ratio of  $Ce^{144}$  to uranium in a sample of irradiated fuel is a direct indication of the atom burnup in the sample, and since the radial and longitudinal fission distributions before meltdown were known in the core, it was hoped that  $Ce^{144}$  determinations in the damaged core would provide information as to the origin of material displaced from the fuel section into the blanket. It was found that the  $Ce^{144}$  content of the solidified material in the blanket sections and lower part of the core was lower than the average content at the center of the core. The results indicate, therefore, that the fuel material which entered the blanket probably originated from the outside of the fuel section. Furthermore, the higher content of  $Ce^{144}$  in the center of the fuel section compared to the outside indicates that little mixing occurred during the period when the fuel section was molten.

When the reactor melted down, 10.5 grams of plutonium in some experimental specimens were present in the fuel section in hole No. 58, approximately 1-3/4 in. from the center line. Since no trace of these specimens could be found during disassembly, it was assumed that they had entered the molten fuel alloy. As originally constituted, the plutonium in the samples contained 94.96%  $Pu^{239}$ , 4.73%  $Pu^{240}$ , 0.30%  $Pu^{241}$ , and 0.012%  $Pu^{242}$ . In contrast, the plutonium produced by neutron capture in the  $U^{238}$  in the fuel is essentially pure  $Pu^{239}$ .<sup>(16)</sup> Therefore, determination of the  $Pu^{240}$  relative to  $Pu^{239}$  in the chemical samples might also provide a means of tracing the movement of the molten fuel, as this ratio would originally have been highest in the vicinity of the experimental plutonium-bearing specimens.

It was found that the  $\text{Pu}^{240}$  content of the sample of fuel alloy which entered the lower blanket was less by a factor of 100 than that shown by the samples from the fuel section. A mass spectrographic analysis was not made on the sample from the upper blanket, due to insufficient material. The relative  $\text{Pu}^{240}$  content of the material at the bottom of the core was similar to that in the center. These results indicate that the fuel material which entered the lower blanket departed from the fuel section at an early stage in the meltdown, i.e., before the plutonium from the experimental specimens arrived at the bottom of the fuel section. In contradiction to the results described earlier from the  $\text{Ce}^{144}$  analyses, the fact that the relative  $\text{Pu}^{240}$  concentration was the same at the bottom of the fuel section as at the center indicates that some mixing did occur in the molten volume.

Corroboration of the results obtained by measurement of the ratio of  $\text{Pu}^{240}$  to  $\text{Pu}^{239}$  was obtained by radiochemical determination of  $\text{Pu}^{238}$ . Since this isotope would be formed primarily by an  $(n, 2n)$  reaction with  $\text{Pu}^{239}$ , the concentration of  $\text{Pu}^{238}$  would be proportional to the total amount of  $\text{Pu}^{239}$  present. Since the composition of the plutonium in any case would be predominantly  $\text{Pu}^{239}$ , the determination of  $\text{Pu}^{238}$ , which is relatively easy because of its high specific activity, furnishes a convenient method of determining relative concentrations of total plutonium. The  $\text{Pu}^{238}$  analyses showed that the concentration of plutonium was significantly higher in the fuel section as compared to material which entered the upper and lower blankets.

The mass spectrographic analyses of the uranium samples taken from the damaged region of the core verified earlier observations made during disassembly that the unenriched blanket had participated to a negligible extent in the meltdown. The mass spectrographic analyses of the uranium also enabled another determination of the relative movement of the molten fuel. The  $\text{U}^{235}$  depletion in this case served as a tracer, since the variation of this quantity as a function of position in the core was known before the meltdown. As might be predicted, measurements of  $\text{U}^{235}$  depletion in the samples corroborated the indications furnished by the  $\text{Ce}^{144}$  analyses and again showed that extensive mixing did not occur in the molten volume and that the fuel which entered the blanket regions originated from the outer part of the fuel section.

## SIMULATED MELTDOWN EXPERIMENTS

The origin of the porous structure in the center of the damaged core could not be definitely established with any of the measurements or analyses made upon the material. Two explanations for the porous structure which gained widest acceptance were (1) release of fission gas, and (2) vaporization of NaK entrained in the molten fuel. Calculations indicated

that, if a temperature of 1200° C were assumed to have developed during the meltdown, the latter mechanism would produce far more gas than could be obtained even with complete fission gas release. Also, as mentioned earlier, it had been observed that many of the pores in the solidified material were filled with NaK. To investigate the NaK mechanism more completely, two experiments were performed in which an alloy similar to the composition of the solidified fuel in the damaged core was poured into NaK.(17)

In the first experiment, an alloy of uranium - 2 w/o zirconium alloy and stainless steel with final composition similar to that resulting from the meltdown was prepared and was observed to melt near 860° C. A charge of 176 grams of this alloy, just above the melting point, was poured into NaK at 400° C in a  $1\frac{7}{8}$ -in. diameter mold. A casting with a small amount of porosity was obtained with a density of 16.0 gm/cm<sup>3</sup>. Figures 55 through 57 show the porosity and microstructure which was obtained. It can be noted that the microstructure of this casting, shown in Figure 57, is not unlike that shown in Figure 54, which is the microstructure of a sample taken from the densest zone in the damaged core.

In the second experiment, an attempt was made to increase the porosity of the casting by reducing the mold diameter to 1/2 in. and by using the more fluid eutectic alloy, uranium - 12 w/o iron. In this experiment a porous mass was obtained, similar in certain respects to the structure observed in the actual meltdown. The density of the second casting was measured to be 13.9 gm/cm<sup>3</sup> by immersion in CCl<sub>4</sub> and 10.6 gm/cm<sup>3</sup> by metallographic sectioning and measurement. The porosity in this casting and the microstructure of the material are shown in Figures 58 through 60. The microstructure of this casting, shown in Figure 60, shows some similarities to that observed in samples from the porous zones of the meltdown, shown in Figures 50 and 51.

On the basis of the above experiments, plus observations made during disassembly, it is believed that the porosity which developed in the damaged EBR-I core could have resulted from vaporization of NaK entrained in the molten fuel alloy and subsequent expansion of the vapor.

## CONCLUSIONS

1. As a result of the temperature excursion on November 29, 1955, approximately 40 to 50% of the fuel section of EBR-I melted and reached temperatures from a minimum of approximately 850° C to a maximum of less than 1400° C.

2. The molten zone consisted of a central column of coarse porosity surrounded at the sides and top by a zone of finer porosity. Underlying both porous areas was a relatively dense mass of material in which was embedded a number of partially dissolved fuel slugs.

3. Although the upper and lower blanket rods were surrounded with molten fuel alloy which was ejected from the fuel section, neither the blanket slugs nor the jackets in which they were contained entered the molten phase.

4. Relatively little mixing apparently occurred in the fuel section during the period in which it was molten, and the molten fuel alloy which entered the blanket sections appeared to have originated primarily from the outer part of the molten zone.

5. Observations during disassembly of the core and subsequent simulated meltdown experiments indicated that the porous structure which formed in the molten core could have resulted from the vaporization of entrained NaK.

#### ACKNOWLEDGMENTS

So many persons at both the Idaho and Lemont sites of Argonne National Laboratory assisted in the disassembly and analytical studies of the damaged reactor that space limitations do not permit individual mention of those who helped. Almost the entire Idaho Division participated in the removal of the core from the reactor and its initial disassembly. The final disassembly at the Lemont site was done by the Metallurgy Division and the Remote Control Division with assistance from the Reactor Engineering Division. Continuous motion picture and still photographic coverage of this phase of the operation was supplied by the Graphic Arts Department. The Metallurgy Division was responsible for the metallographic examinations and simulated meltdown experiments. Chemical and mass spectrographic analyses were performed by the Chemistry Division, assisted by the Special Materials Division.

## REFERENCES

1. H. V. Lichtenberger, F. W. Thalgott, W. Y. Kato, and M. Novick, Operating Experience and Experimental Results Obtained from a NaK-Cooled Fast Reactor, Proc. Int. Conf. on the Peaceful Uses of Atomic Energy, (United Nations, New York, 1955), Vol. 3, pp 345-360.
2. S. H. Paine and J. H. Kittel, Irradiation Effects in Uranium and Its Alloys Proc. Int. Conf. on the Peaceful Uses of Atomic Energy (United Nations, New York 1955), Vol. 7, pp. 445-454. Also published in Problems in Nuclear Engineering, edited by D. J. Hughes, S. McLain, and C. Williams, 1, 107-117, (Pergamon Press, New York, 1957).
3. J. H. Kittel, S. H. Paine and H. H. Chiswik, Effect of Heat Treatment on Irradiation-Induced Dimensional Changes in Some Uranium-Zirconium Alloys, ASTM Symposium on Radiation Effects on Materials (September 1956).
4. J. H. Kittel and S. H. Paine, Effects of High Burnup on Natural Uranium, ANL-5539(May 1957).
5. F. L. Yaggee, The Manufacture of Centrifugally Cast Reactor Fuel Slugs, Mark II Fuel Loading for EBR-I, ANL-5724 (to be published).
6. J. H. Kittel, Layer Formation by Interdiffusion Between Some Reactor Construction Metals, ANL-4937 (June 1949).
7. R. A. Noland and D. E. Walker, Special Heat of Austenitic Stainless Steel Used in the Experimental Breeder Reactor (EBR-I), ANL-5548 (October 1956).
8. W. H. Zinn, A Letter on EBR-I Fuel Meltdown, Nucleonics, 14, No. 6, 35 (1956).
9. R. O. Brittan, The EBR-I Meltdown - Analysis of the Incident, ANL-5756 (to be published).
10. A. B. McIntosh and K. Q. Bagley, Selection of Canning Materials for Reactors Cooled by Sodium/Potassium and Carbon Dioxide, Inst. Metals, 84, 259 (1956).
11. E. W. Rylander and R. A. Blomgren, Operating Procedures of a Hot Lab for Solid-State Tests, Nucleonics, 12, No. 11, 98-100 (1954).
12. R. B. Wehrle, Booting Assembly for the Model 8 Master-Slave Manipulator, Proc. Fifth Hot Laboratories and Equipment Conf. (March 1957), to be published.

13. I. Hartmann, J. Nagy, and M. Jacobson, Explosive Characteristics of Titanium, Zirconium, Thorium, Uranium and Their Hydrides, U. S. Bureau of Mines Report on Investigation 4835 (December 1951).
14. A. Fenstermacher, Private Communication, Argonne National Laboratory (April 11, 1957).
15. H. A. Saller and F. A. Rough, Compilation of U. S. and U. K. Uranium and Thorium Equilibrium Diagrams, BMI-1000, 35 (1955).
16. M. Levenson, Determination of the Conversion Ratio of the Experimental Breeder Reactor by Radiochemical Methods, ANL-5095 (1953).
17. N. J. Carson, Private Communication, Argonne National Laboratory (March 21, 1957).

Table I

LOCATION OF AREAS IN WHICH METALLOGRAPHIC AND CHEMICAL SAMPLES  
WERE TAKEN (SEE ALSO FIGURES 42 AND 43)

Sample No.	Location
1	Coarse Sponge
3	Same
6	Same
18	Same
26	Same
29	Coarse Sponge
4	Junction Between Coarse and Fine Sponge
17	Fine Sponge
19	Same
21	Same
27	Same
30	Same
5	Solidified Material Near Outer Row of Fuel Elements, Near Midplane of Fuel Section
7	Same
8	Solidified Material Near Outer Row of Fuel Elements, Near Bottom of Fuel Section
10	Same
11	Solidified Material on Outside of Lower Blanket Jackets, Just Under Fuel Section
12	Same
15	Same
14	Same, Further Down
24	Same
25	Same
31	Same
9	Same, Near Limit of Downward Travel
13	Same
36	Solidified Material on Outside of Upper Blanket Jacket
20	Non-Porous Mass at Bottom of Fuel Section
23	Same
33	Same
22	Same, Plus Some Partially Dissolved Fuel
32	Same
28	Partially Dissolved Fuel Slug

Table II

MICROHARDNESS VALUES OBTAINED ON SAMPLES FROM EBR-I CORE.  
FIVE DETERMINATIONS WERE MADE ON EACH SPECIMEN, USING A  
1-KG LOAD AND A VICKERS DIAMOND INDENTER.

Sample No.	Hardness, DPH	Standard Deviation	Sample No.	Hardness, DPH	Standard Deviation
29	431	±33	32 (fuel)	301	±12
30	446	±15	32 (adjoining material)	384	±15
31	456	±25	33	444	±25

Table III

CHEMICAL AND MASS SPECTROGRAPHIC ANALYSES OF SAMPLES FROM DAMAGED CORE ASSEMBLY  
SEE TABLE I AND FIGURES 42 AND 43 FOR LOCATIONS FROM WHICH SAMPLES WERE TAKEN

Sample No.	K, %	Fe, %	U, %	Ce <sup>144</sup> cpm/mg U <sup>(a)</sup>	% of Uranium Present				Pu <sup>238</sup> <sup>(b)</sup>	% of Plutonium Present			
					U <sup>234</sup>	U <sup>235</sup>	U <sup>236</sup>	U <sup>238</sup>		Pu <sup>239</sup>	Pu <sup>240</sup>	Pu <sup>241</sup>	Pu <sup>242</sup>
1	1.7	6.98	74.7	1.2 x 10 <sup>6</sup>	1.14	92.55	0.244	5.97	2.09				
3	0.53	8.26	83.8	8.9 x 10 <sup>6</sup>	1.13	92.57	0.246	6.03	2.14	95.06	4.67	0.253	0.015
4	0.60	8.62											
5	0.24	7.21	88.5		1.14	92.92	0.252	5.67					
6	0.74	6.75											
7	0.03	9.47											
8	0.02	10.47											
9	0.13	8.96											
10	0.52	8.06											
11	0.50	8.06											
12	0.59	9.68											
13	0.43	8.44	82.9	3.9 x 10 <sup>6</sup>	1.15	93.15	0.256	5.42	0.48	99.9	0.04		
14	0.75	7.34											
15	0.29	9.58											
17	0.34	6.90											
18	<0.02	8.57											
19	0.12	14.25											
20	0.017	7.55	73.0	1.5 x 10 <sup>6</sup>	1.15	92.67	0.243	5.92	2.01	95.10	4.63	0.262	
21	0.22	8.05											
22	<0.02	8.39											
23	0.07	6.71											
24	1.2	6.63											
25	0.1	5.04											
26	0.02	7.30											
27	0.02	8.98											
28	<0.02	0.50			1.12	92.88	0.235	5.75					
36	0.065	3.01	90.2	2.2 x 10 <sup>6</sup>	1.16	92.71	0.245	5.72	0.51				

(a) Counting date: March 21, 1957.

(b) Reported as per cent alpha activity with Am<sup>241</sup> removed.

Figure 1. Horizontal cross section of EBR-I at the reactor midplane.  
 (Dimensions are given in inches.)

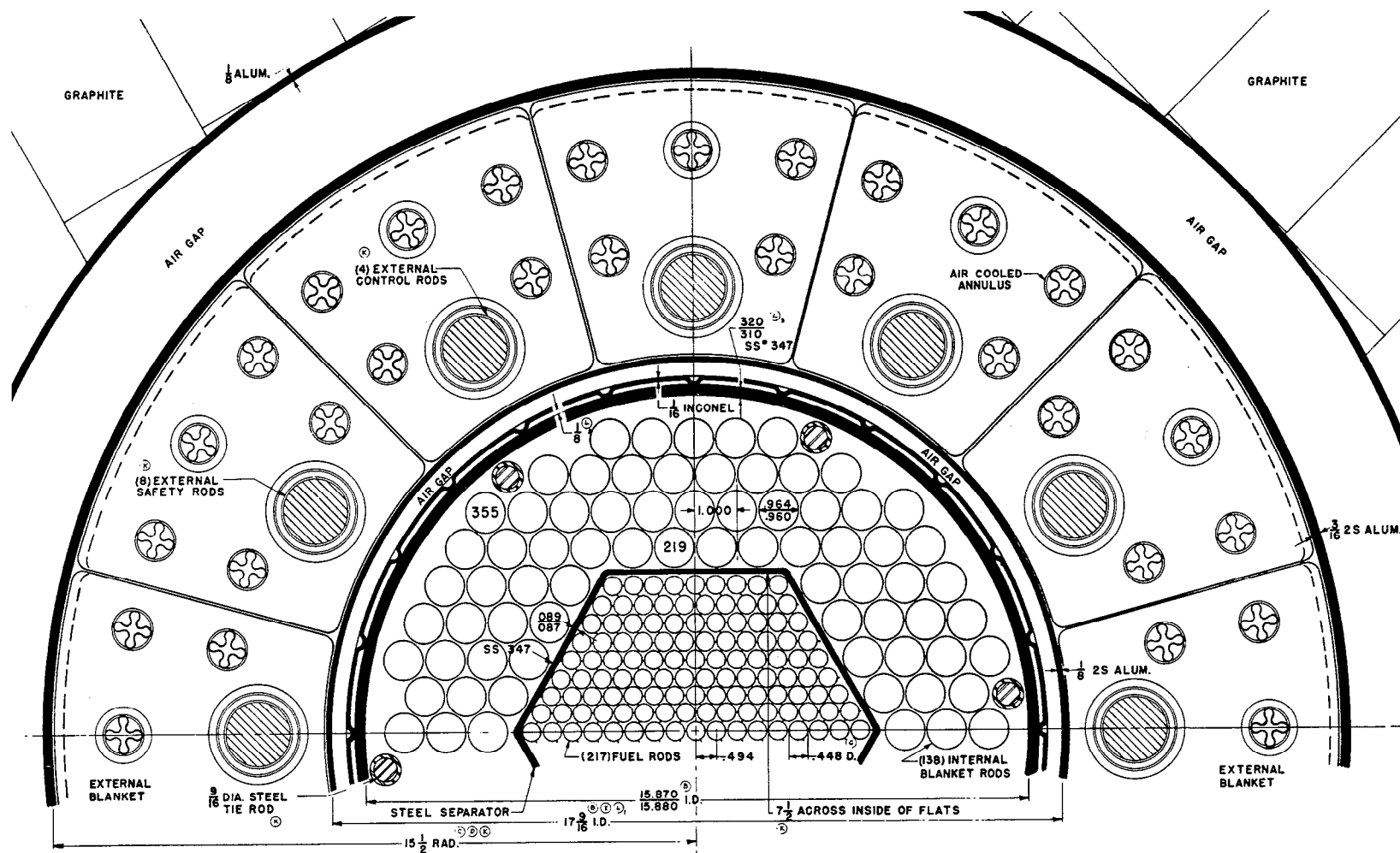
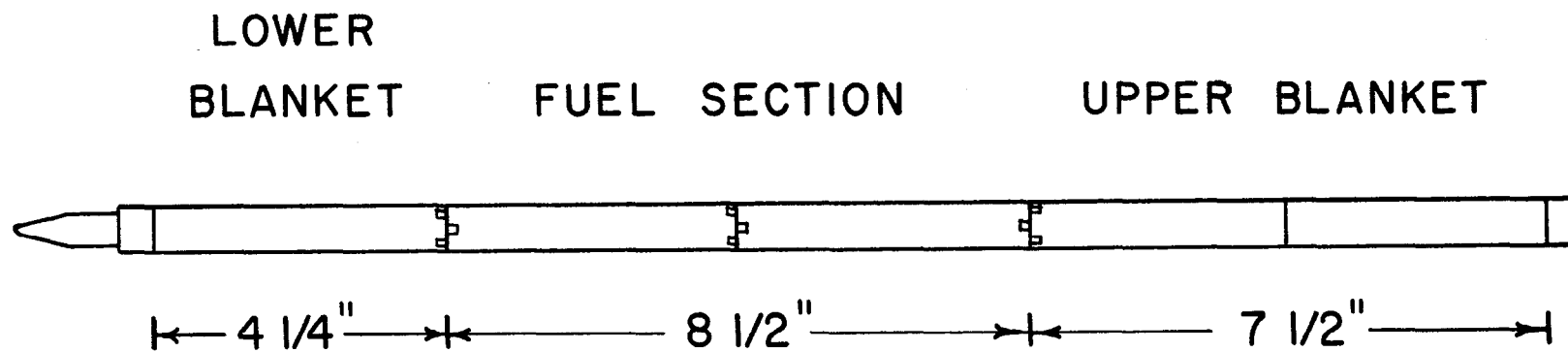
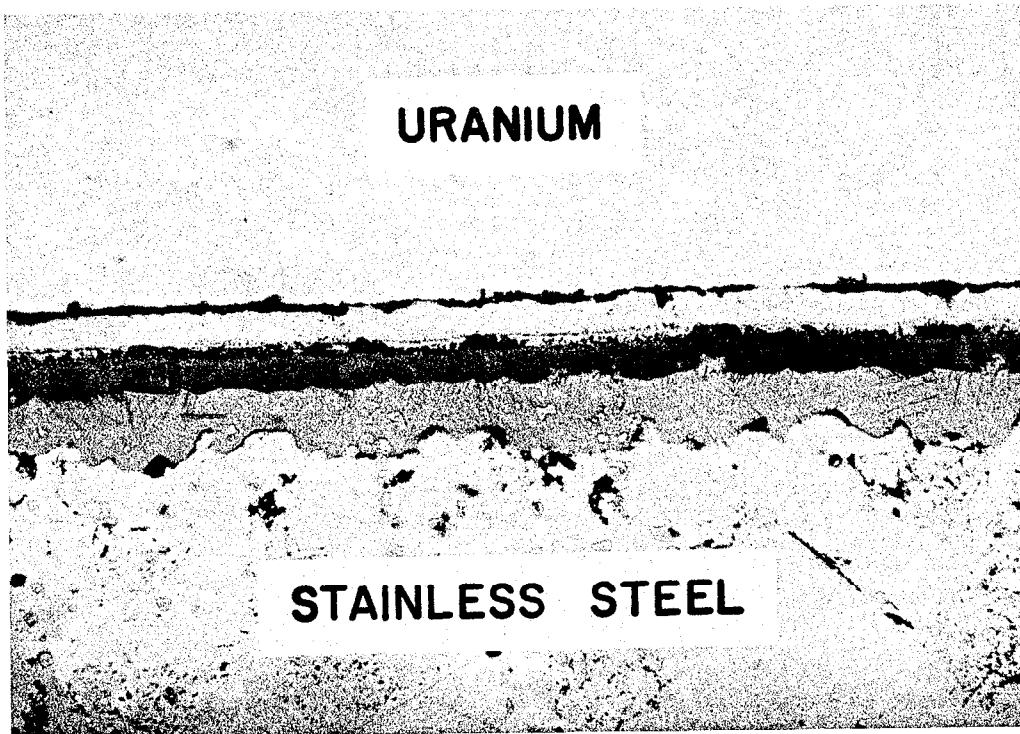


Figure 2. Simplified drawing of a typical fuel element from the EBR-I second loading. The diameter of the assembled fuel element is 0.45 in.



106-3230

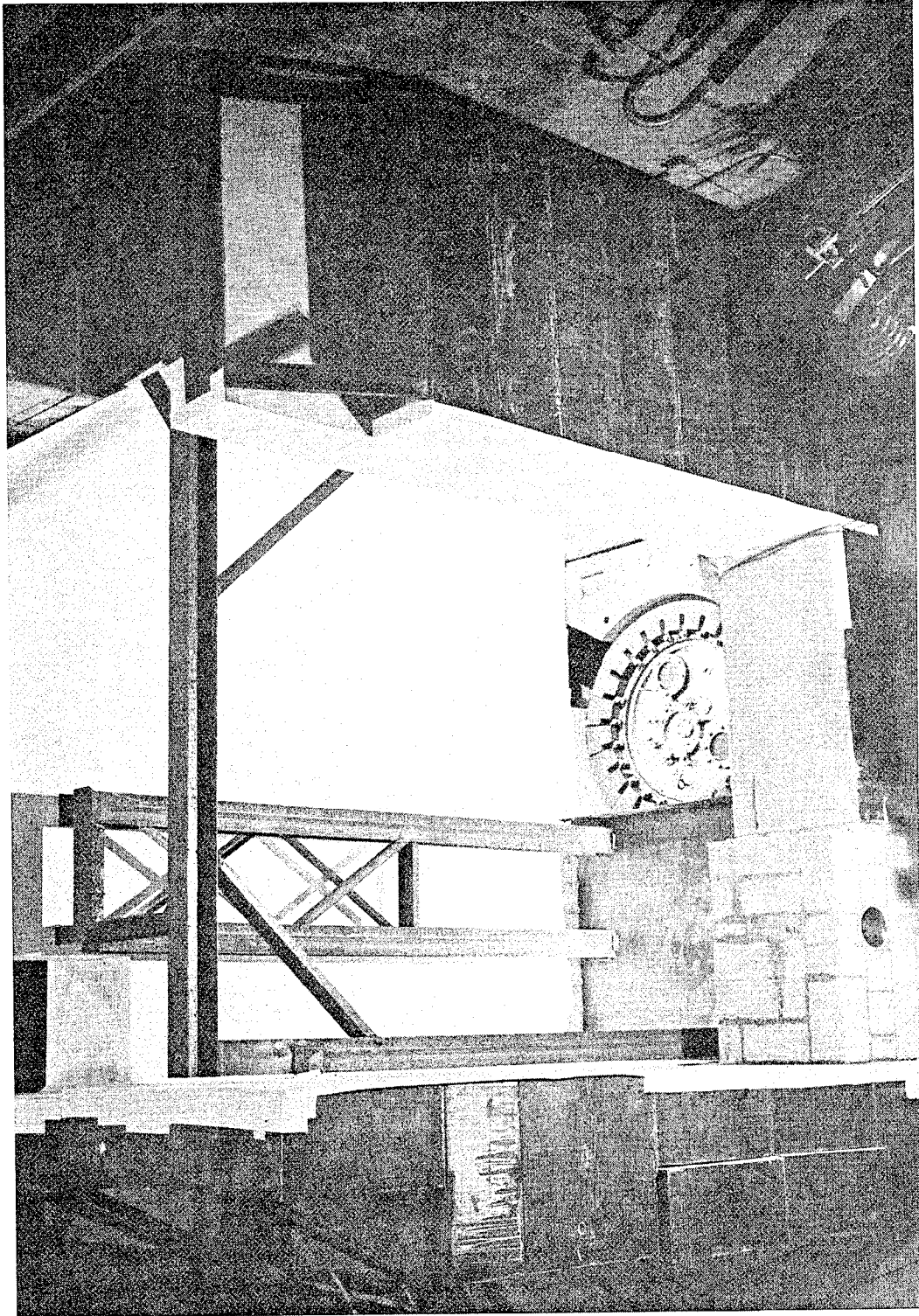
Figure 3. Intermetallic compound layers formed as a result of interdiffusion between uranium and Type 347 stainless steel after six days at 700°C. Total thickness of the layers is 0.0018 in.



103-282

500X

Figure 4. Construction of temporary cave above EER-I before closure of front face. The top of the reactor is shown at the center of the cave floor. After lifting the core assembly from the reactor tank, it was suspended from the bracket shown at the upper left.



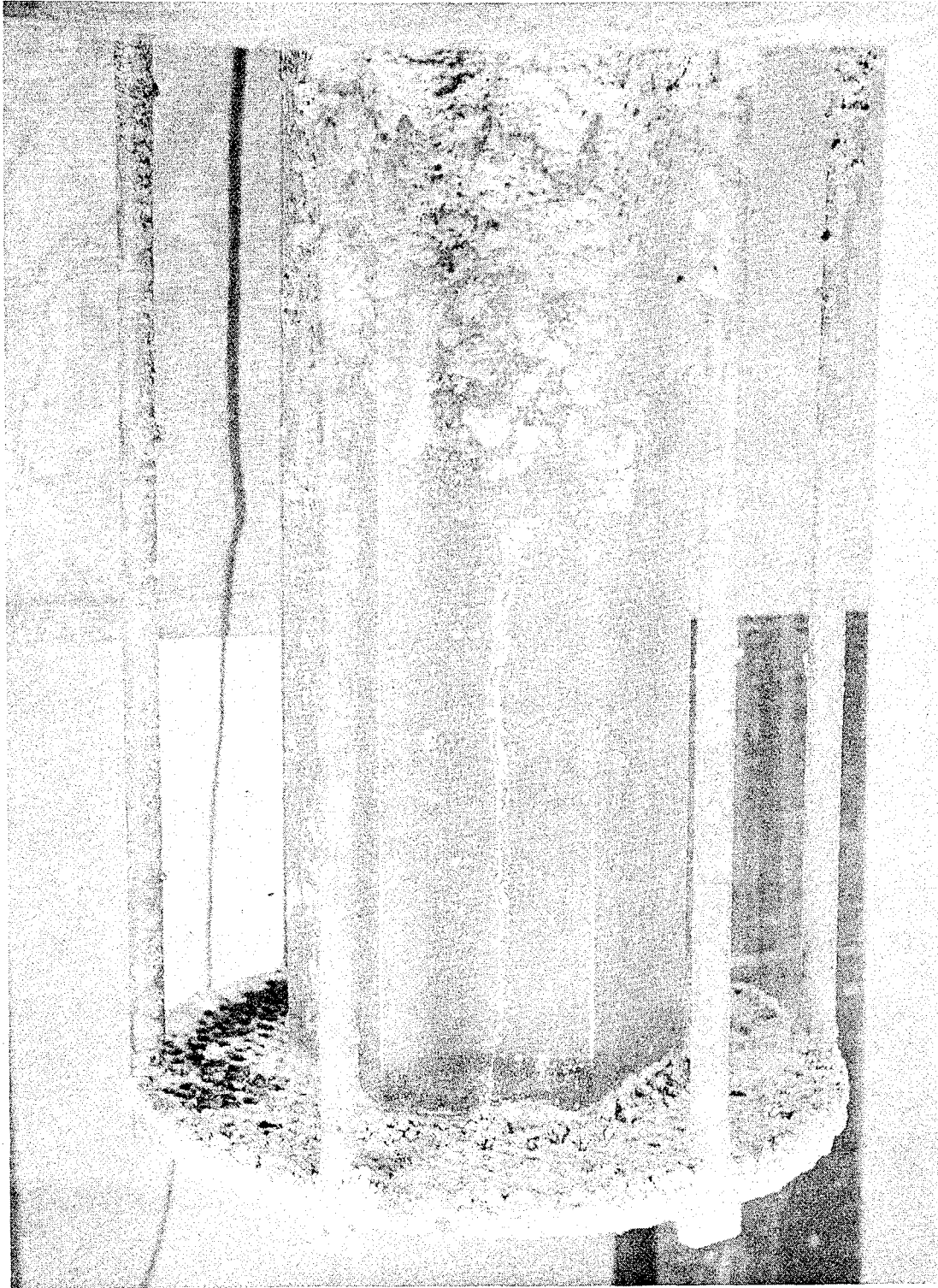
103-188

Figure 5. Completed temporary cave built over EBR-I for removal of core assembly.



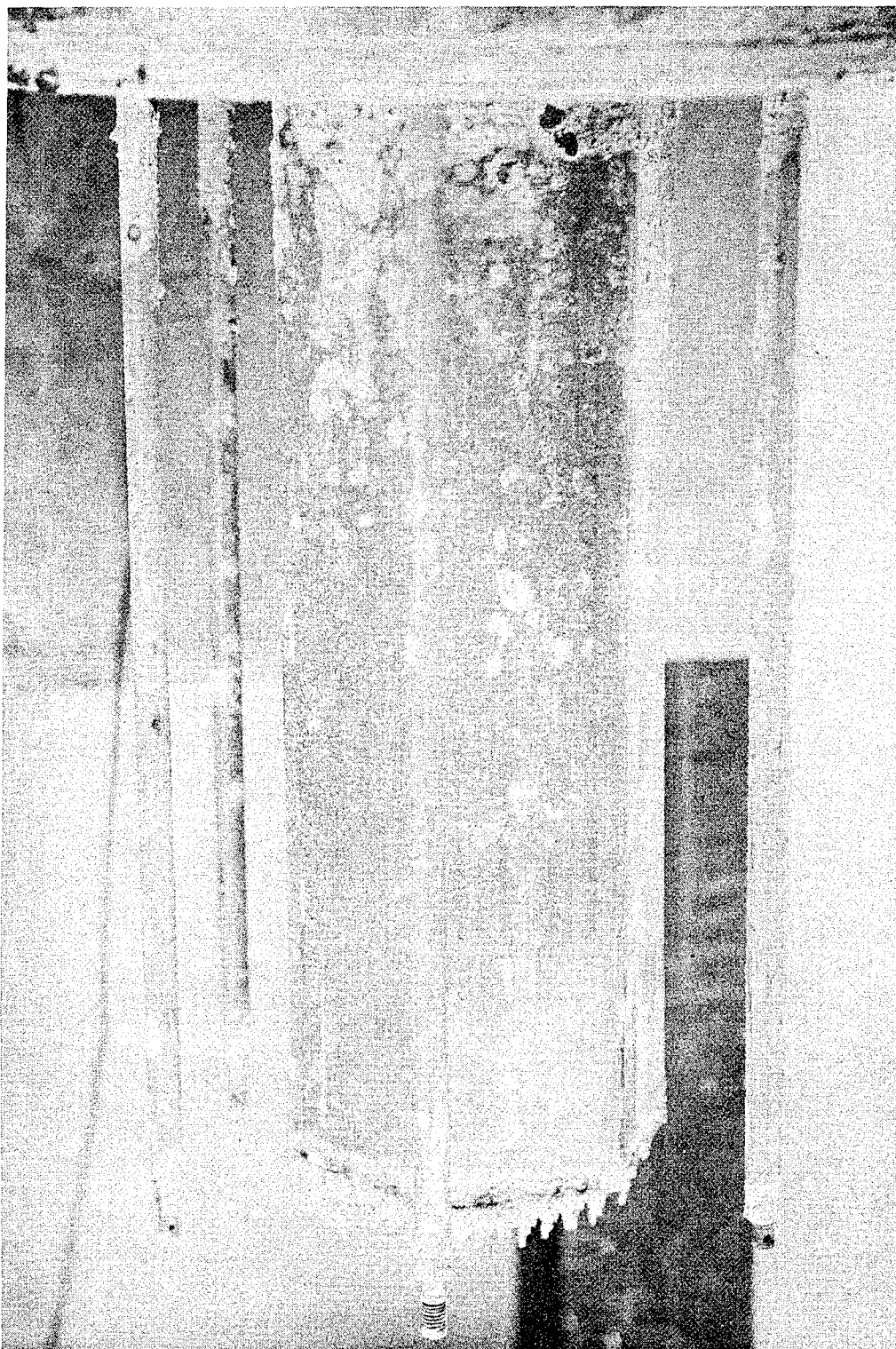
103-199

Figure 6. Core assembly after removal of blanket rods. The fuel section is enclosed in the hexagonal separator.



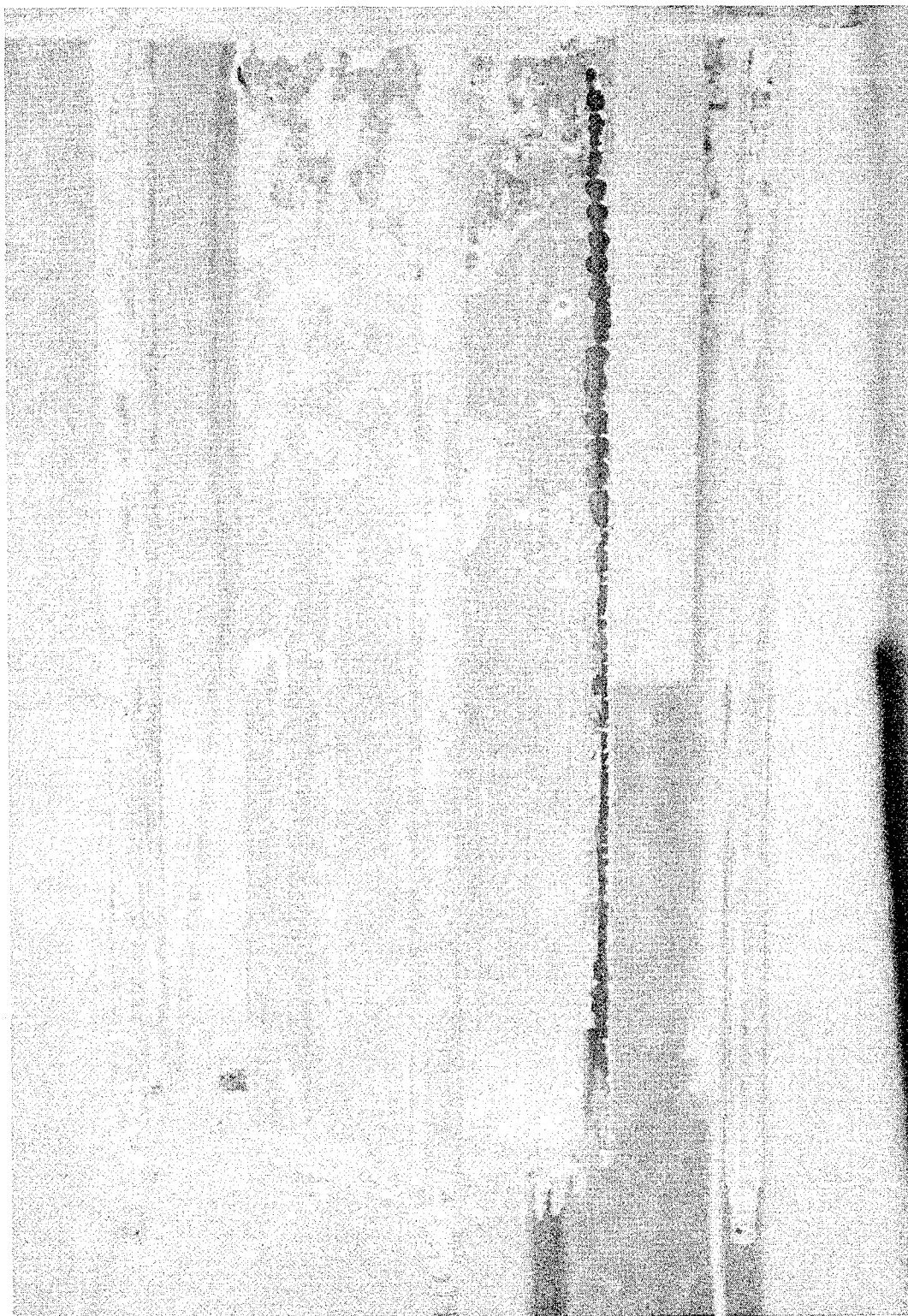
103-178

Figure 7. Core assembly after removal of bottom plate. The tips of the fuel rods in the hexagonal separator are visible.



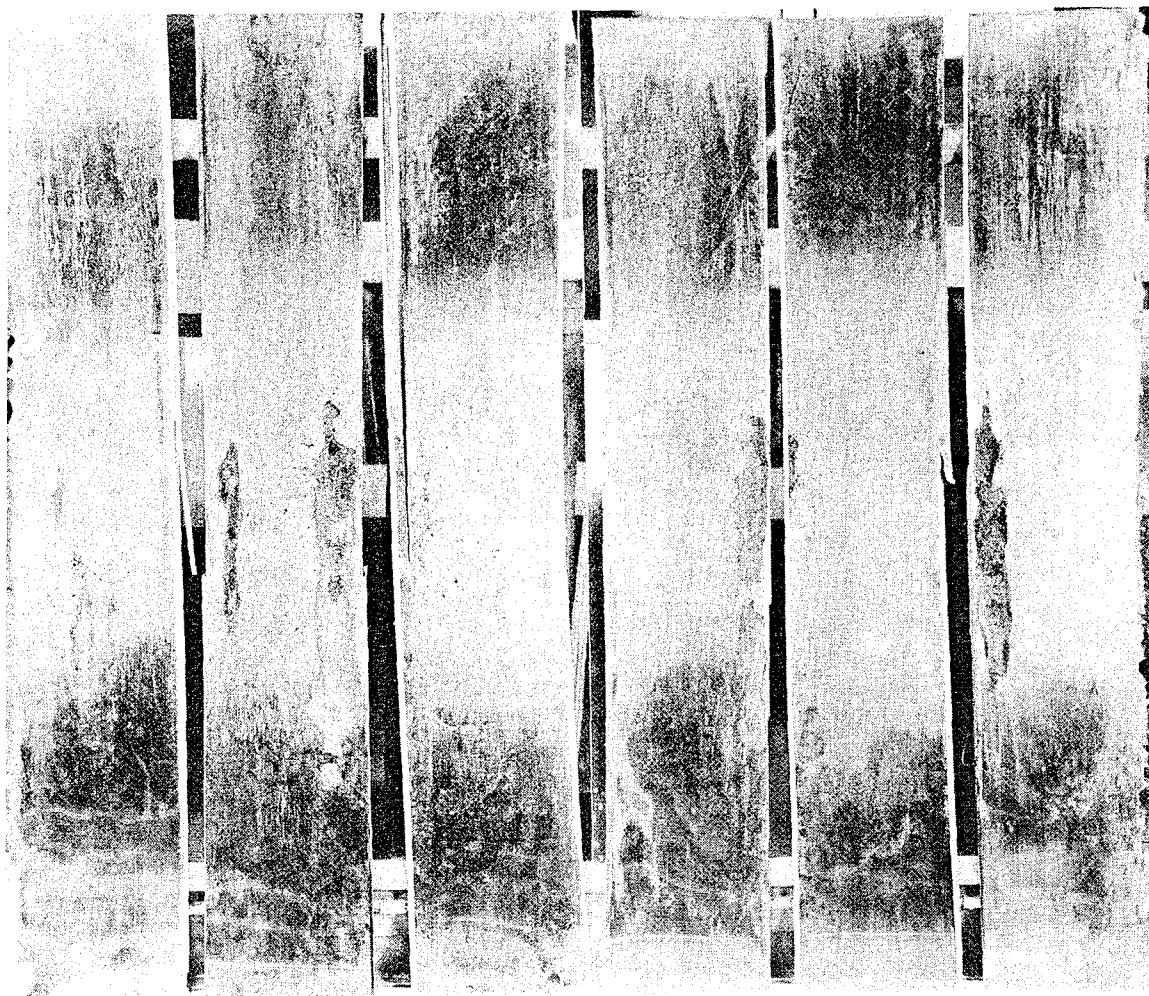
103-182

Figure 8. Holes drilled in hexagonal separator to facilitate removal from core assembly.



103-181

Figure 9. Interior surfaces of hexagonal separator, showing superficial alloying of molten phase with separator, particularly on sides 2, 4, and 6.



SIDE NO. 1

2

3

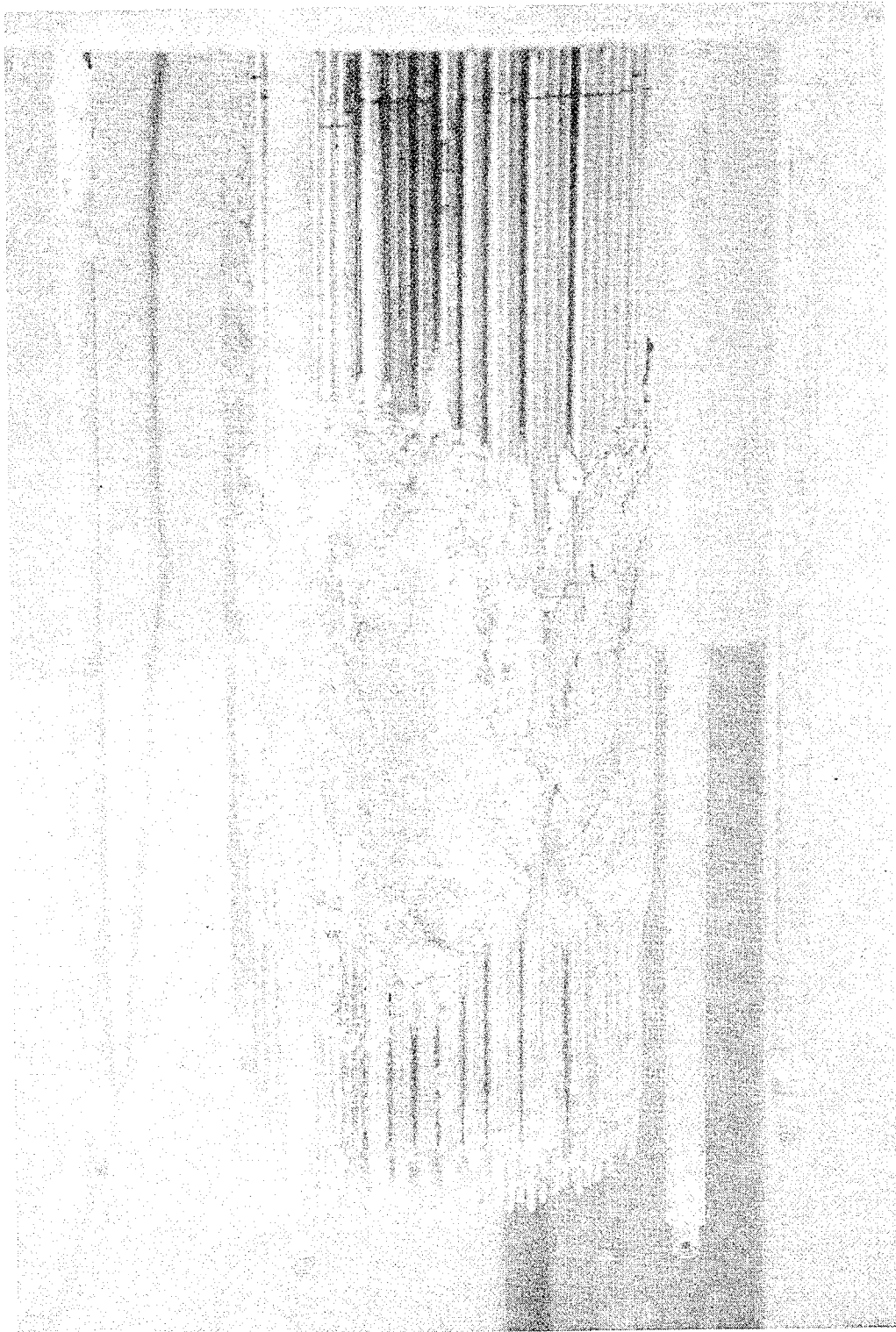
4

5

6

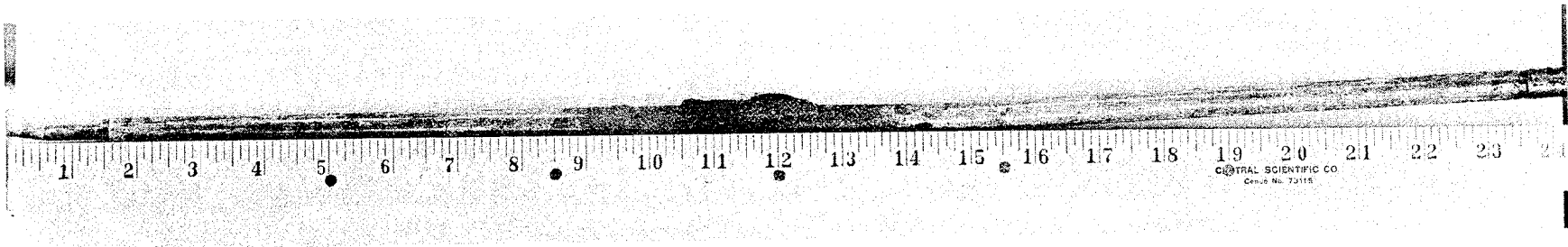
106-3188

Figure 10. Damaged EBR-I core after removal of hexagonal separator.



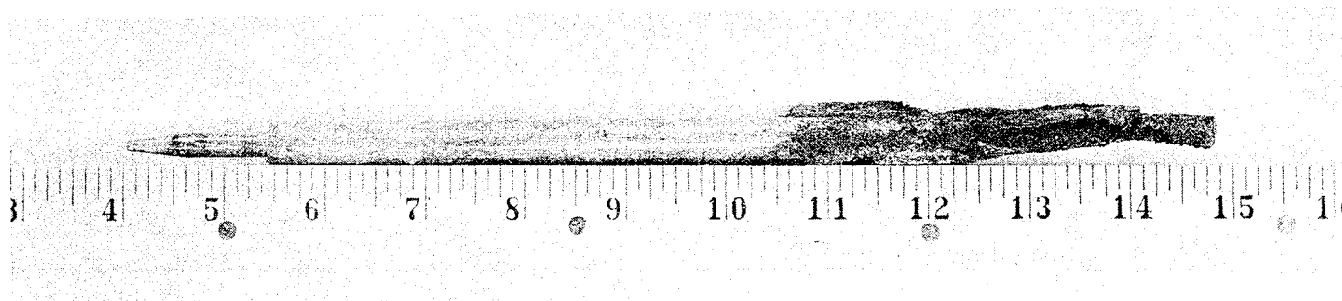
103-201

Figure 11. Typical fuel element from the first (outer) row of the damaged EBR-I core.



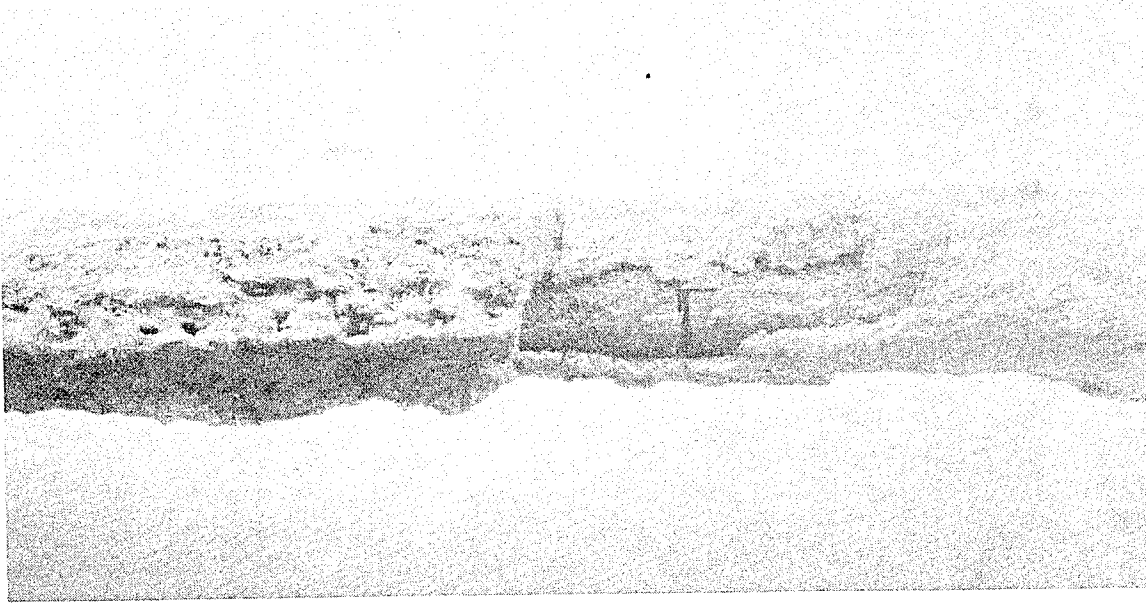
106-2622

Figure 12. Typical fuel element from the second row of the damaged EBR-I core.



106-2623

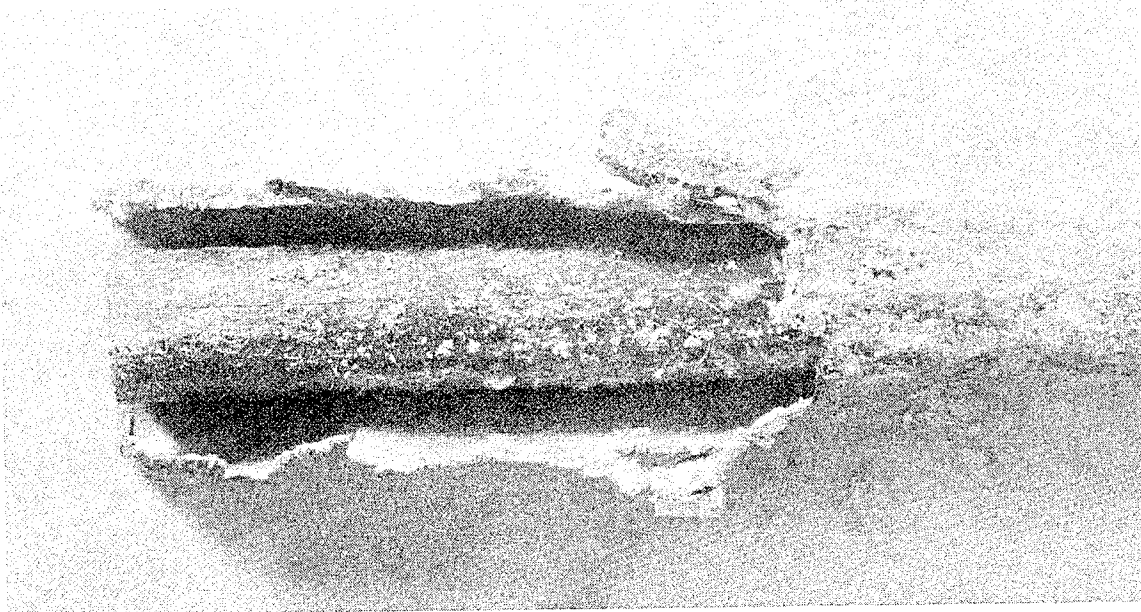
Figure 13. Fuel element from outer row of damaged EBR-I core assembly, showing that although the outer jacket has been severely damaged by melting, the stainless steel spacer between adjacent fuel slugs is undamaged.



20037

2X

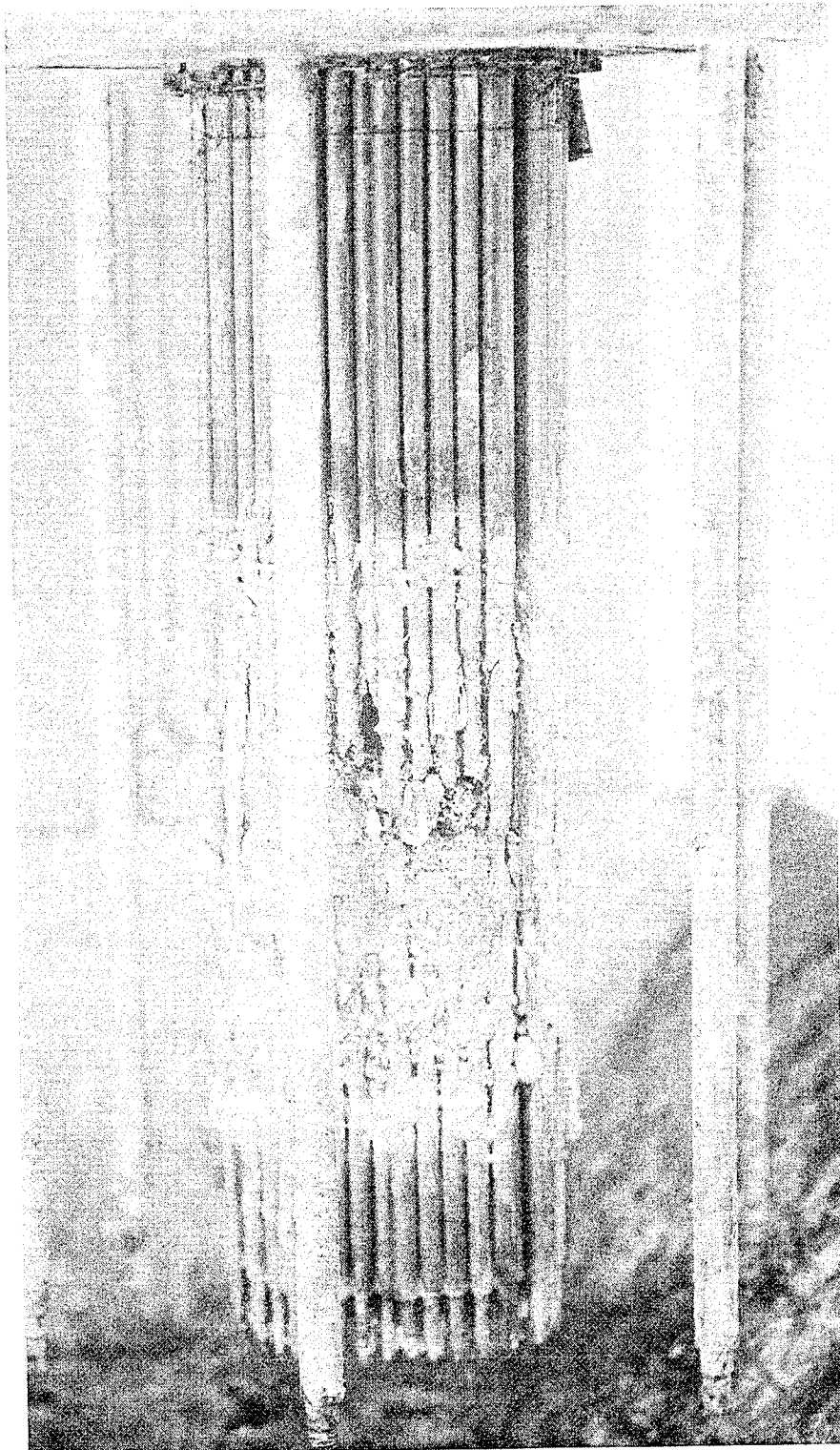
Figure 14. The stainless steel jacket shown above in Figure 13 has been peeled back, and it can be noted that the surface of the fuel slug and the interior surface of the jacket were unaffected by the meltdown.



20036

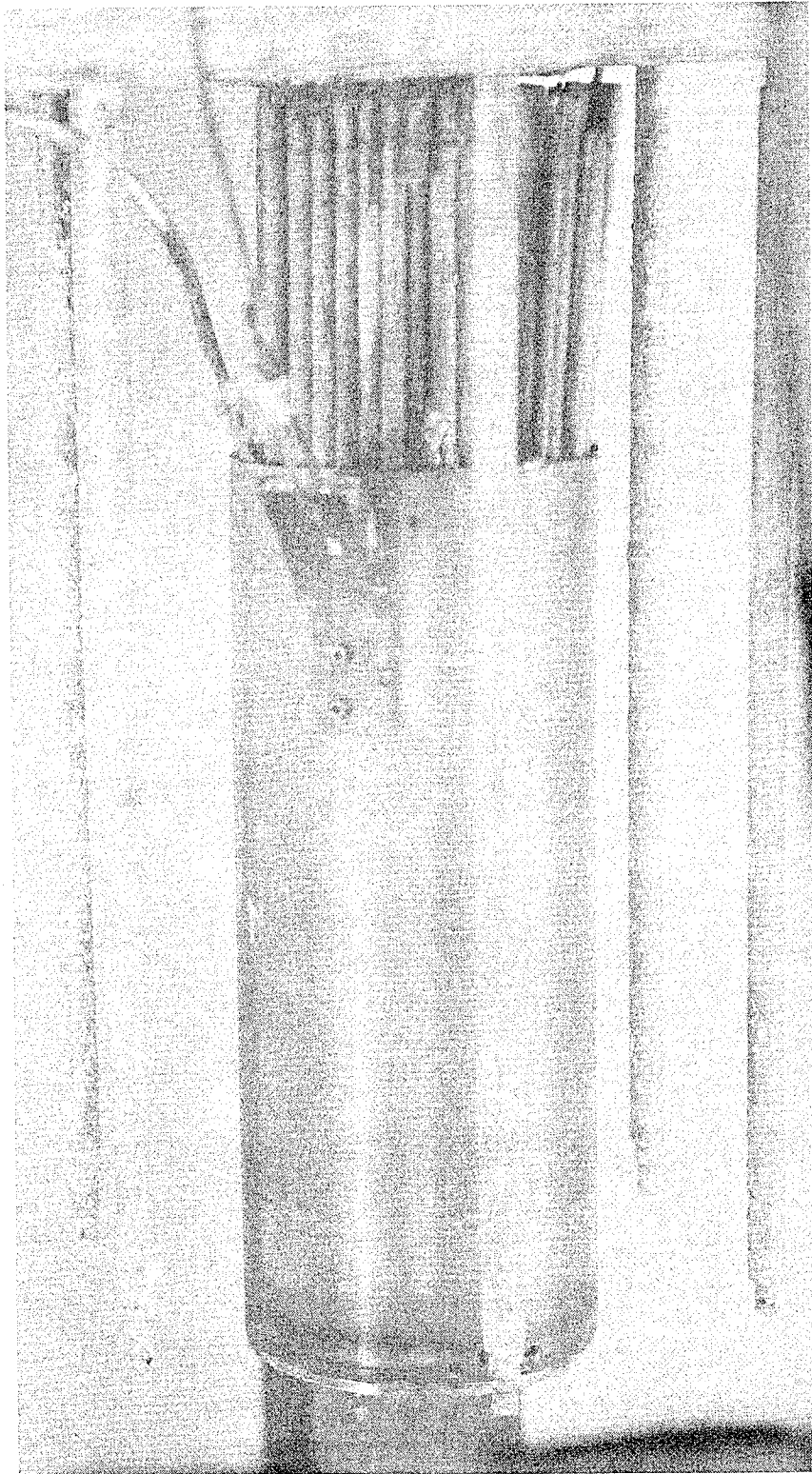
2X

Figure 15. Damaged EBR-I core after removal of outer fuel elements.



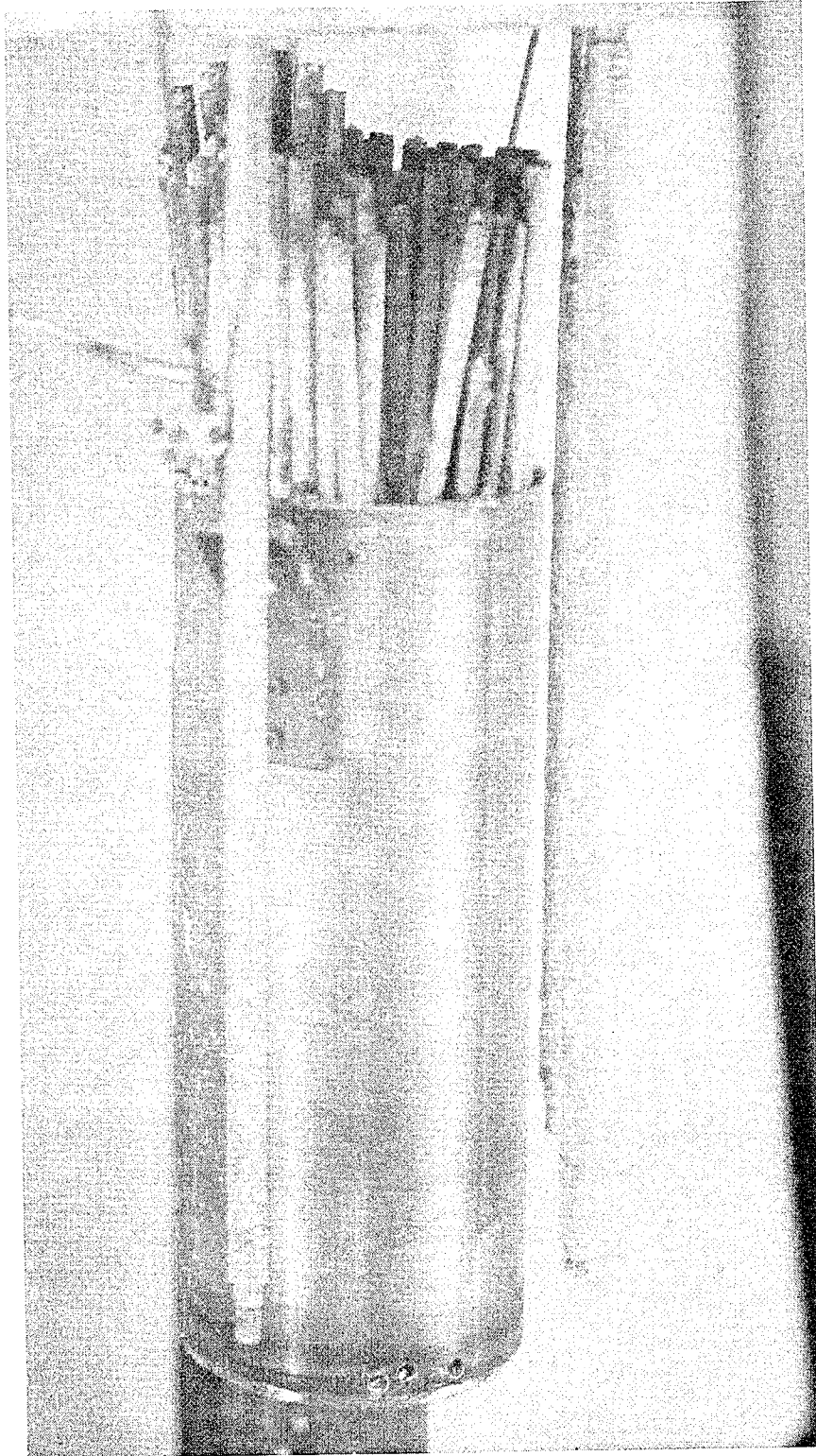
103-198

Figure 16. Thimble used to contain damaged core. Argon gas is being led into the thimble by the tube on the left.



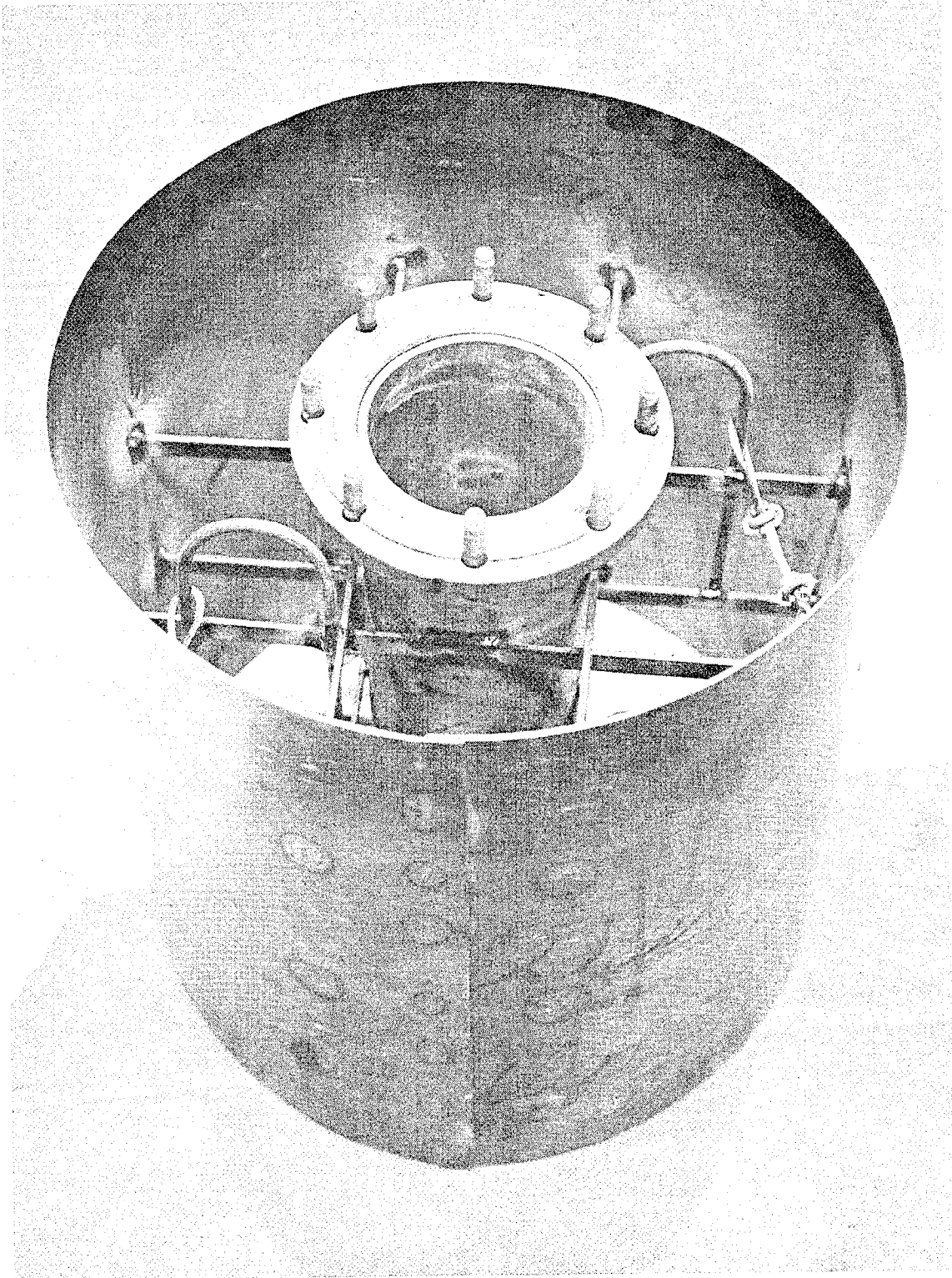
103-195

Figure 17. Appearance of core assembly after all remaining fuel rods had been sawed through.



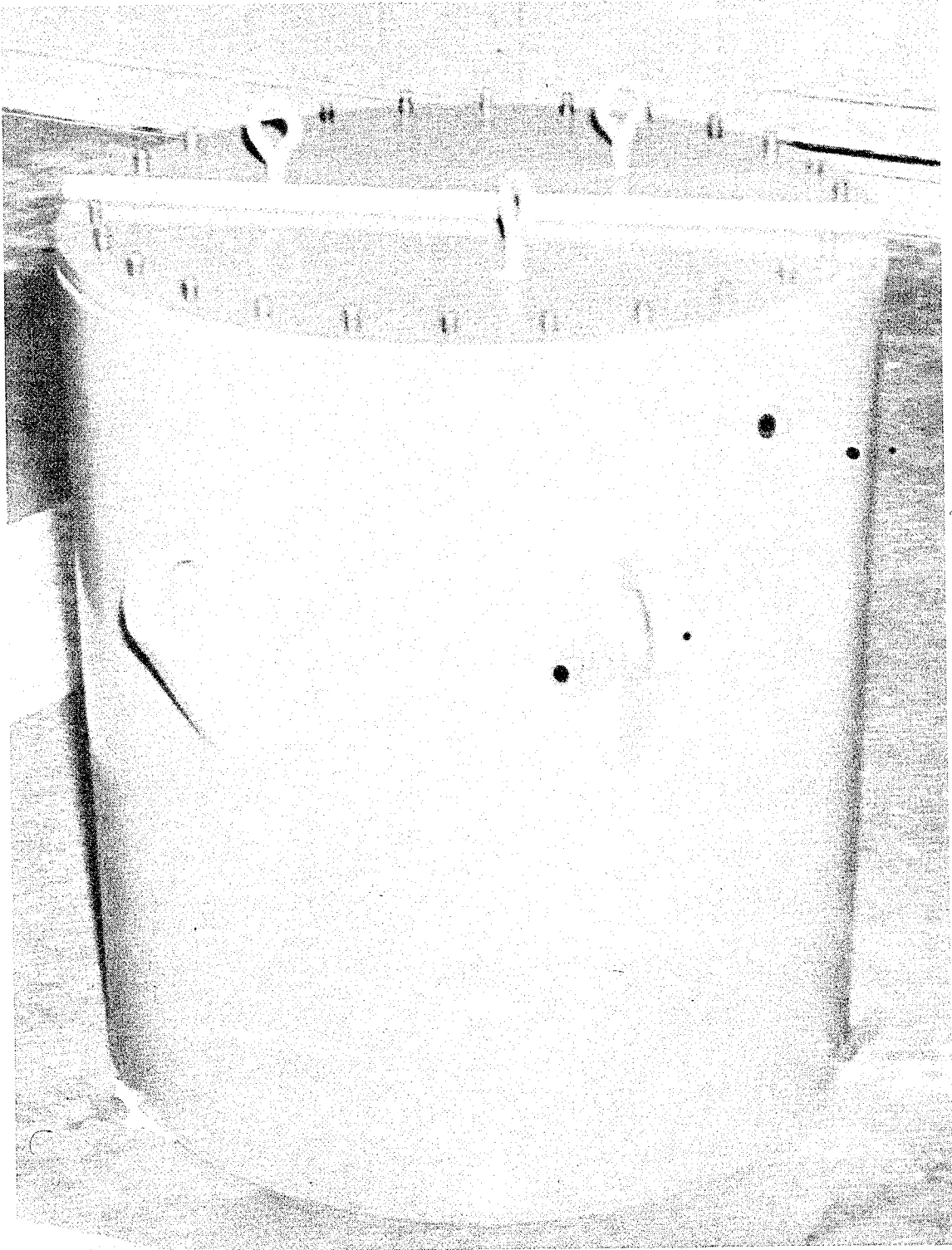
103-197

Figure 18. Gas-tight container and cage assembly used for shipment of the damaged EBR-I core assembly.



103-194

Figure 19. Lead cask used to ship the damaged EBR-I core assembly. The cask is 43 inches high, 40 inches in diameter, and weighs 10,800 lb.



103-202

Figure 20. View of some of the instrumentation outside the cave used for final disassembly of the EBR-I core. The equipment at the left recorded air-borne particulate activity in the cave atmosphere. The equipment at the center recorded oxygen level in the cave atmosphere. Other instruments, not visible, measured nitrogen flow rate, temperature, humidity, and gamma and neutron levels in the cave.

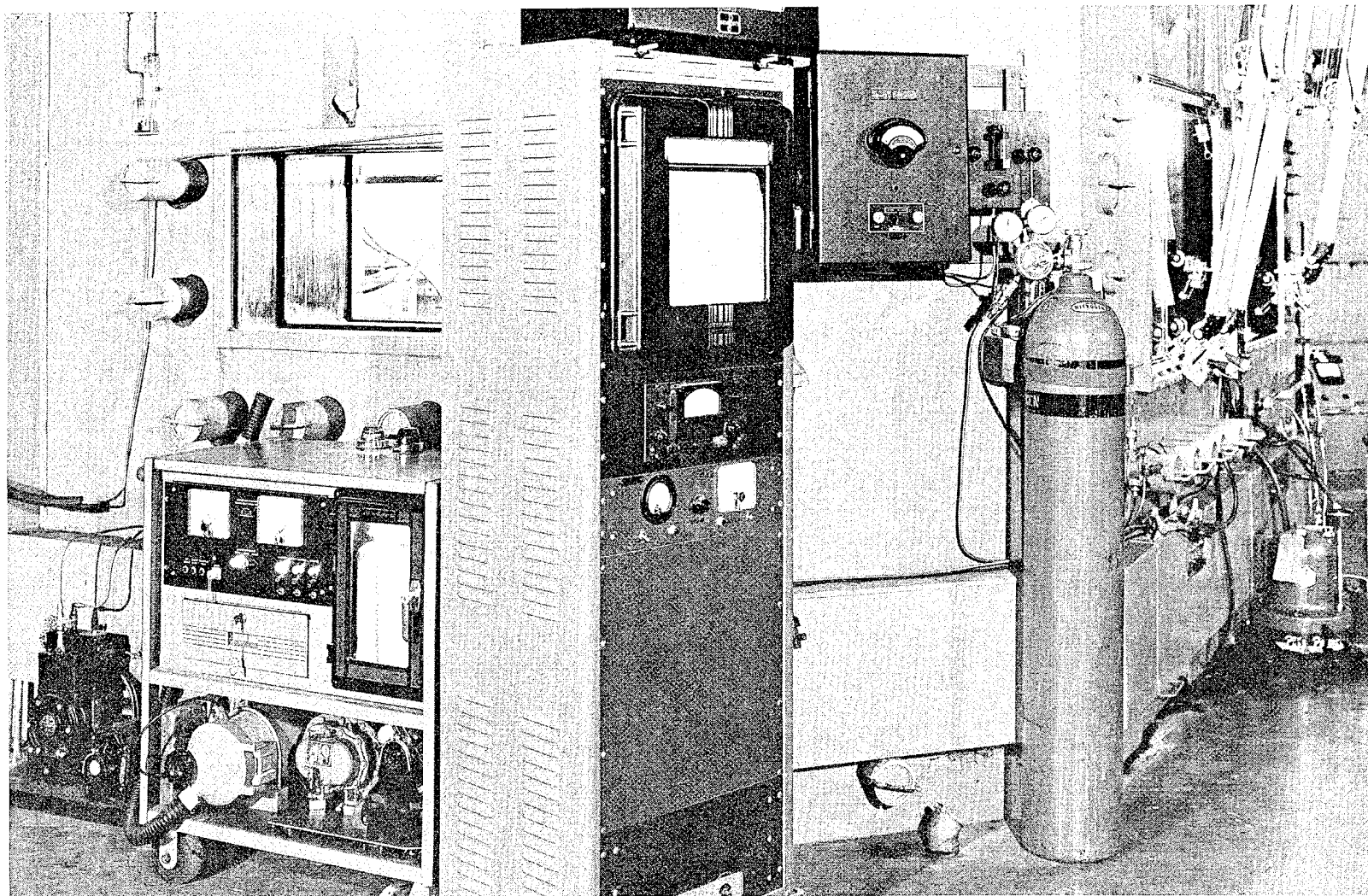


Figure 21. Area in left part of cave used for disassembly of EBR-I core. The top of the cage assembly used for shipment, shown in Figure 18, is at the lower left. The device in the center background is a pipe cutter, and the object in the right background is a hydraulic chisel. An electric impact chisel is suspended at the extreme right. All powered equipment was remotely operated.

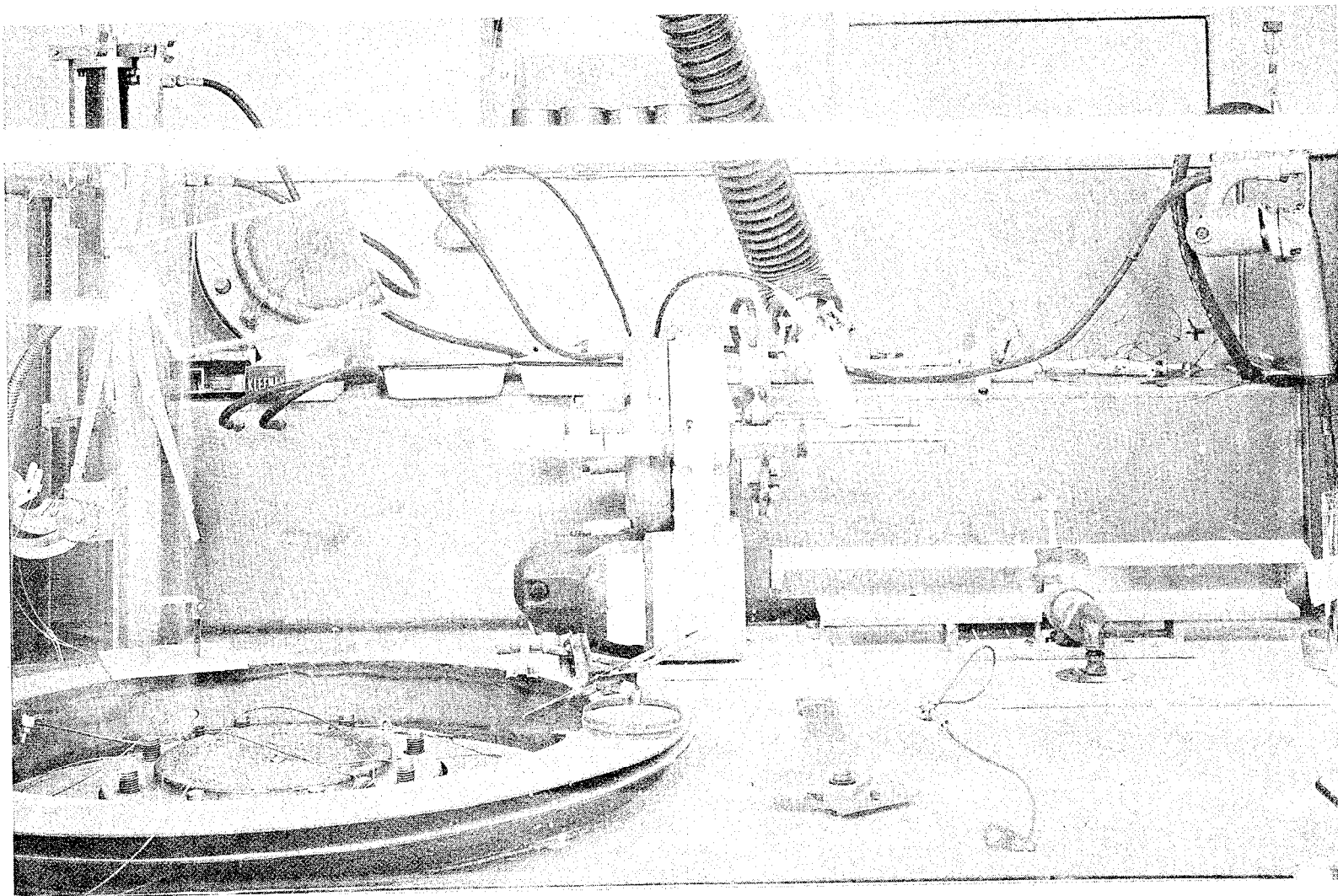
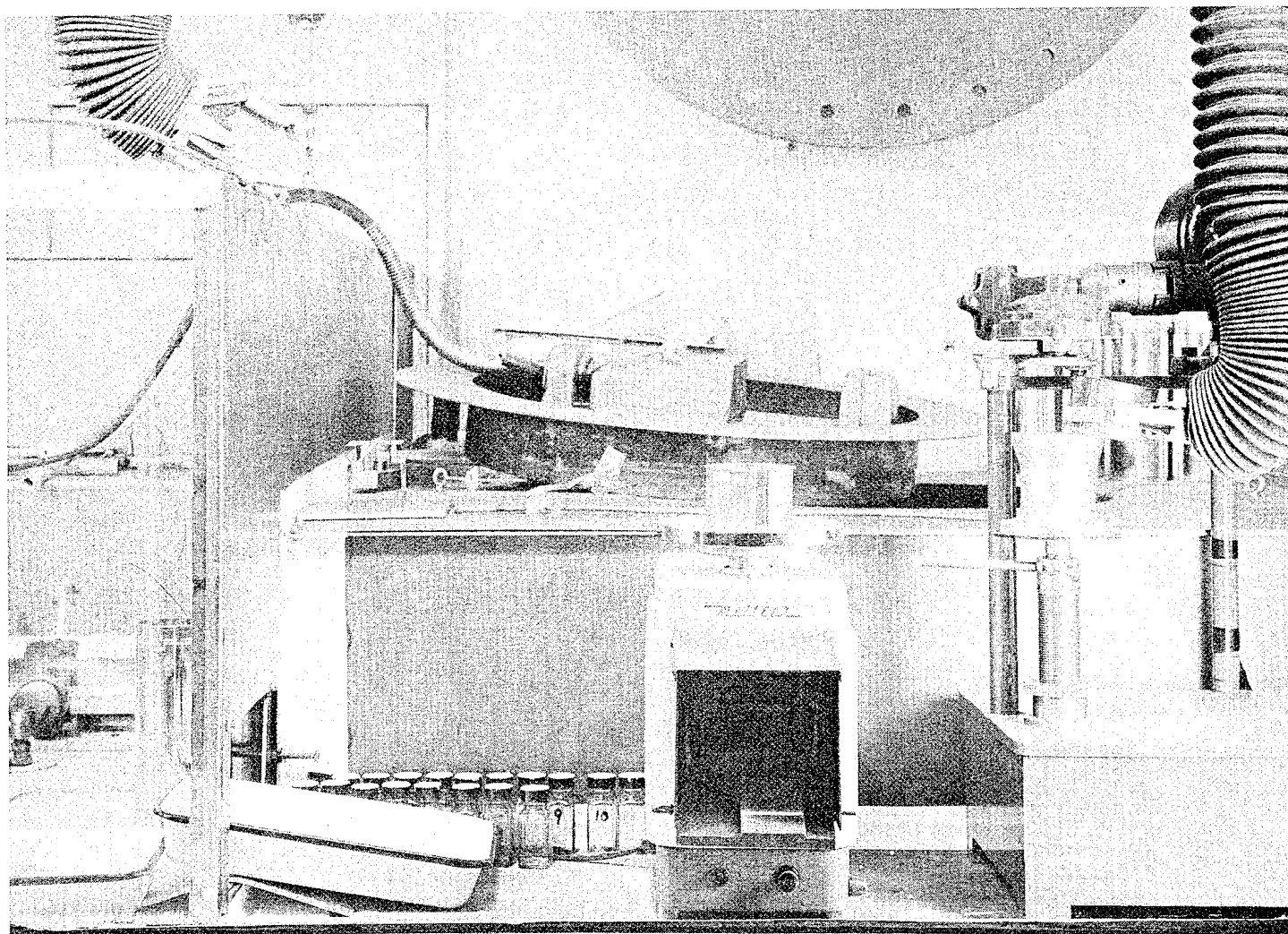
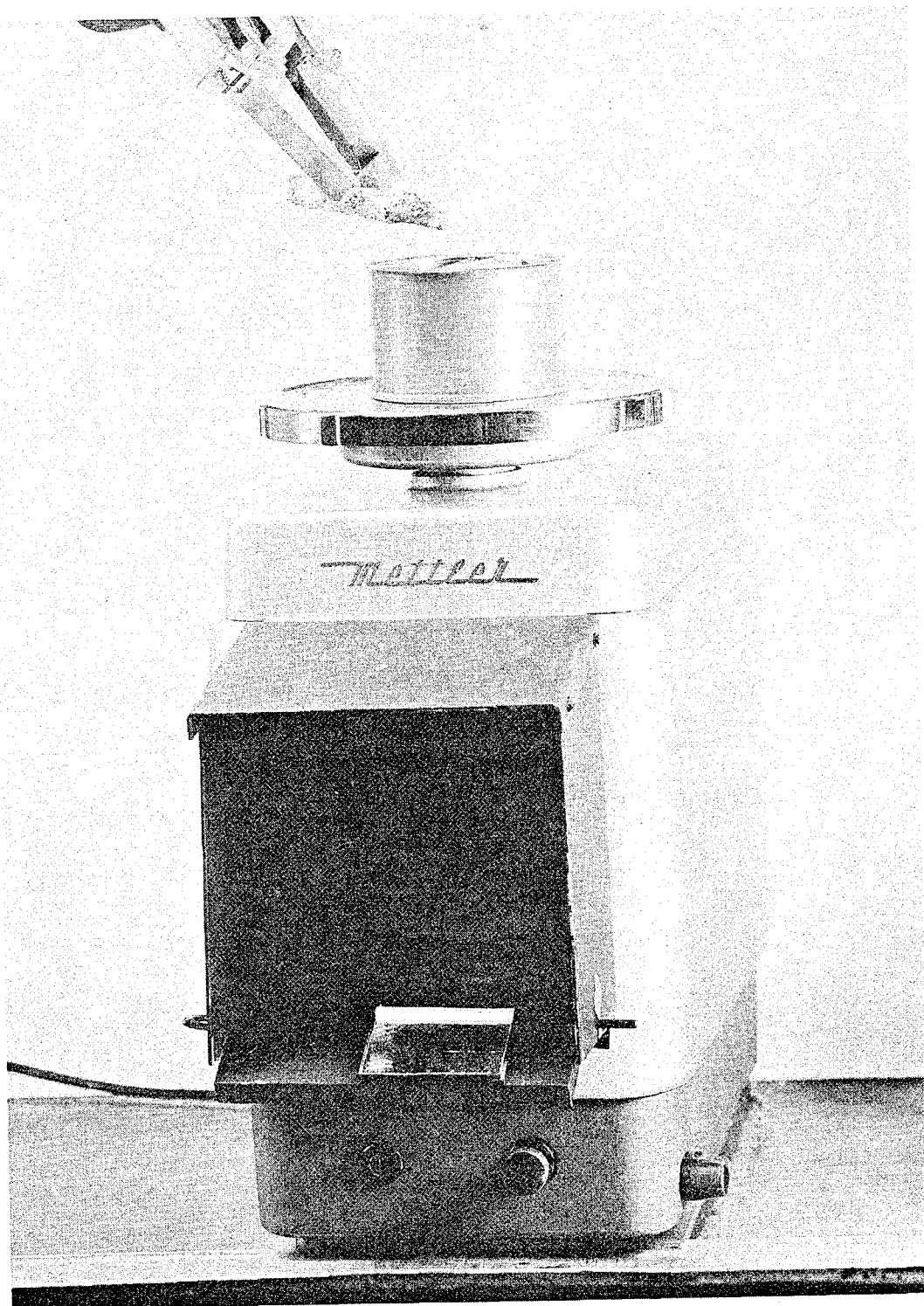


Figure 22. Area in right part of cave used for weighing and sealing cans of separated enriched material. The numbered bottles in the foreground were used for chemical samples. A partition at the left divided this area of the cave from the disassembly operations in the left area.



103-260

Figure 23. Typical piece of fuel being loaded into a storage can. After each filled can was weighed it was moved to the can sealer shown in Figure 24.



103-219

Figure 24. Remotely operated equipment shown sealing a can of enriched fuel.

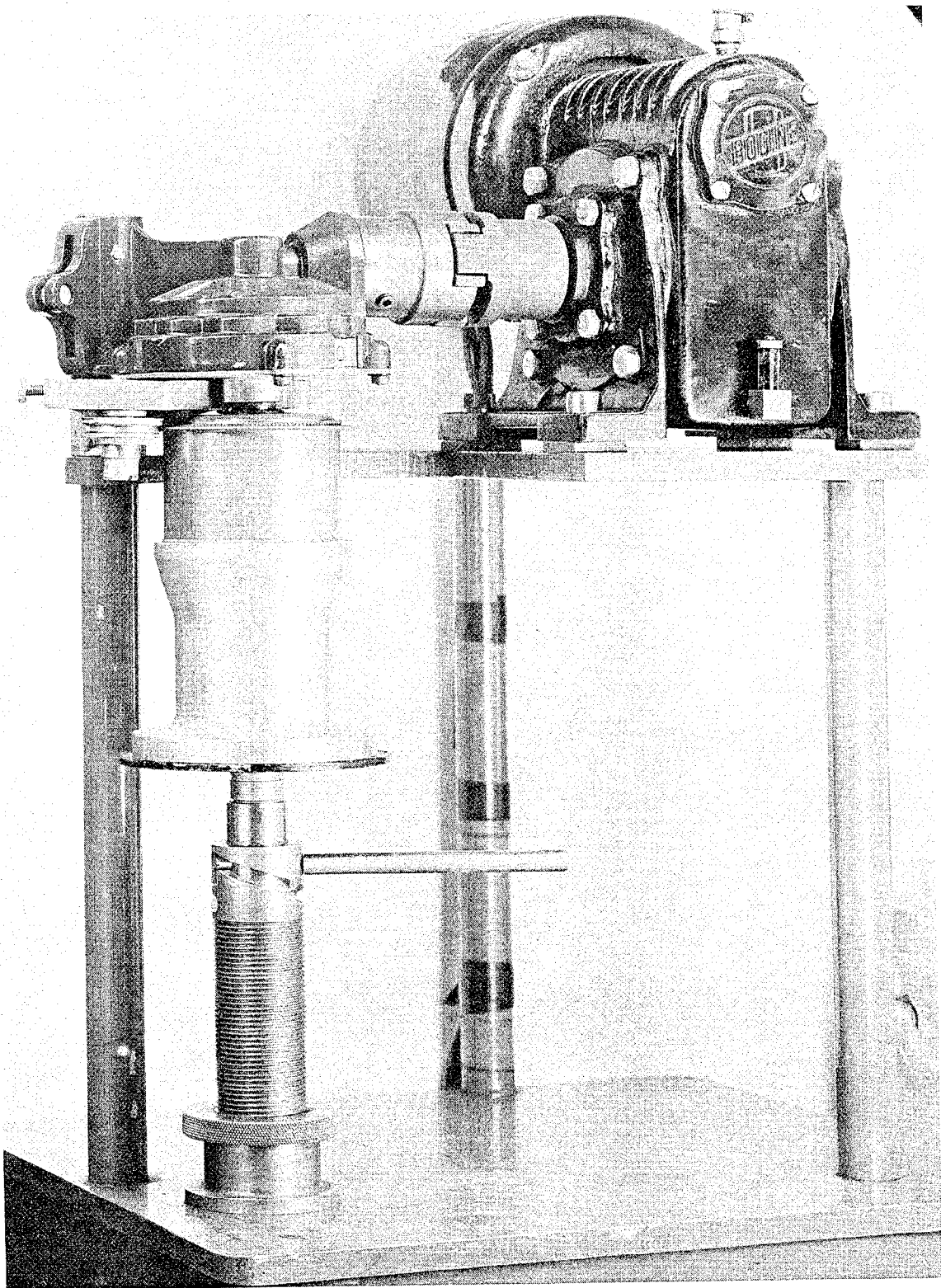
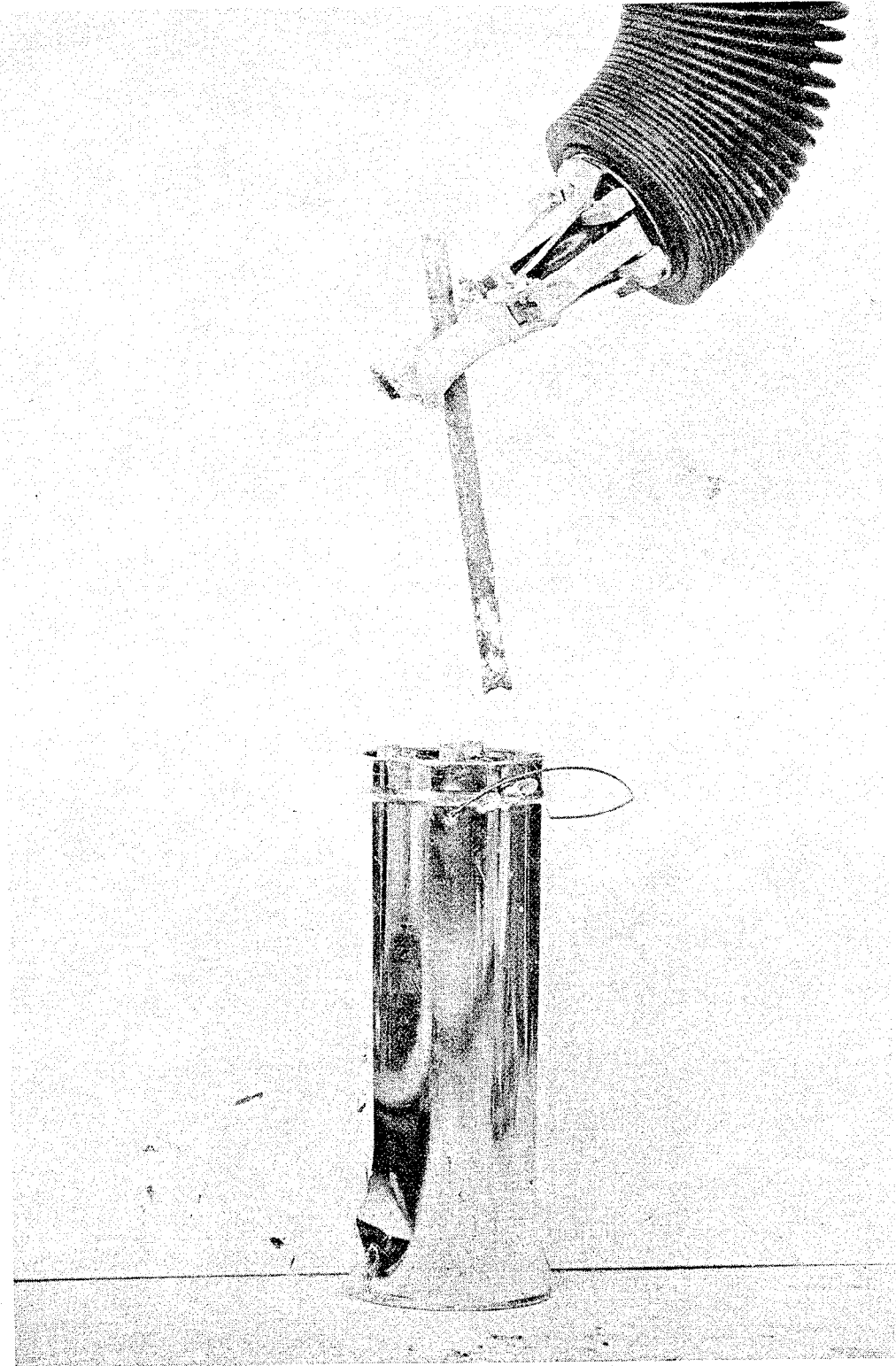
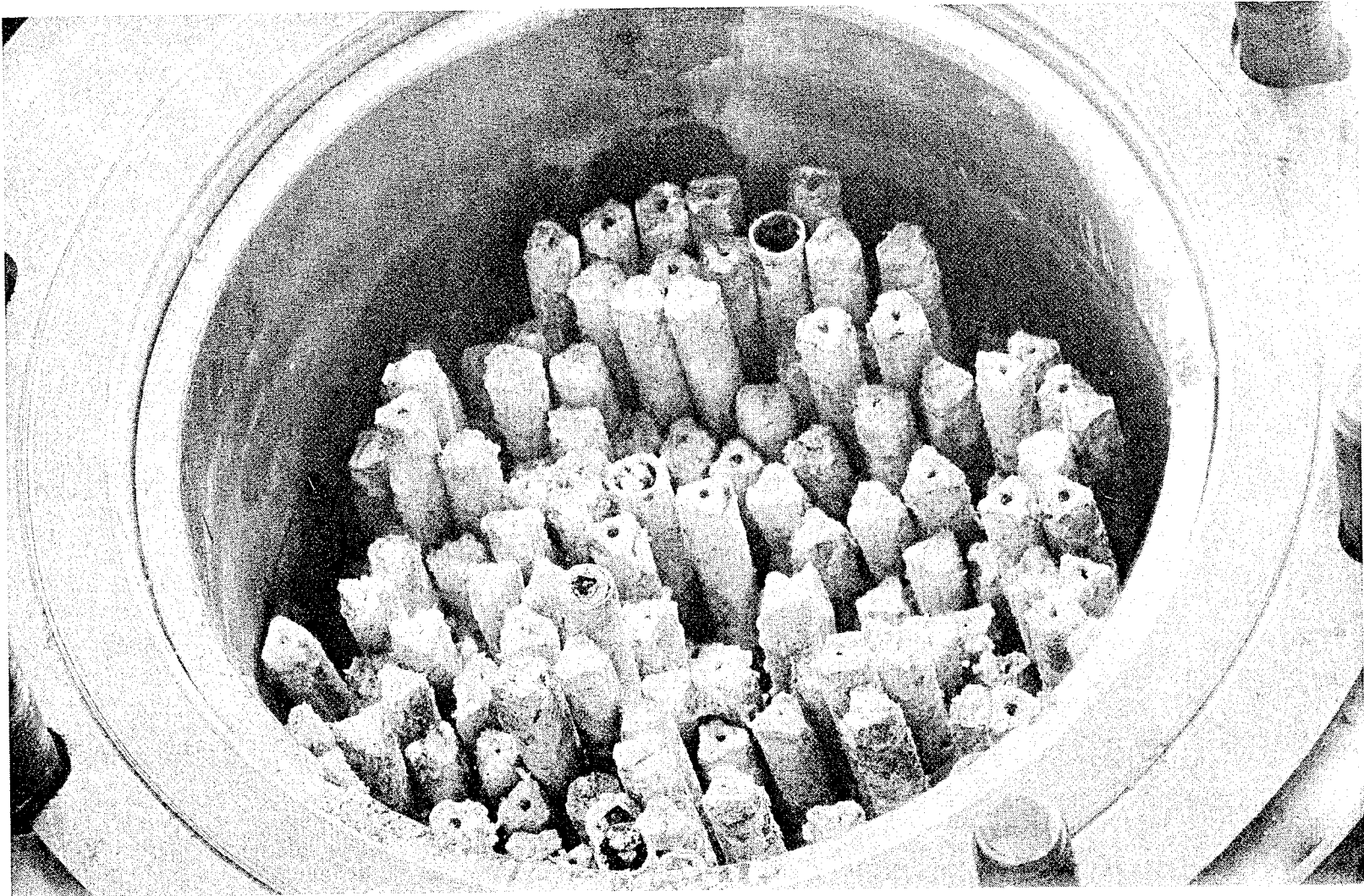


Figure 25. Procedure used for loading unenriched blanket material.



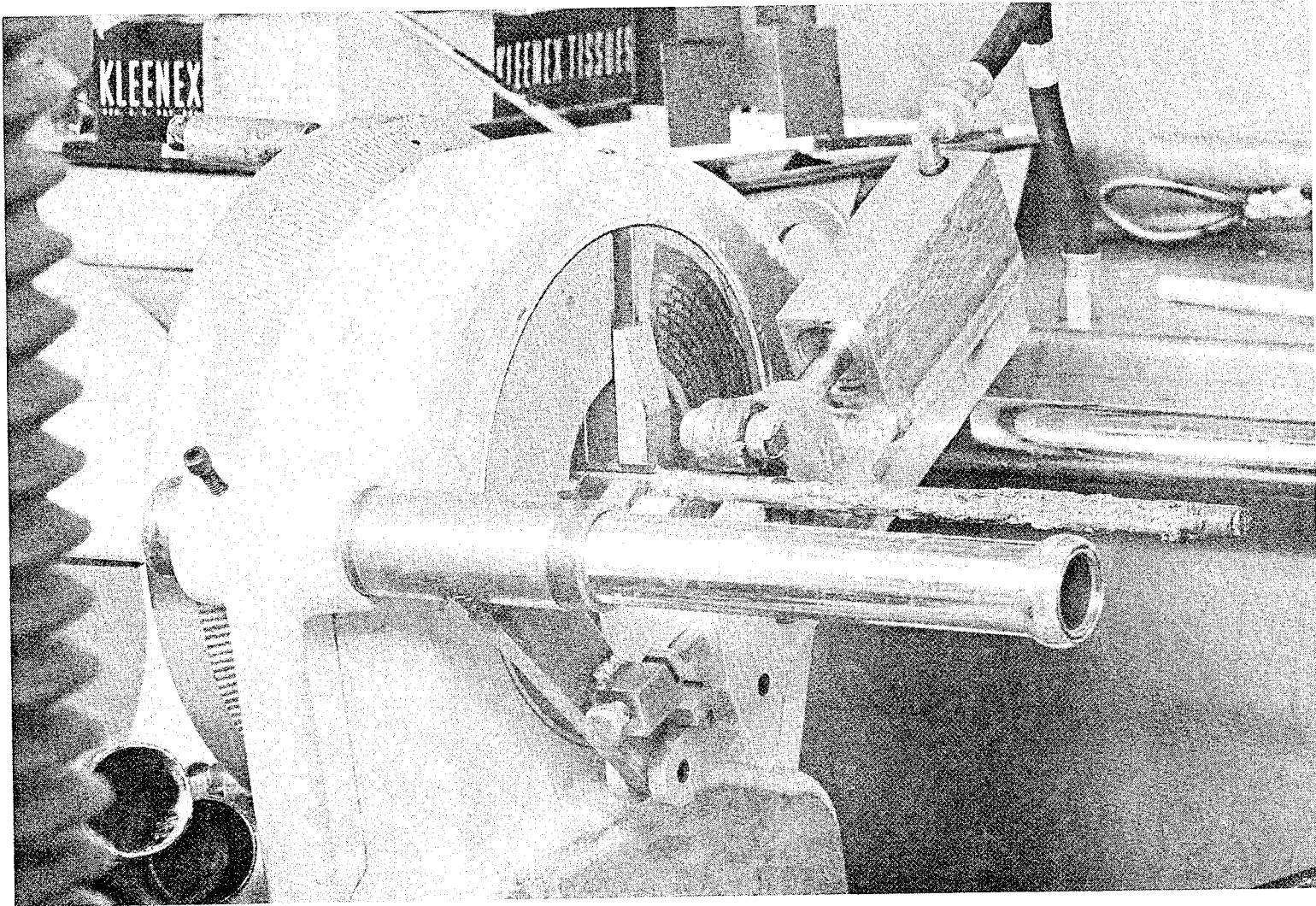
103-226

Figure 26. Appearance of the top of the damaged EBR-I core before final disassembly operations were started.



103-216

Figure 27. Remotely operated pipe cutter being used to cut outer jacket on a fuel element near the junction of fuel and blanket. The blanket section at the right end of the element has already been removed with the pipe cutter, and the tip of a fuel slug is visible.



103-214

Figure 28. Clump of upper blanket rods from near the center of the core assembly. The blanket section begins about one-half in. above the lower end, and it can be noted that the molten fuel alloy has moved upward between the rods for approximately 5 in.

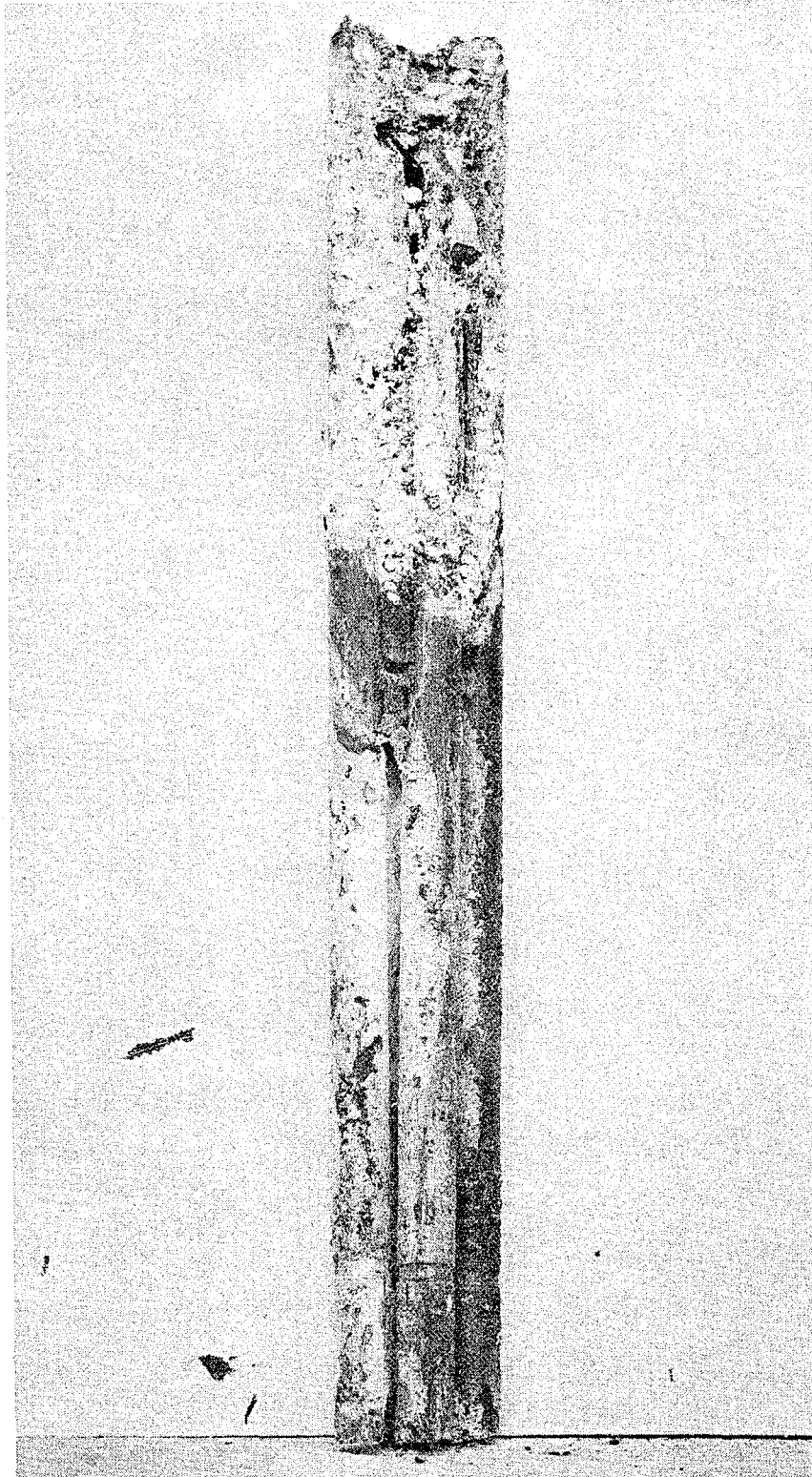
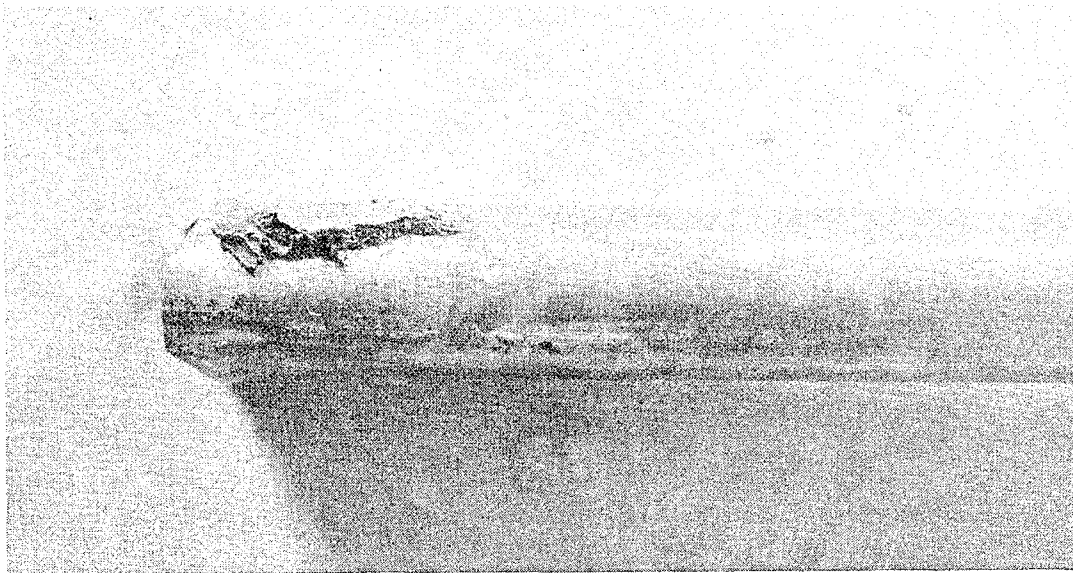


Figure 29. Stainless steel outer jacket from the upper blanket. The left end originally was attached to the fuel section. Most of the adhering fuel alloy has been removed, and it can be noted that the jacket does not appear to have been damaged by melting.



20544

2X

Figure 30. Use of thermocouple wires embedded in the fuel section to lift the fuel and lower blanket assembly from the thimble used for shipping.

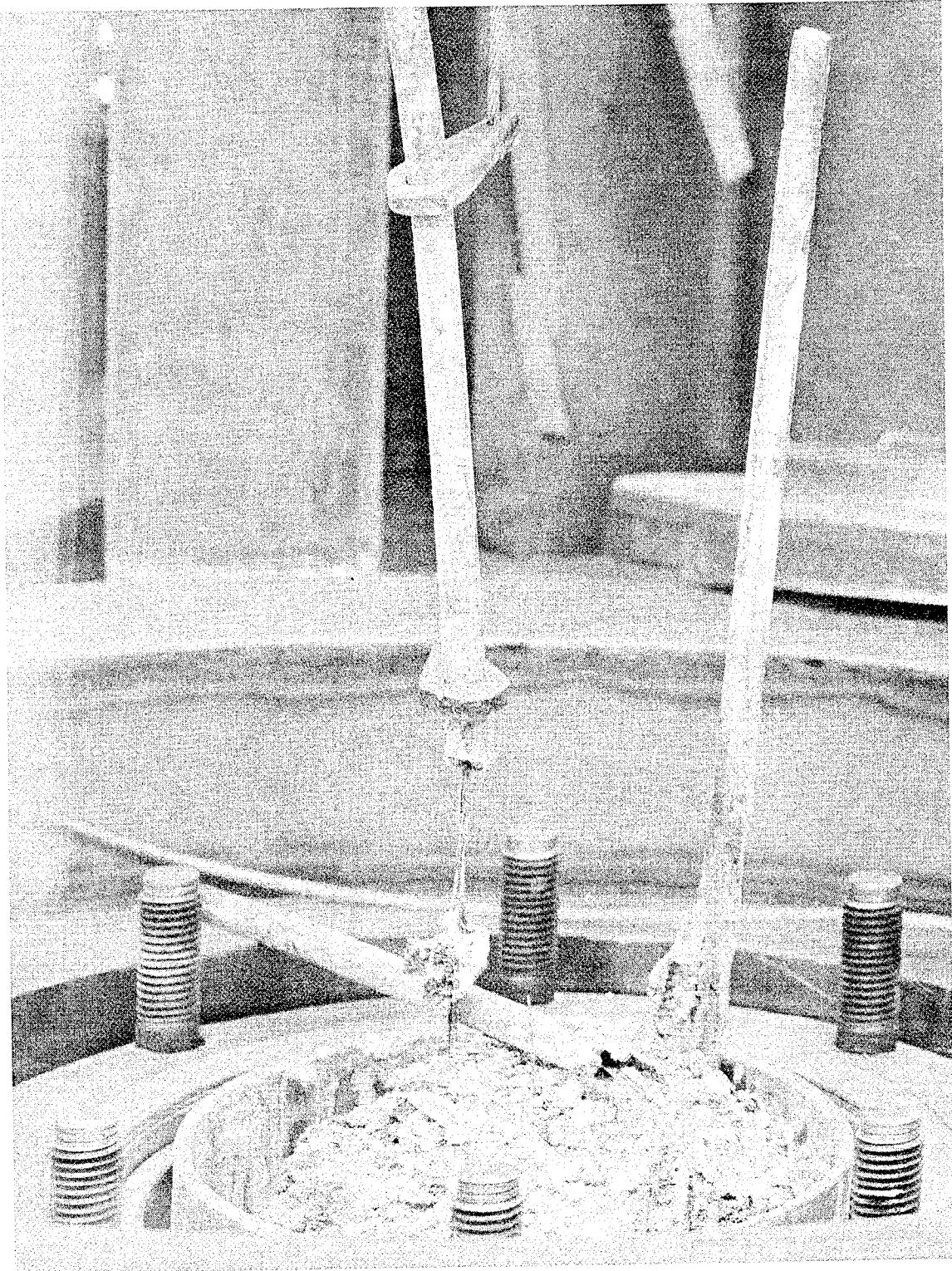
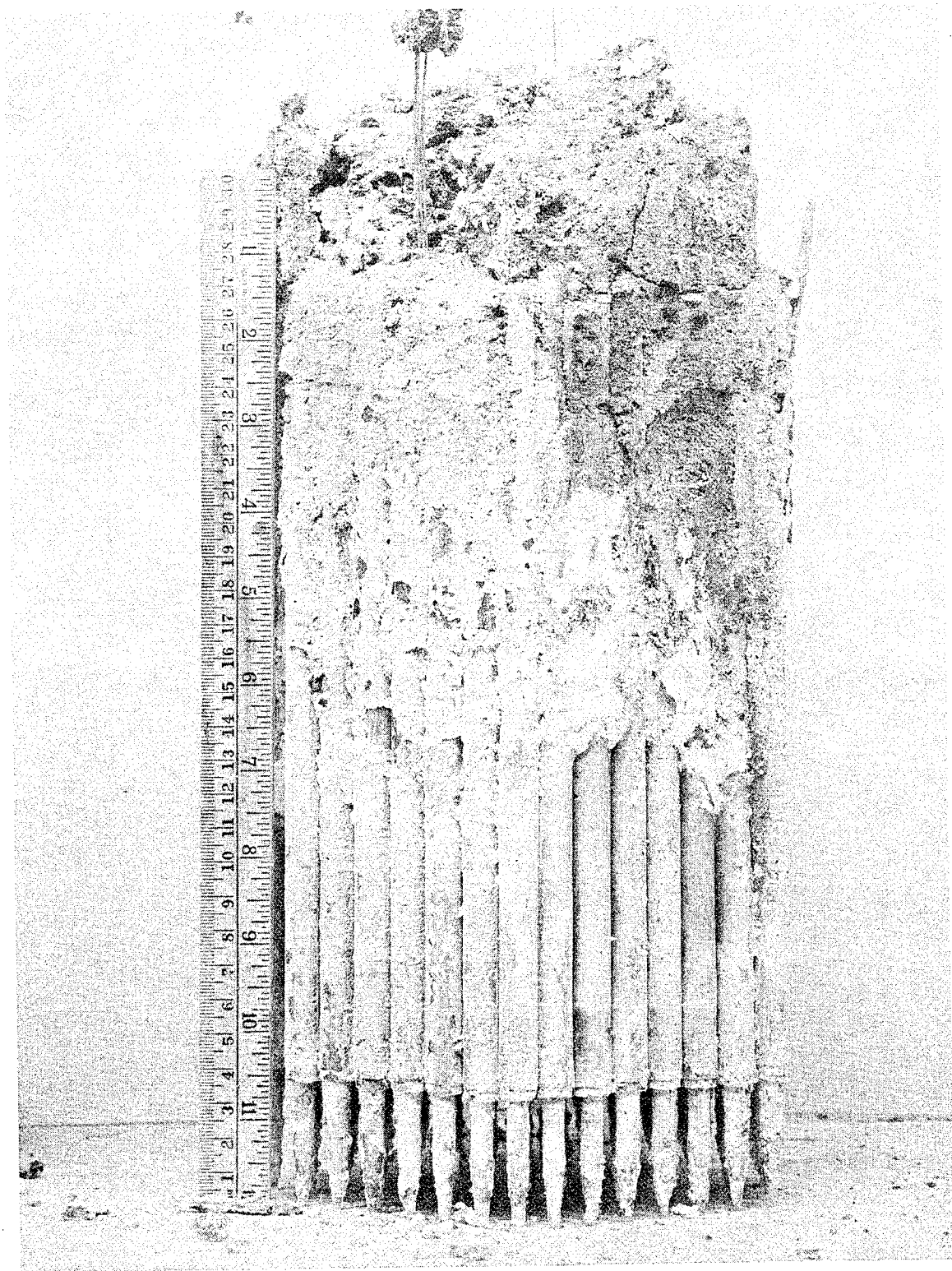


Figure 31. Appearance of the damaged EBR-I core after removal of the upper blanket section.



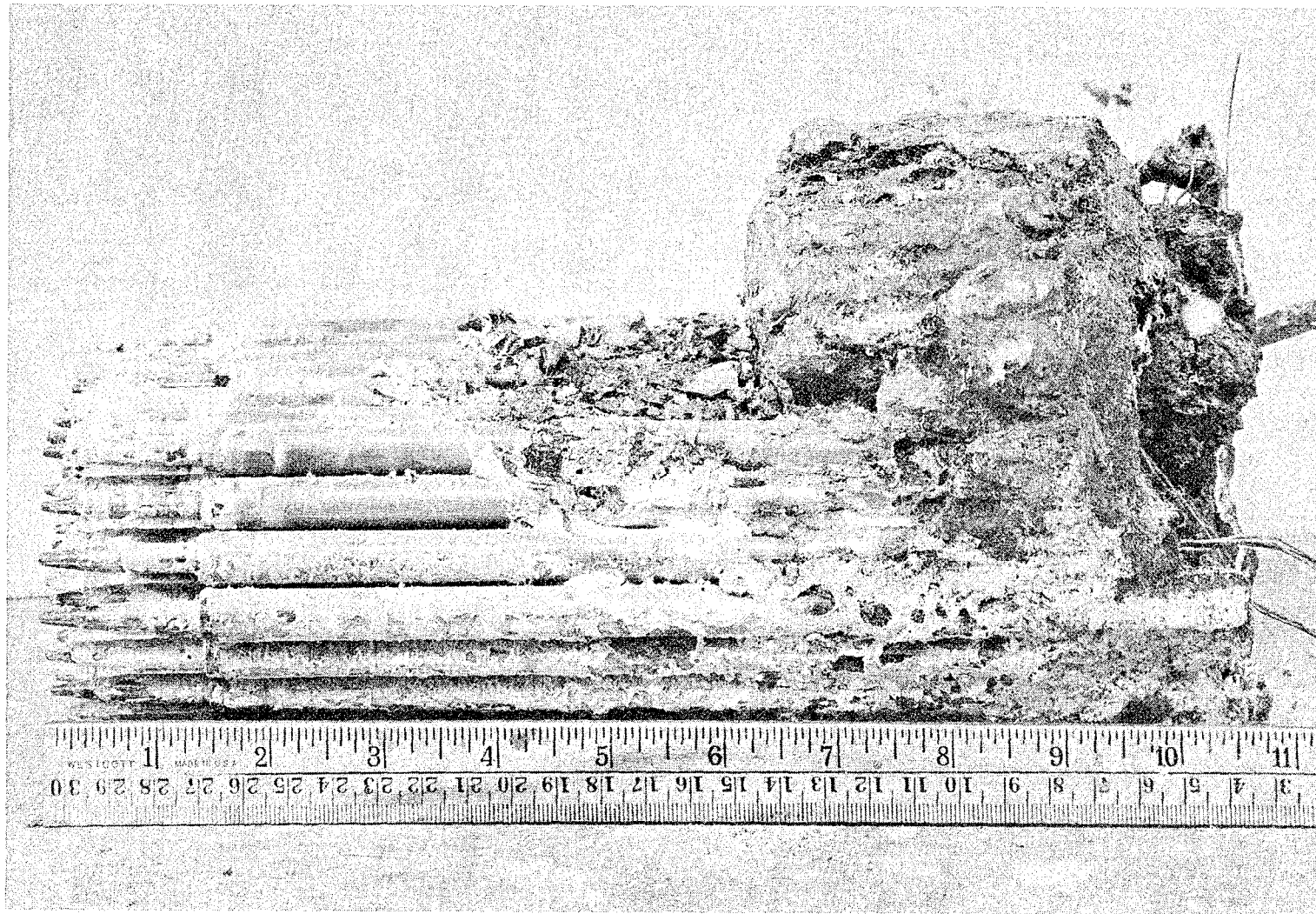
103-235

Figure 32. Cross section of damaged EBR-I core at the midplane of the fuel section. Two distinct sponge-like zones are present. Thermocouple wires in the fused mass are undamaged.



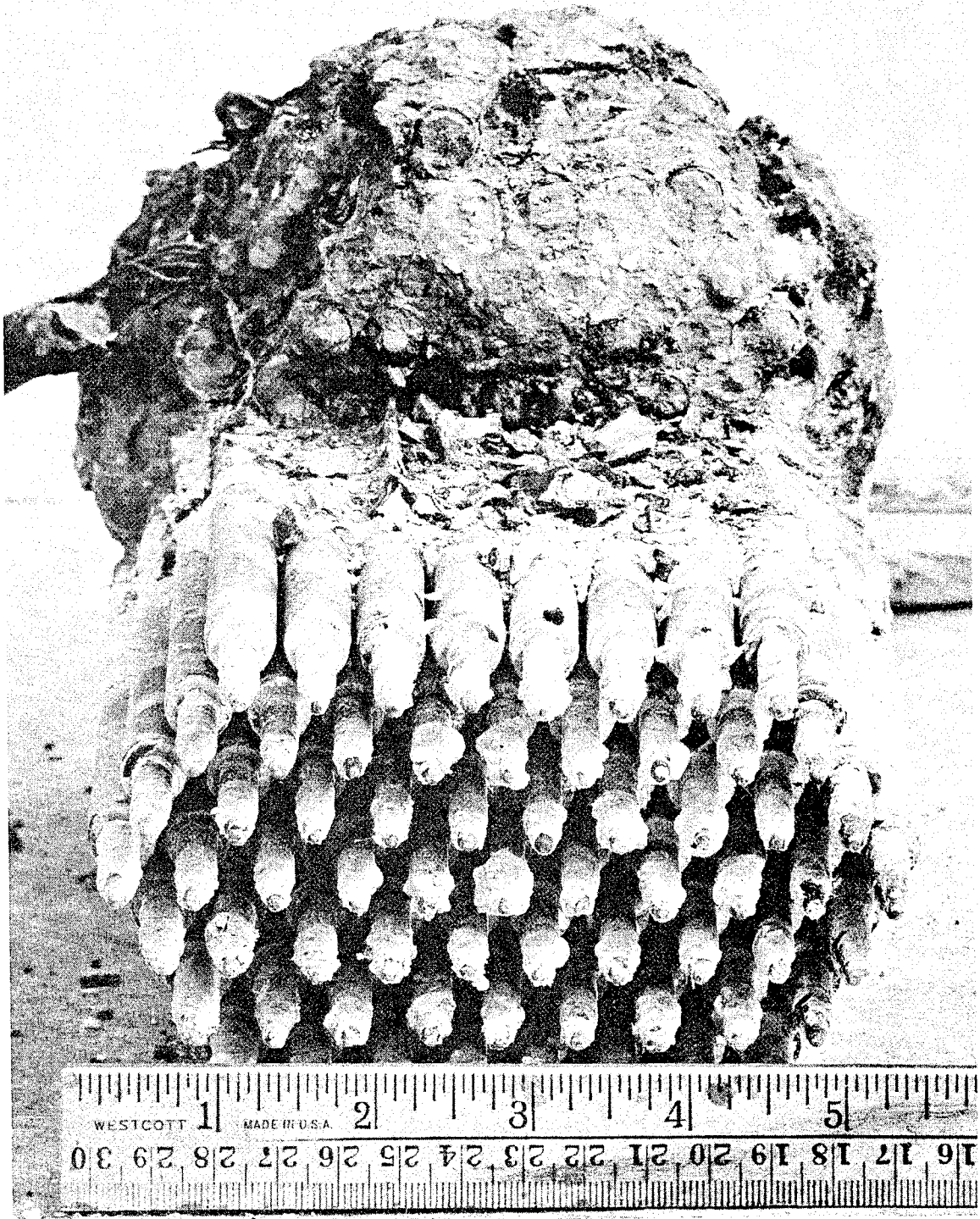
103-234

Figure 33. Side view of core assembly after partial removal of lower blanket section.



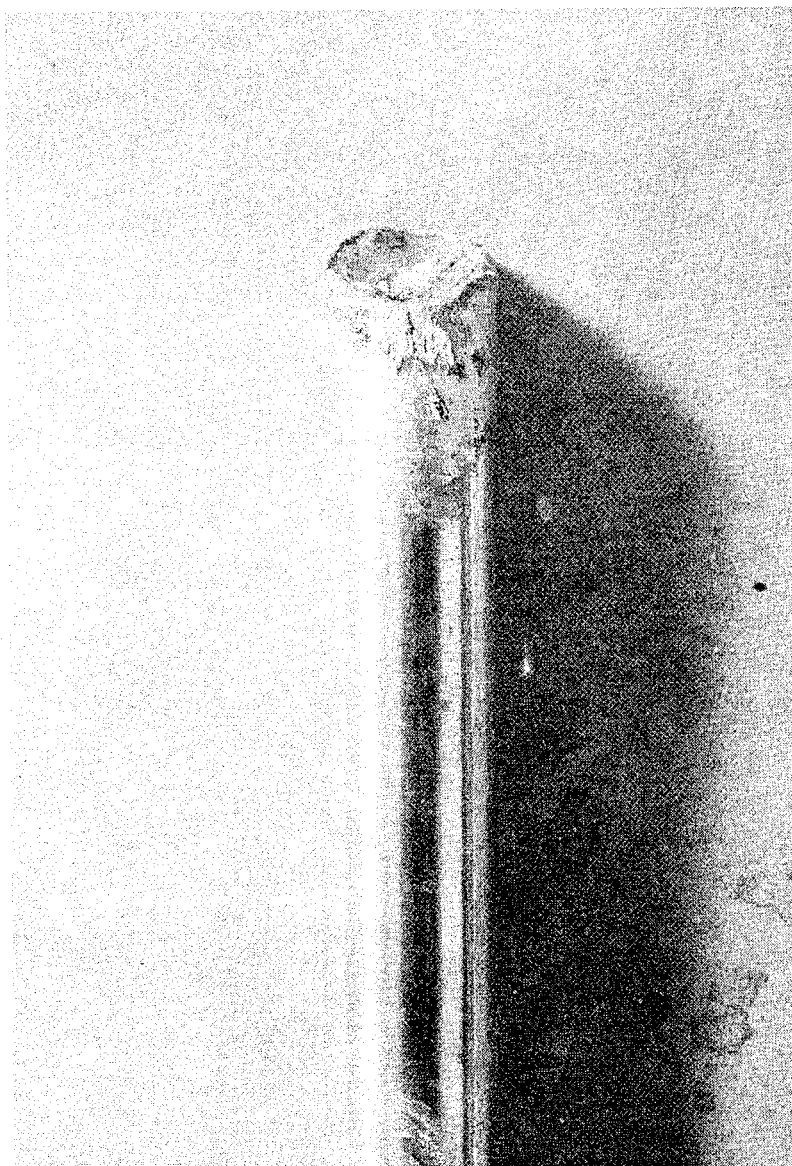
103-222

Figure 34. Bottom of fuel section, after partial removal of lower blanket rods.



106-3100

Figure 35. Stainless steel outer jacket from the lower blanket. The upper end was originally attached to the fuel section. Most of the adhering fuel alloy has been removed, and it can be noted that the jacket does not appear to have been damaged by melting.



20546

2X

Figure 36. Vertical cross section of the lower half of the core. The junction between fuel and lower blanket is at the 6-1/4 in. level.

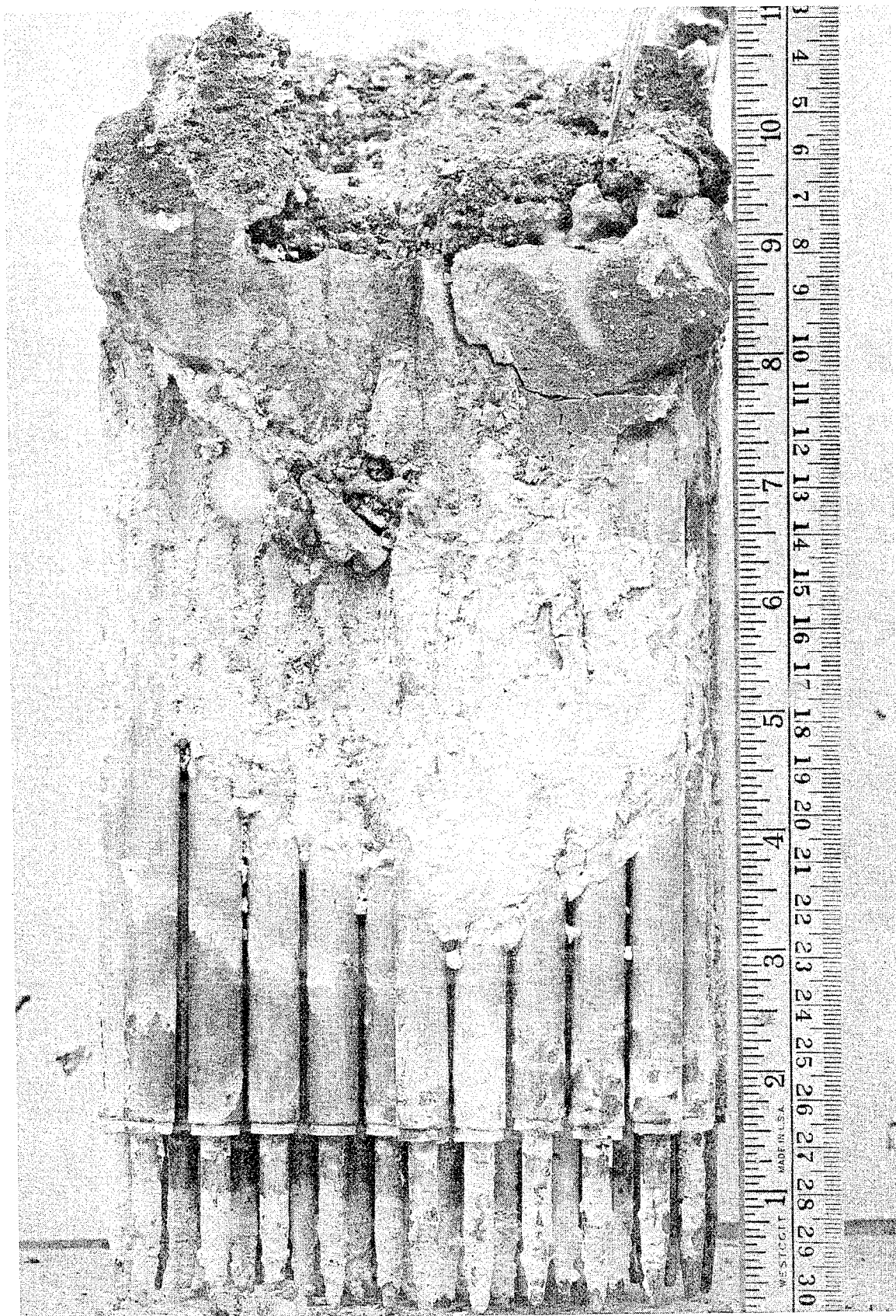
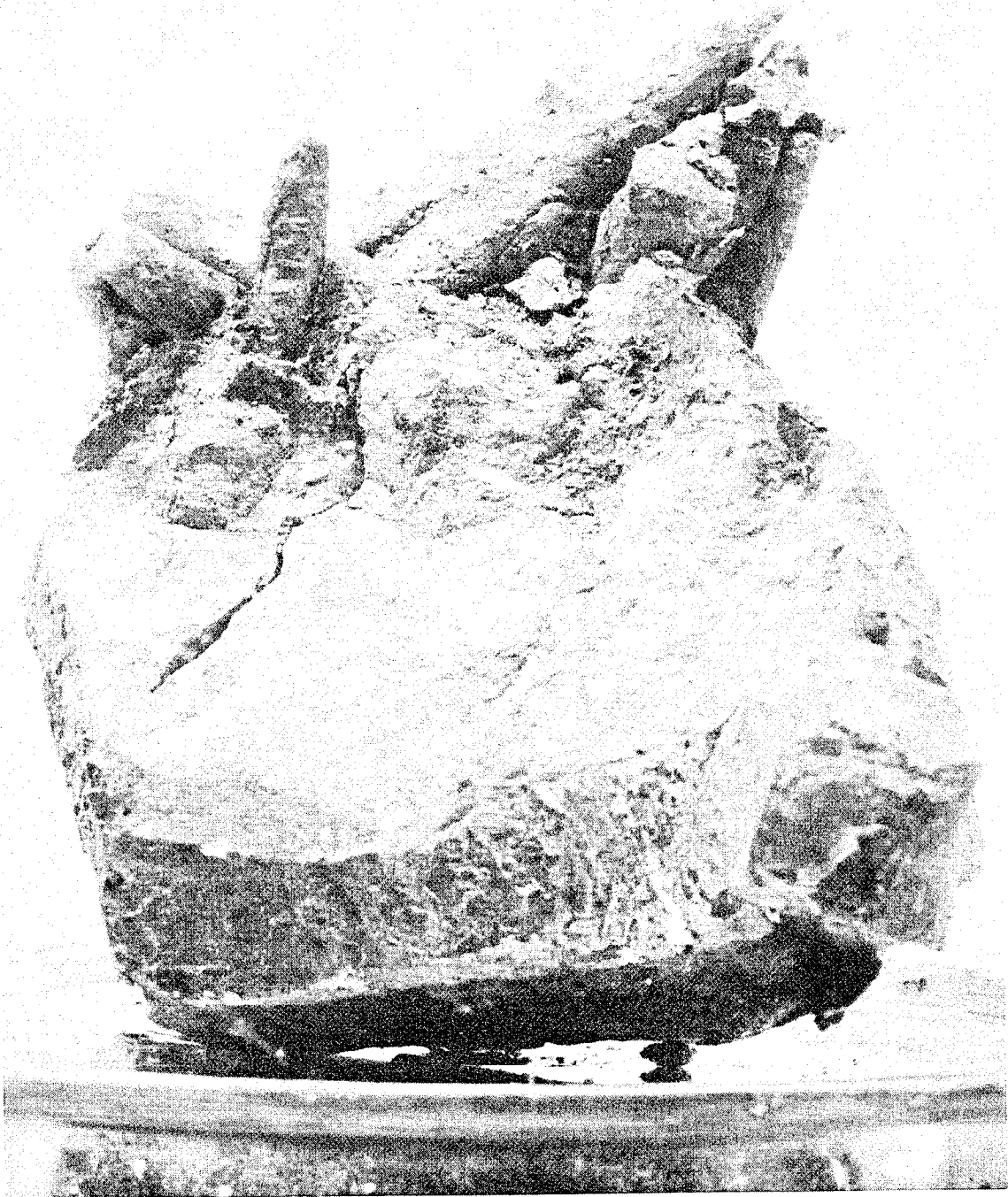


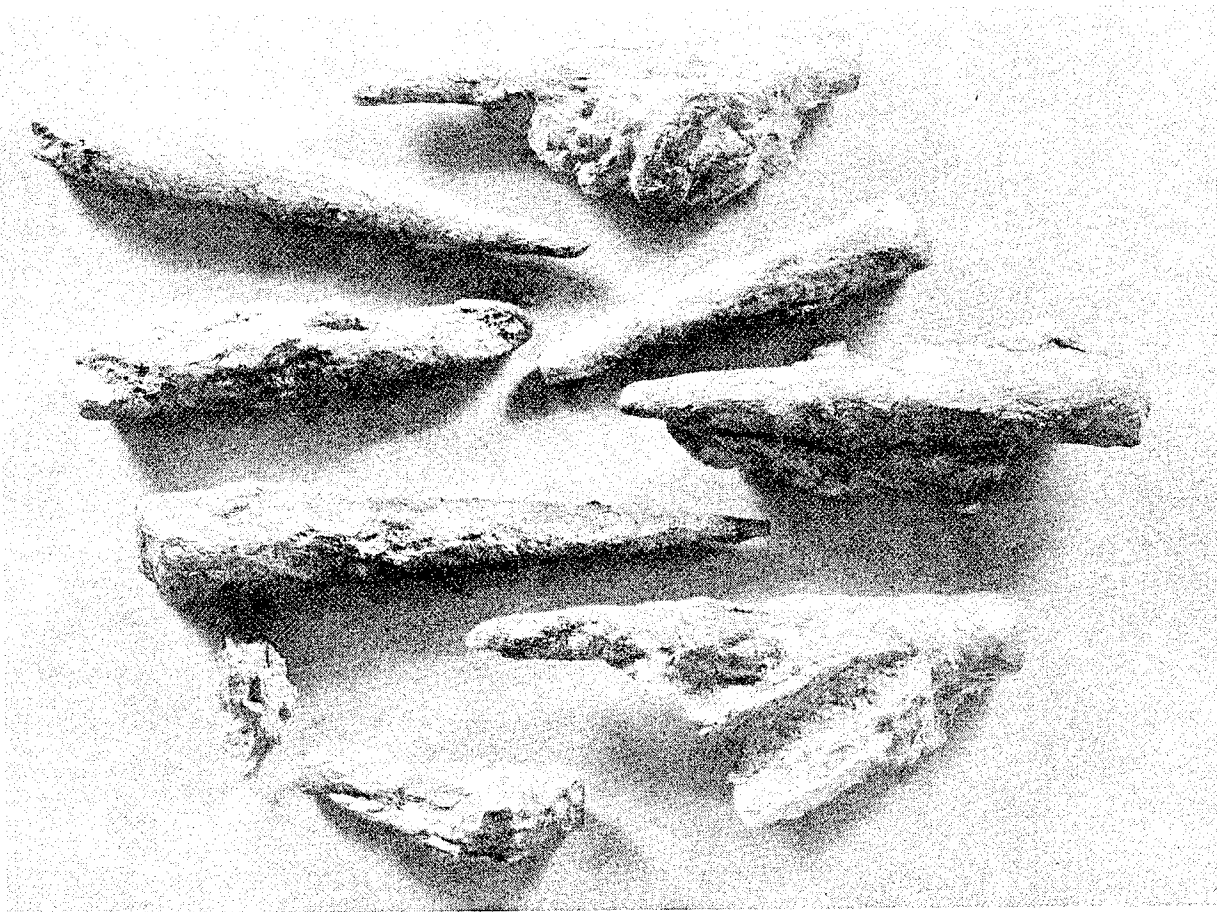
Figure 37. Partially dissolved fuel slugs embedded in dense material from near bottom of fuel section.



103-251

2X

Figure 38. Partially dissolved fuel slugs separated from adjoining material.



20564

2X

Figure 39. Illustration of voids which were found in the dense zone in the lower fuel section.

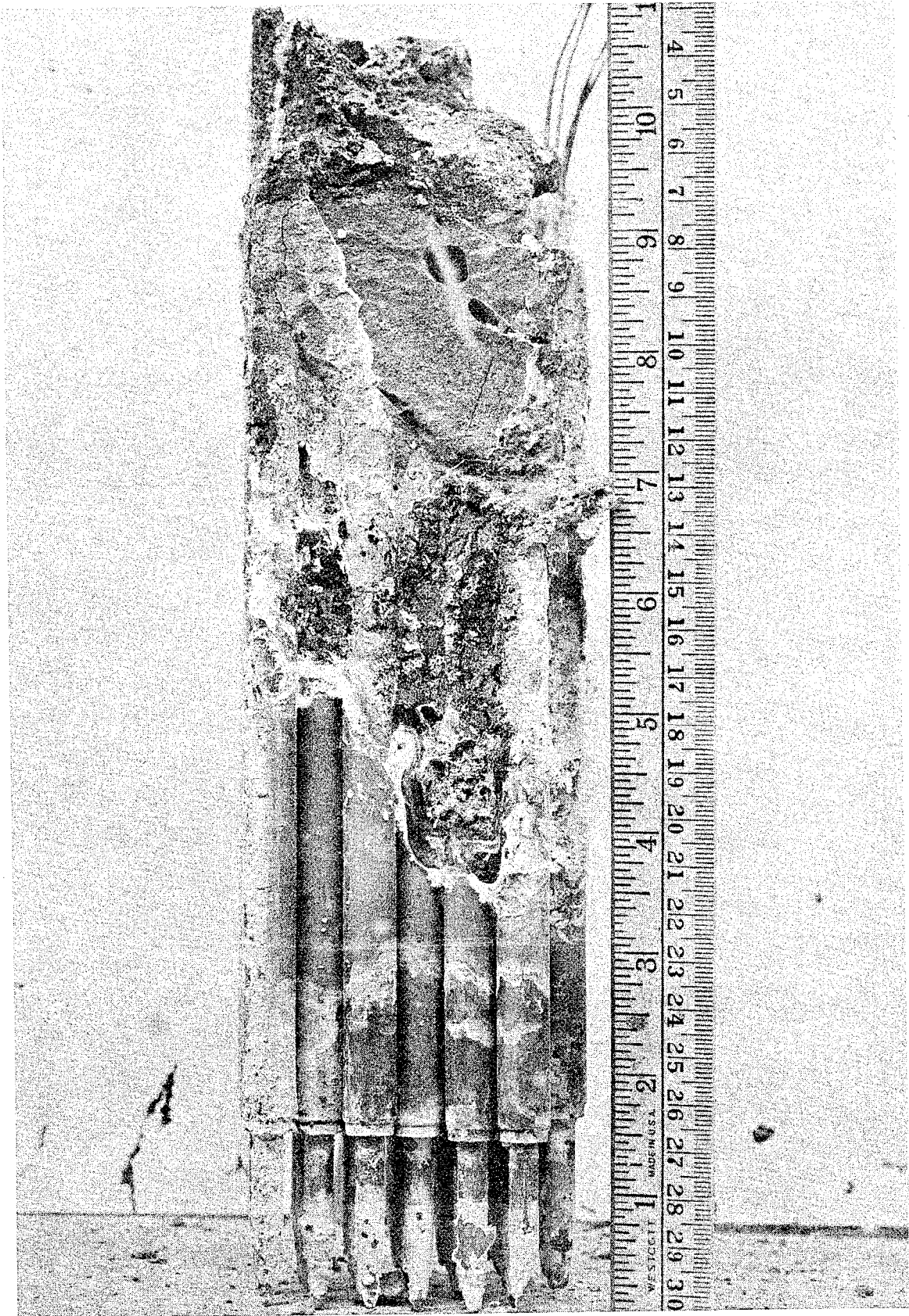


Figure 40. Artist's reconstruction of a vertical cross section through the damaged EBR-I core. The most reliable values for the densities of the various areas are shown at the left.

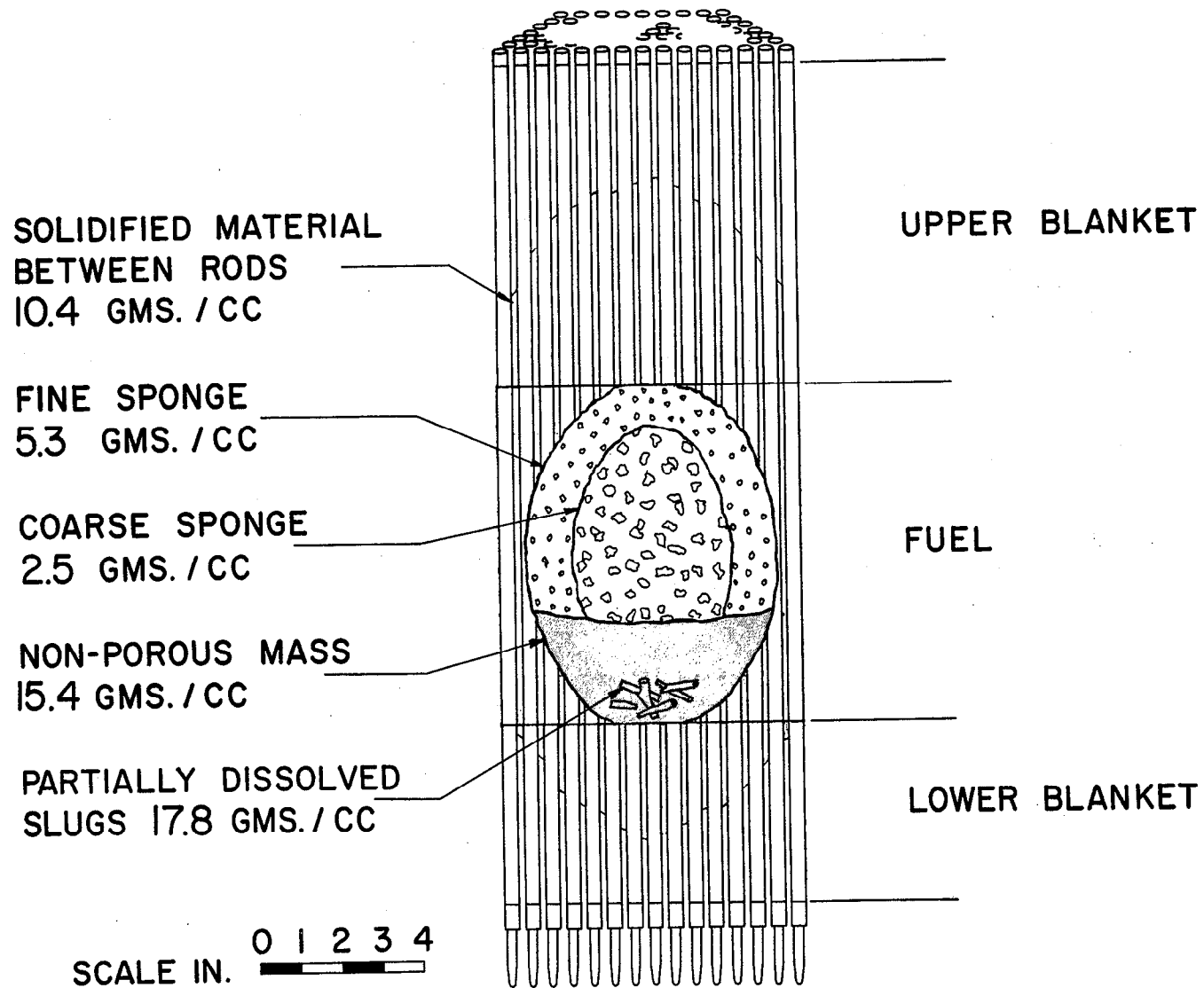


Figure 41. Appearance of samples removed for metallographic examination. Reading left to right, sample numbers are; top, 31 and 32; bottom, 33, 29, and 30. Locations from which the samples were taken are given in Table I.

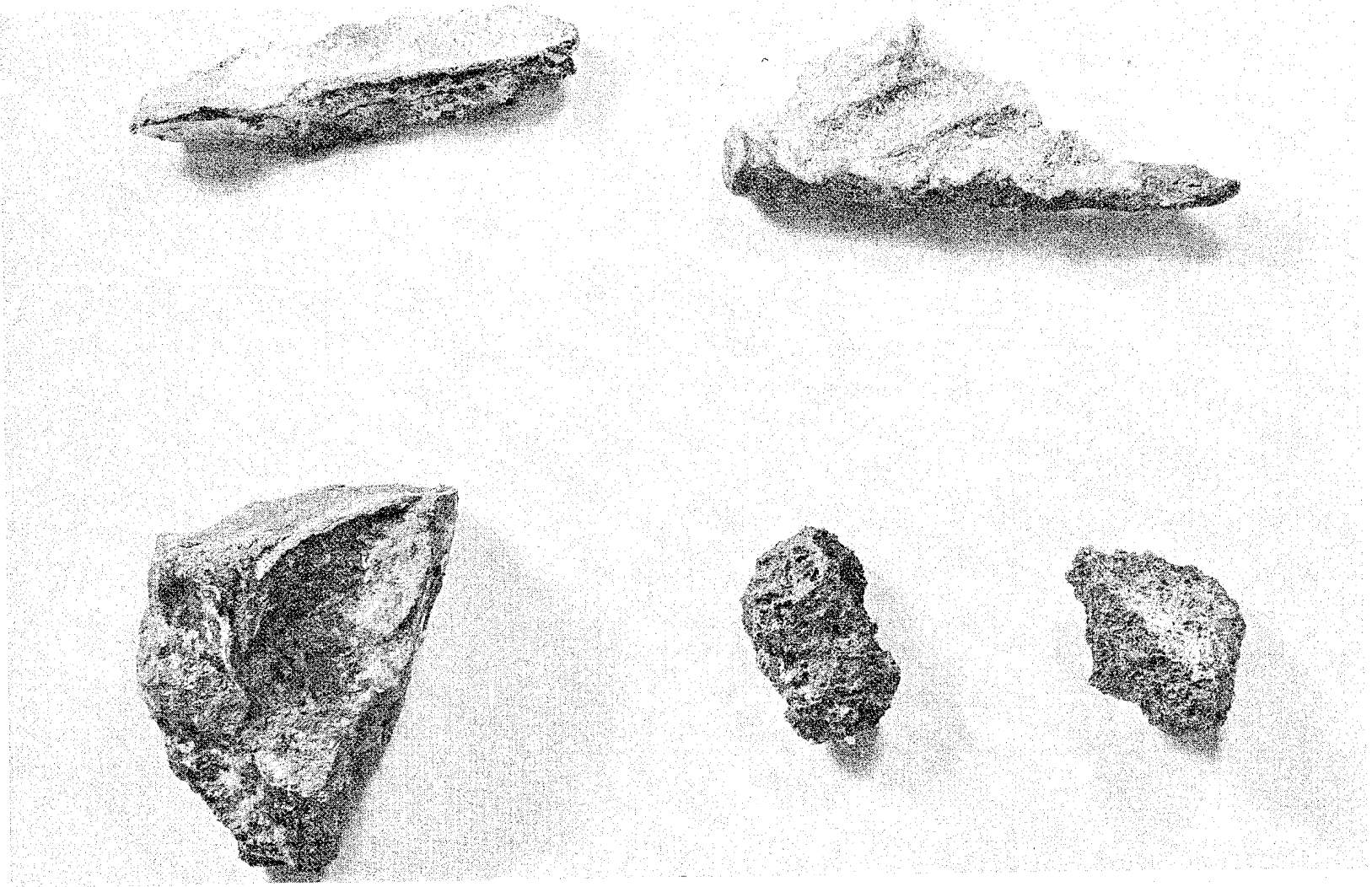
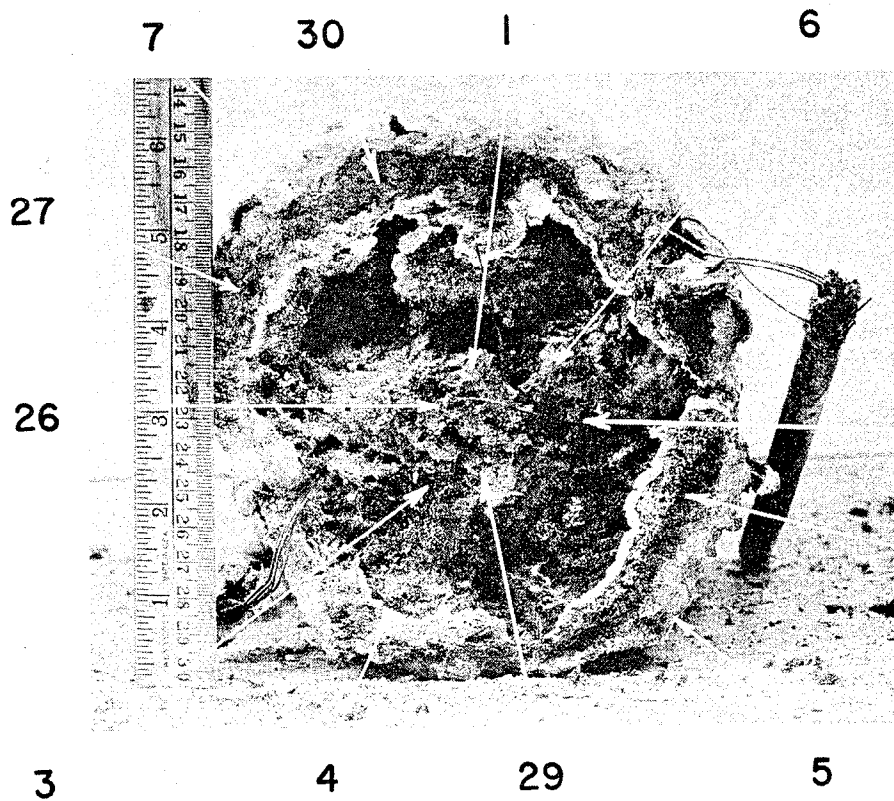


Figure 42. Approximate location of samples taken from a horizontal cross section of the core for chemical analyses and metallographic studies.



103-281

Figure 43. Approximate location of samples taken from a vertical cross section of the core for chemical analyses and metallographic studies.

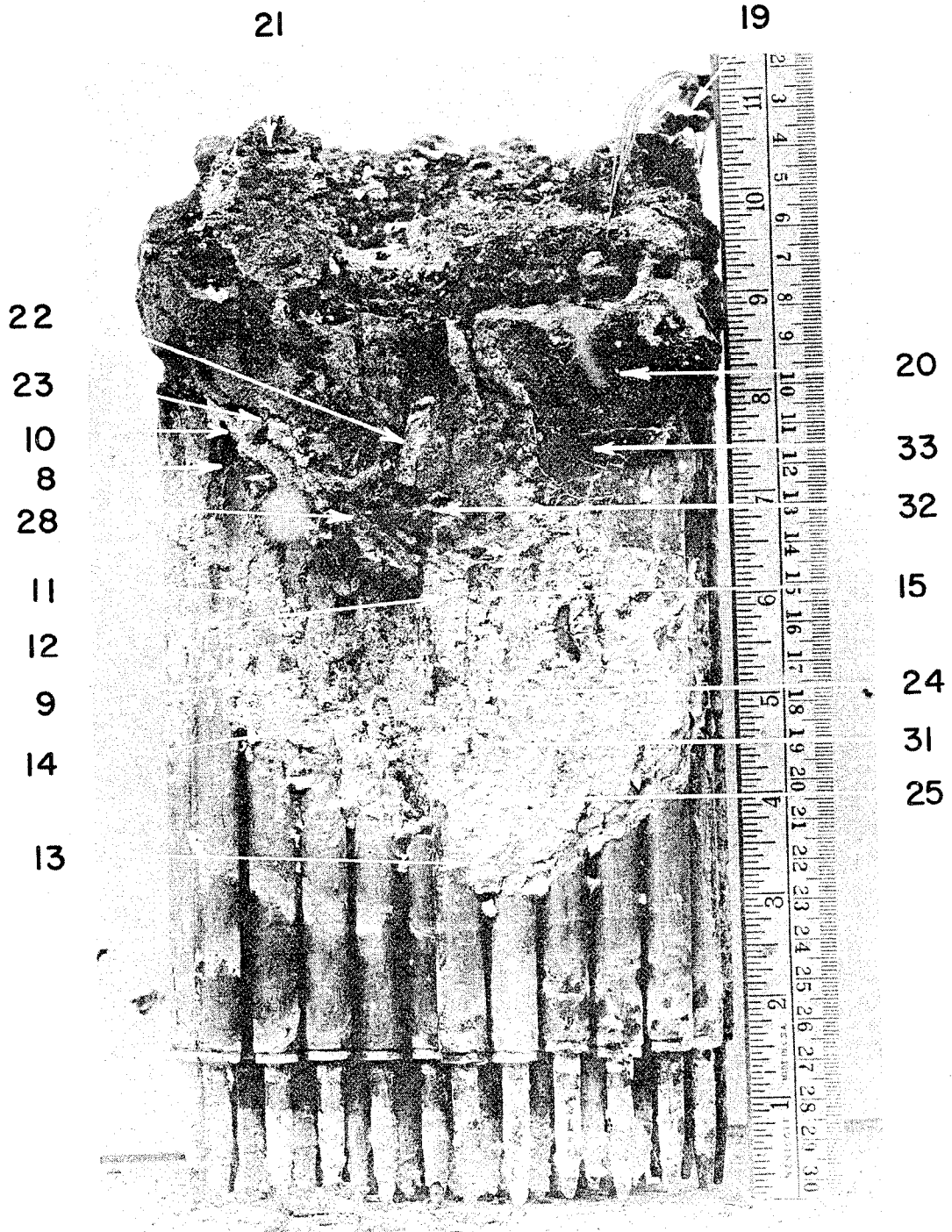
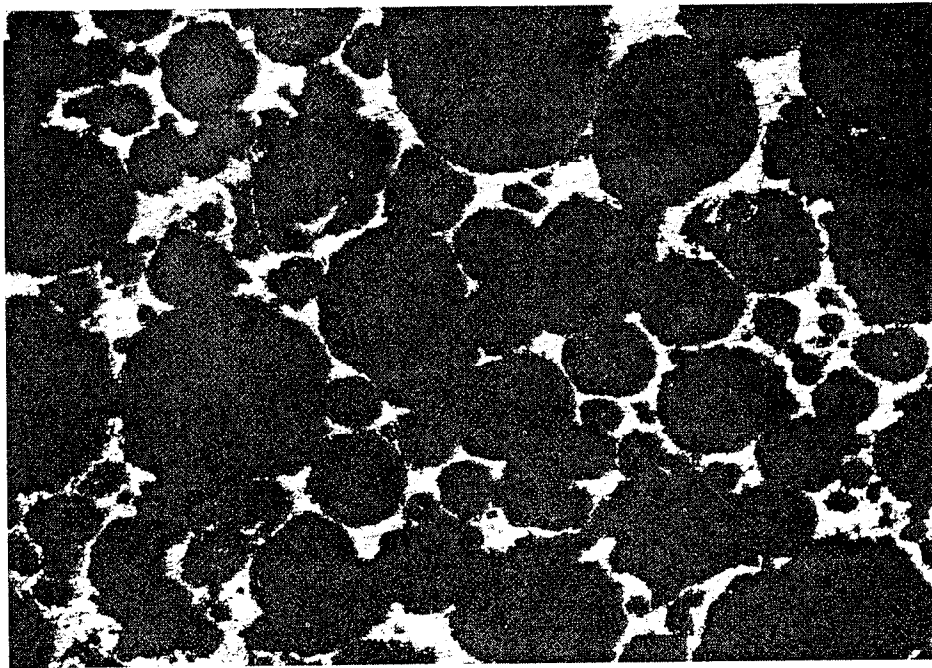


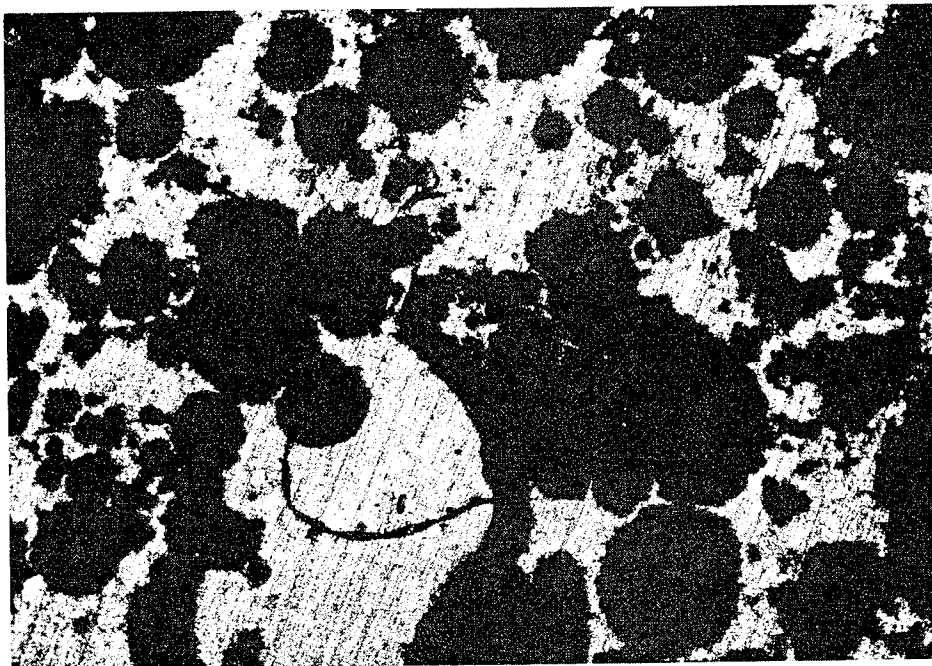
Figure 44. Typical porosity in sample No. 29, from coarse sponge zone.



21237

50X

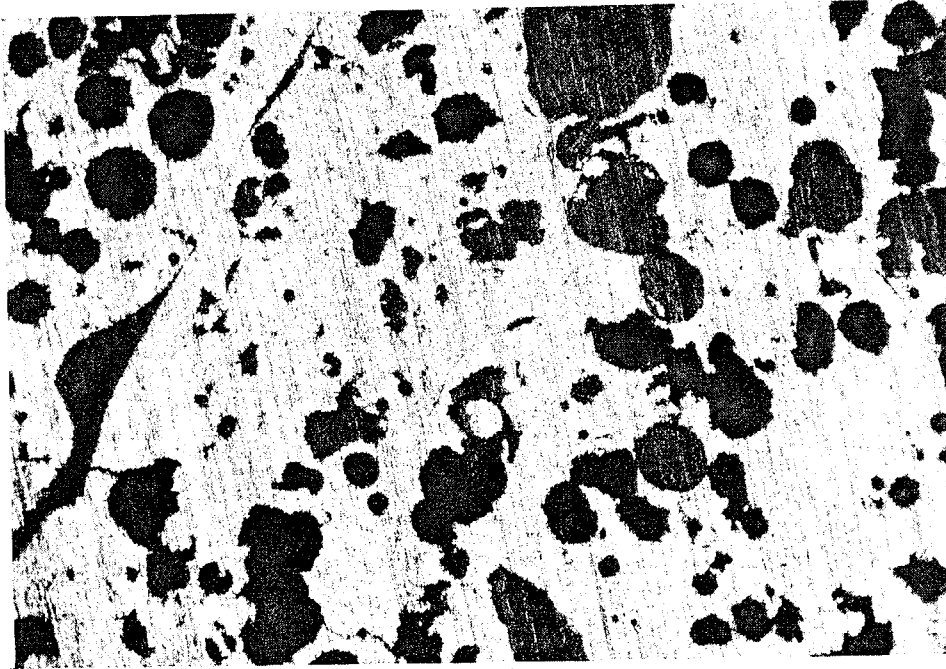
Figure 45. Typical porosity in sample No. 30, from fine sponge zone.



21234

50X

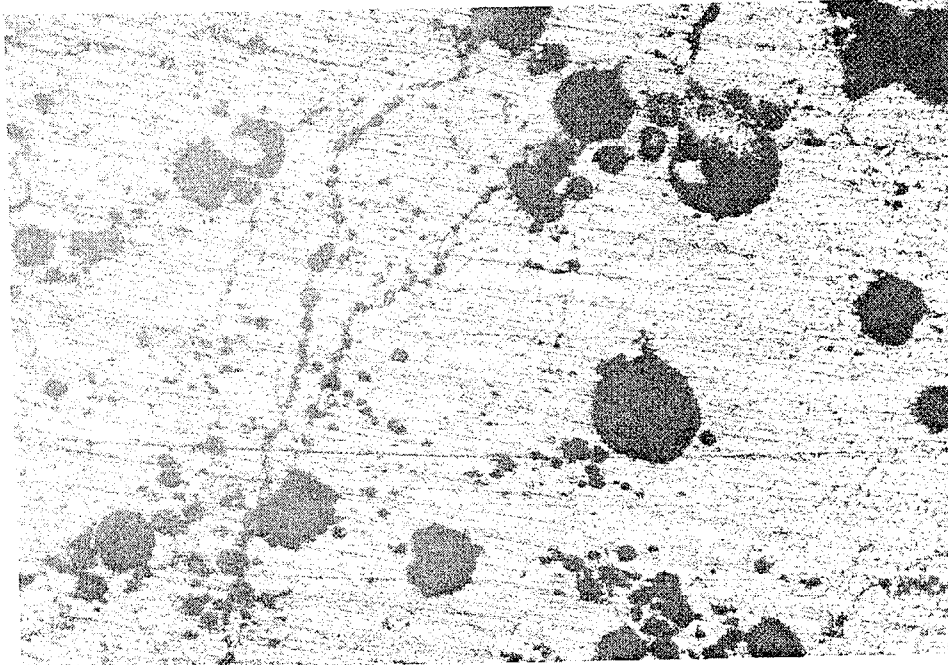
Figure 46. Typical porosity in sample No. 31, from material between blanket rods.



21231

50X

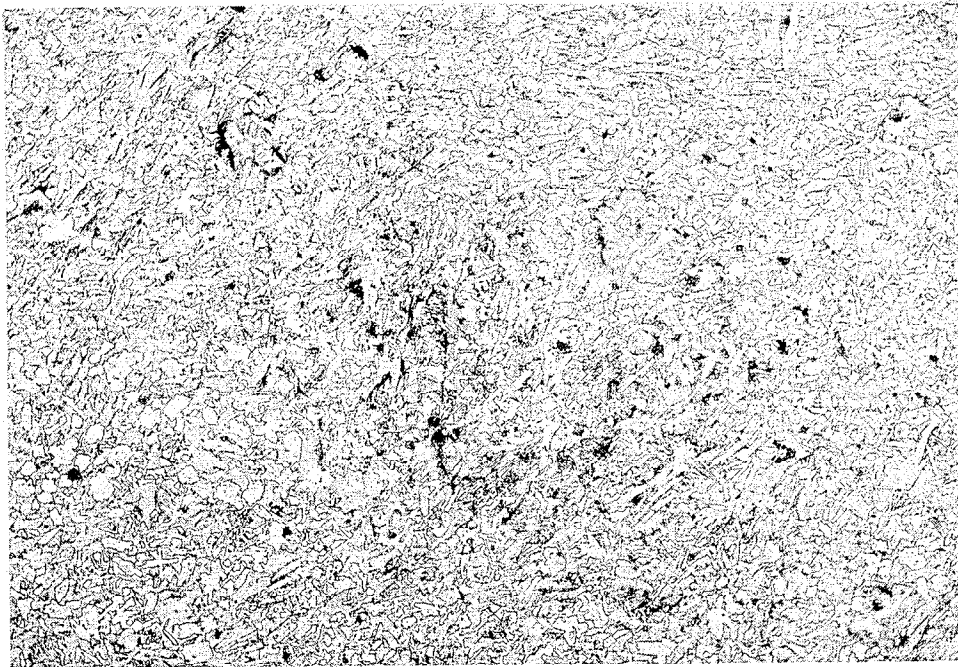
Figure 47. Porosity in material adhering to partially dissolved fuel slug, in sample No. 32.



21349

50X

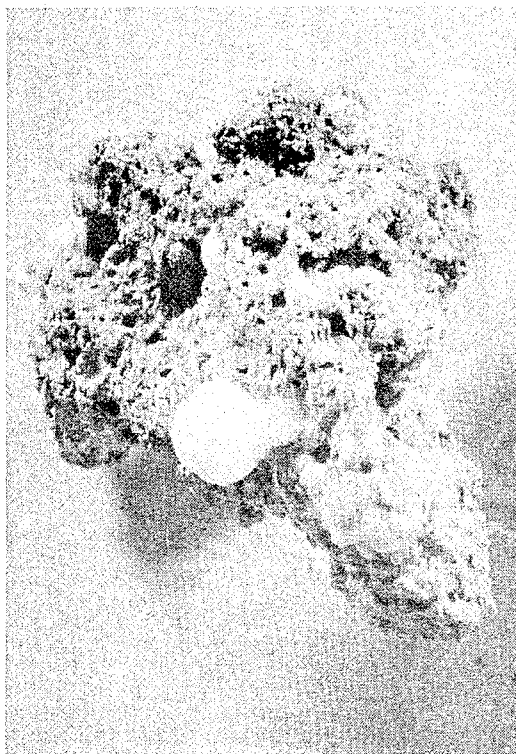
Figure 48. Typical porosity in sample No. 33, from high-density zone.



21224

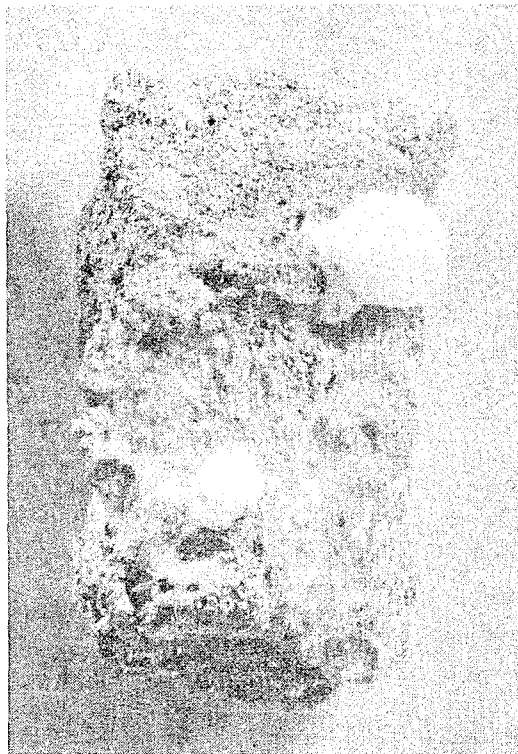
100X

Figure 49. Exudation of NaK oxide and resulting deliquescence in porous samples removed from damaged core. From left to right, the samples are from the coarse sponge zone, the fine sponge zone, and material solidified between lower blanket rods.



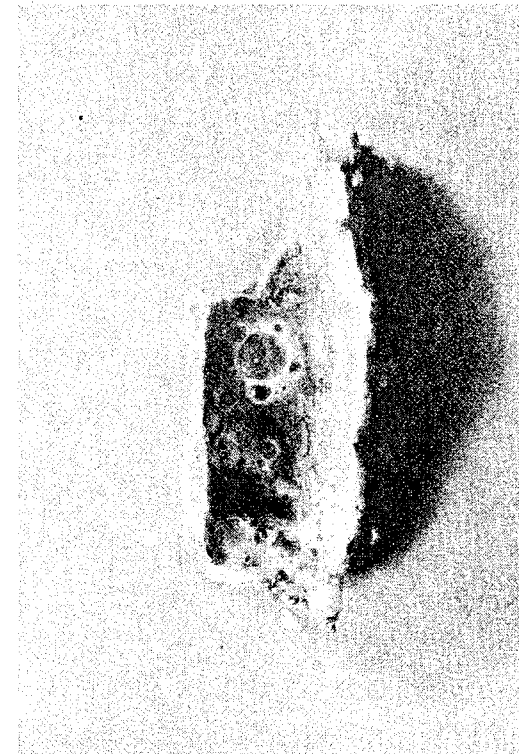
20479

2X



20479

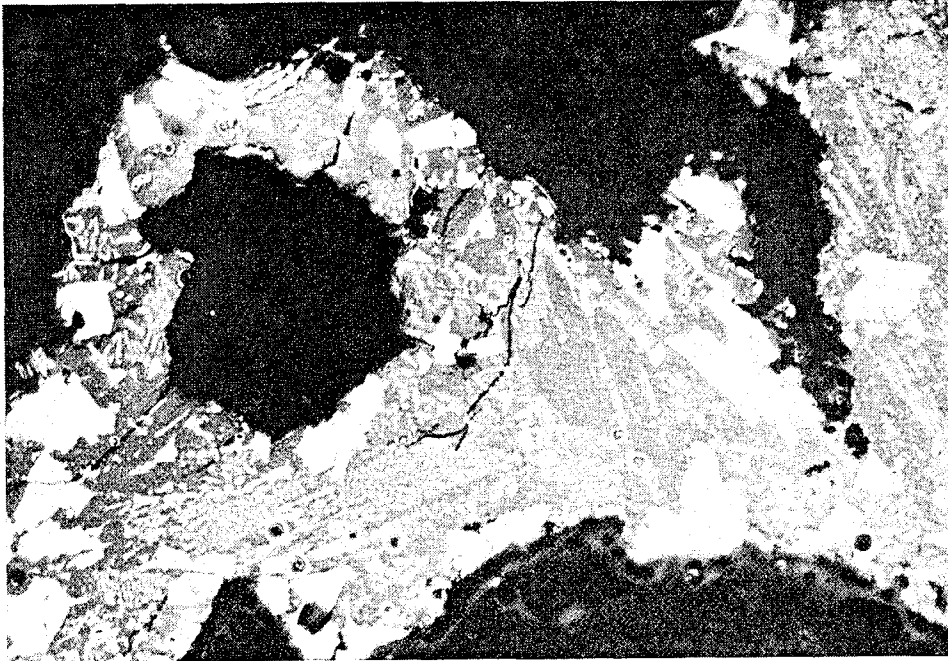
2X



20489

2X

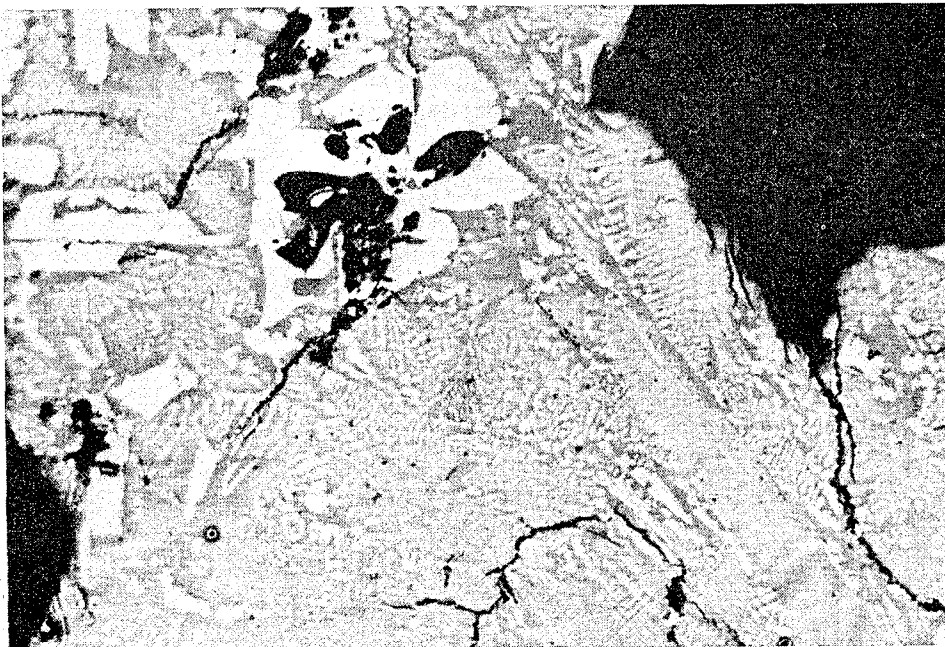
Figure 50. Microstructure in sample No. 29, from coarse sponge zone. The light phase is believed to be analogous to  $UFe_2$  and the dark phase analogous to  $U_6Fe$ .



21238

500X

Figure 51. Microstructure in sample No. 30, from fine sponge zone. The light phase is believed to be analogous to  $UFe_2$  and the dark phase analogous to  $U_6Fe$ .



21236

500X

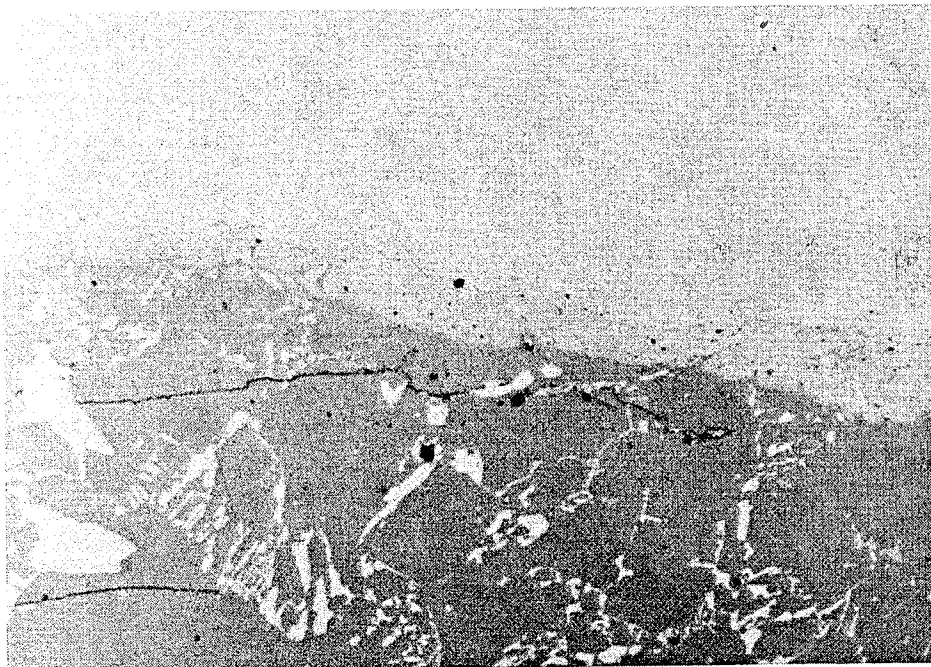
Figure 52. Microstructure in sample No. 31, from material between blanket rods. The light phase is believed to be analogous to  $UFe_2$  and the dark phase analogous to  $U_6Fe$ .



21233

50X

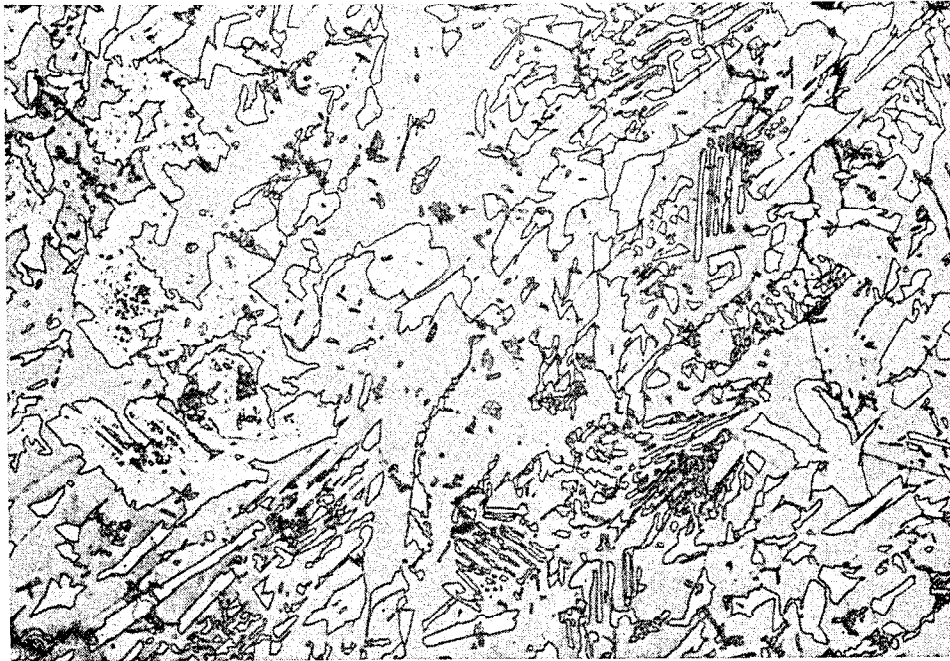
Figure 53. Microstructure of sample No. 32, showing junction between embedded fuel slug and adjoining material. The undissolved fuel slug is shown in the upper half of the photograph. The light phase is believed to be analogous to  $UFe_2$  and the dark phase analogous to  $U_6Fe$ .



21229

500X

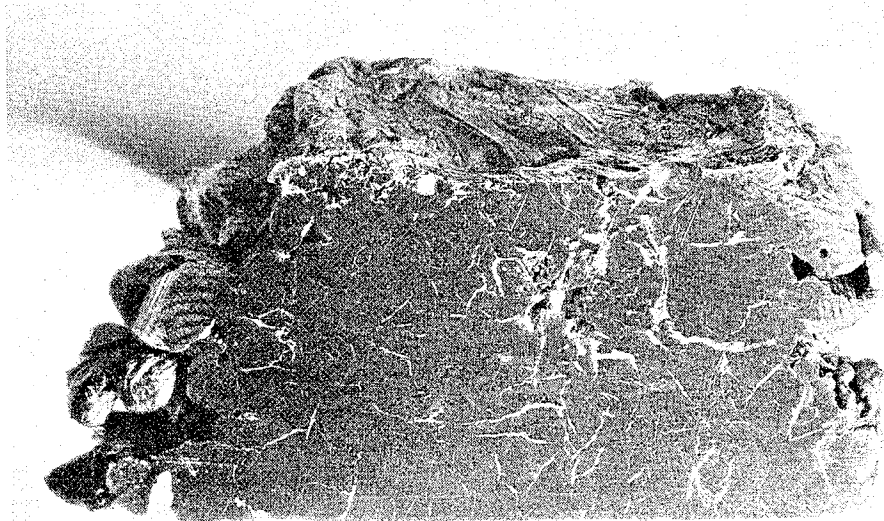
Figure 54. Microstructure in sample No. 33, from high-density zone. The light phase is believed to be analogous to  $UFe_2$  and the dark phase analogous to  $U_6Fe$ .



21225

500X

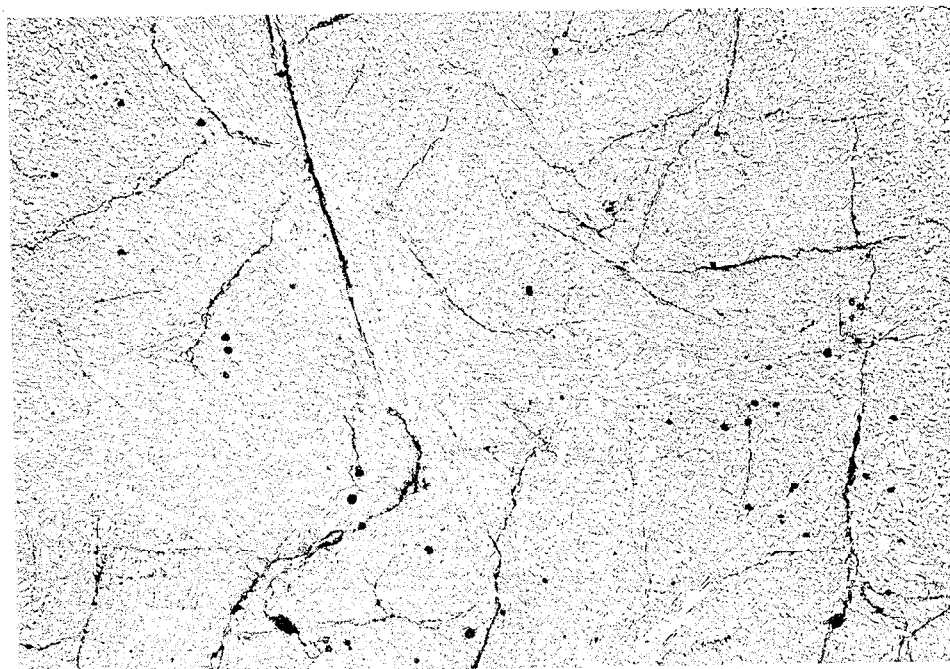
Figure 55. Cross section of first casting made by pouring uranium-stainless steel alloy into NaK. A small amount of NaK was trapped in the casting, evidenced by the traces of NaK oxide.



21015

5X

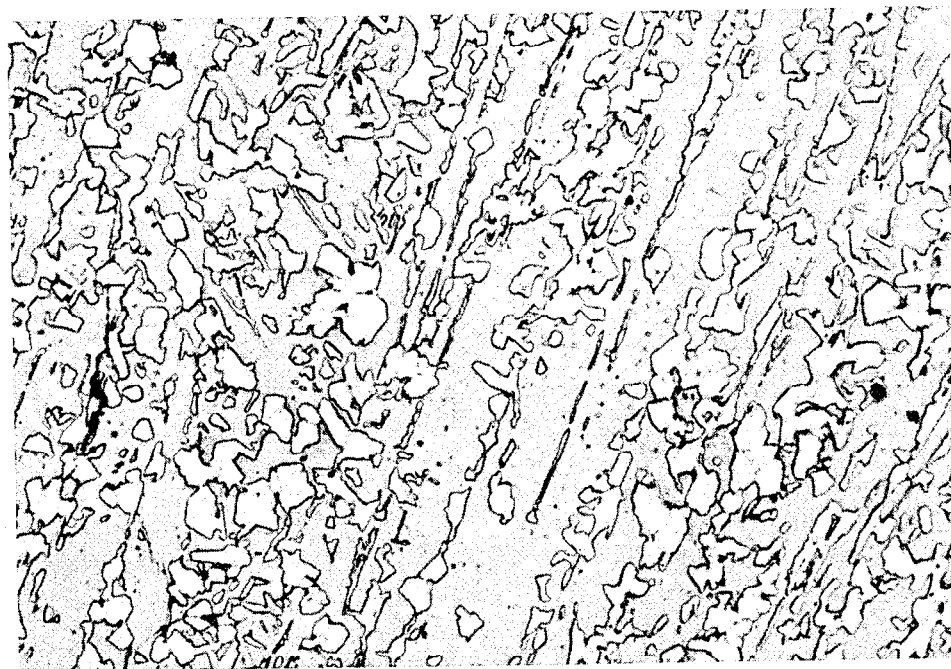
Figure 56. Porosity in casting shown in Figure 55.



21222

100X

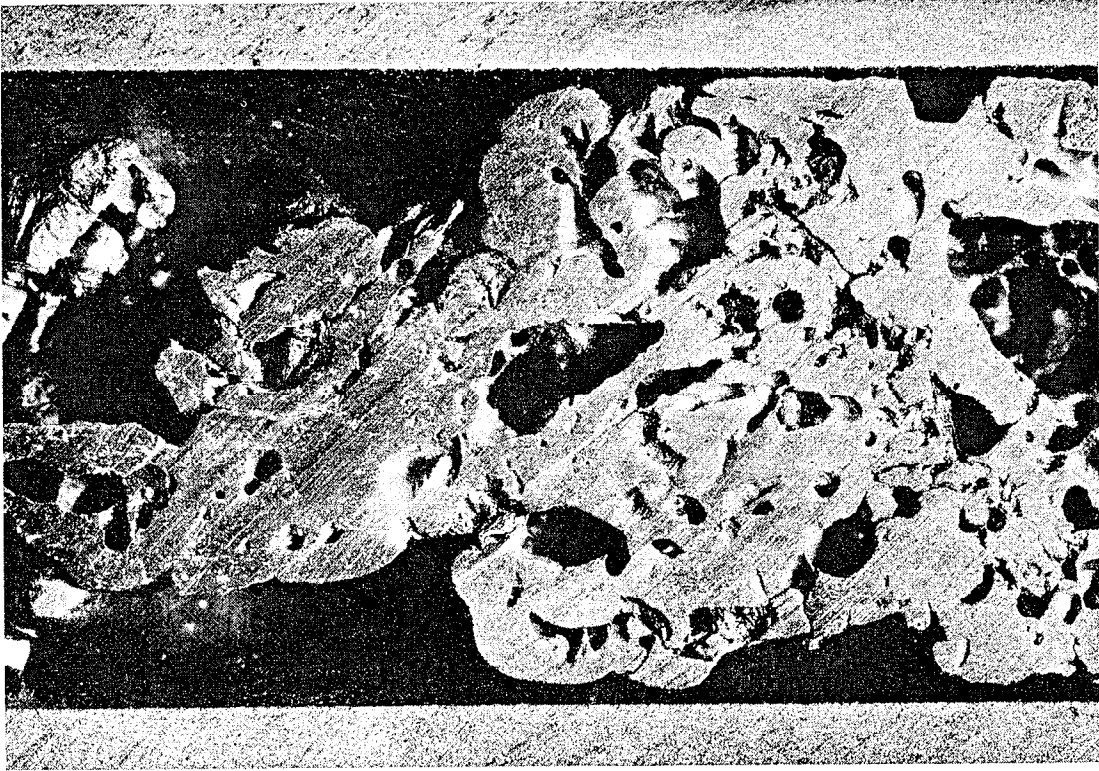
Figure 57. Microstructure of casting shown in Figure 55. The light phase is believed to be analogous to  $UFe_2$  and the dark phase analogous to  $U_6Fe$ .



21223

500X

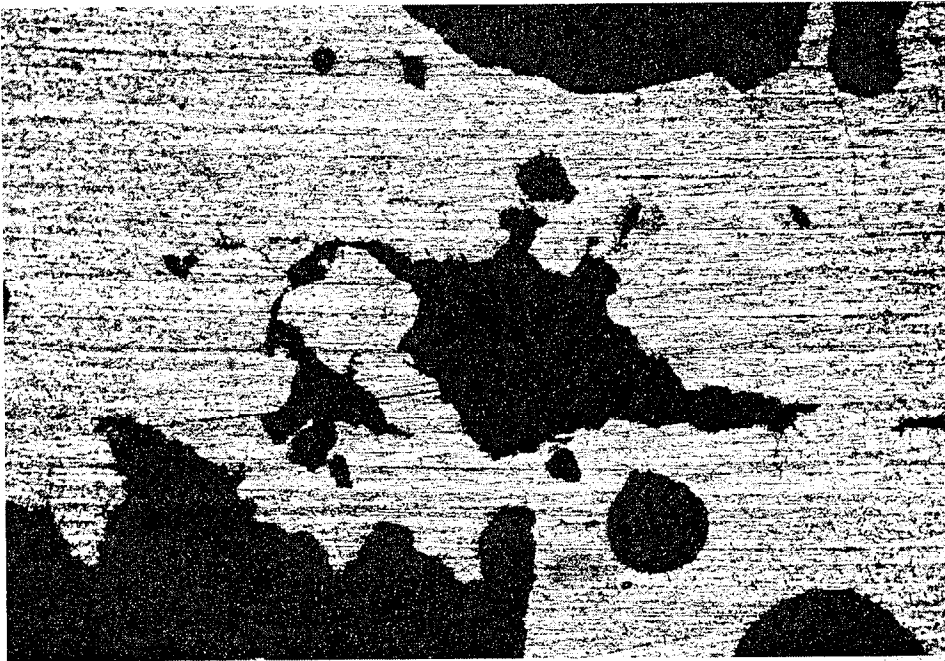
Figure 58. Cross section of second casting made by pouring uranium-iron alloy into NaK.



21201

7X

Figure 59. Metallographic section of above casting.



21348

50X

Figure 60. Microstructure of casting shown in Figure 58. The light phase was identified as  $UFe_2$  and the dark phase is believed to be  $U_6Fe$ .



21350

500X